Mechanisms of electron transfer from cytochrome P450 reductase to cytochrome P450 3A4

Thesis submitted for the degree of
Doctor of Philosophy
at the University of Leicester

by

Yassar Farooq

Biochemistry
University of Leciester

April 2010

Acknowledgements

I like to express my sincere deepest gratitude to my supervisor Prof. Gordon Roberts for giving me an opportunity to work in his laboratory and for all his help, constant encourangement and tolerance throughout my studies. I have had some hard times during my studies and I am grateful for Gordon's full support and patience.

I wish to say thank you to all lab member's past and present from NMR centre/Lab 102, Drs. Andrew Westlake, Jackie Ellis, Aldo Gutierrez, Alex Granua, Wei-Cheng (Vincent) Huang and Richard Ward that have helped me and made my studies enjoyable. I also like to say thanks to everyone in the Department of Biochemistry for their help, friendship and appreciation during my time. I am also grateful for Biotechnology and Biological Sciences Research Council (BBSRC UK) for financial support.

Lastly, I like to say thanks to my family, my parents, and in particular my wife, Tahira for the love, and support throughout my studies.

The thesis is dedicated to my children E'sa and Nimrah.

Abstract

The study demonstrates that CPR and P450 3A4 can be prepared to highly pure state by the use of detergent CHAPS. Optimisation of published methods led to pure flavoprotein, ~90% full-length with a small amount of truncated CPR. The reconstitution of CPR and P450 3A4 into liposomes using CHAPS and Superose 6 column purification has achieved a homogenous highly functional proteoliposomes with good catalytic activity and almost completely reducible P450 3A4 in a simple controllable system. The spectroscopic data has shown that reduction of P450 3A4 in proteoliposomes was at least 10 fold higher than in the simple reconstituted system suggesting that isolation of proteoliposomes from unbound protein aggregates had marked effect on the catalytic activity of P450. Negative staining electron microscopy has revealed proteoliposomes of having mean diameter of 200 ±15 nm in size; the lipid:protein ratio indicated that they incorporated 350 proteins per liposome. Type 1 difference spectral changes were observed upon binding of testosterone and erythromycin. Measurements of the first electron transfer have shown that the reduction of P450 3A4 is highly dependent on the presence of substrate. P450 3A4 reduction in proteoliposomes in the presence of testosterone was rapid and biphasic, with 90% of the P450 reduced in the fast phase, whereas reduction in the presence of erythromycin was monophasic, but substantially slower. Changes in the CPR:P450 molar ratio did not alter the rate of reduction and thus the data strongly indicates that first electron transfer occurs through preformed CPR:P450 complexes in the proteoliposomes that have a lifetime of about order of hundreds of milliseconds. The origin of the slow phase of reduction of P450 is not conclusive from our experiments, but it may be due to P450 heterogeneity. NADPH oxidation and 6β-hydroxytestosterone formation results have revealed that P450 3A4 is highly uncoupled enzyme with rates limited by CPR to P450

3A4 ratio. Hyperbolic plots of rates of NADPH consumption and 6β hydroxytestosterone formation vs CPR concentration indicate apparent *Ks* of 0.4 μM. This suggests that CPR:P450 complex can dissociate and reform between first and second electron transfer, which in turn indicates that second electron transfer occurs by diffusion mechanism.

Table of Contents

List of Figures

List of Tables

Abbreviations

ΔA(max)	(maximum) absorbance change
δ-ALA	δ-aminolevulinic acid
Amp	Ampicillin
b_5	Cytochrome b_5
CHAPS	3-[(3-cholamidopropyl)dimethylammonio]-1-propane-sulfonate
CPR	Cytochrome P450 reductase
CPRox	CPR oxidised
CPRred	CPR reduced
CMC	Critical micelle concentration
CYP	Cytochrome P450
ddH_2O	Double distilled water
DTT	Dithiothreitol
EDTA	Ethylene diamine tetraacetic acid
E. coli	*Escherichia coli*
EM	Electron microscopy
FAD	Flavin adenine dinucleotide
FMN	Flavin mononucleotide
HPLC	High performance liquid chromatograpy
IPTG	Isopropyl β-D-1-thiogalactopyranoside
K_d	Apparent dissociation constant
K_s	Equilibrium dissociation constant
K_m	Mechalis constant
KCl	Potassium chloride
kDa	Kilo Dalton
KPB	Potassium phosphate buffer
L:P	Lipid to protein ratio
LB	Luria-Bertoni medium
LB_{amp}	Luria-Bertoni medium containing ampicillin
MW	Molecular Weight
MWCO	Molecular weight cut-off
NADH	Reduced nicotinamide adenine dinucleotide

NADPH	Reduced nicotinamide adenine dinucleotide phosphate
NMR	Nuclear magnetic resonance
OD_{600}	Optical density at 600 nm
PMSF	Phenylmethylsulfonyl fluoride
PNACL	Protein and Nucleic Acid Chemistry Laboratory
POPC	1-palmitoyl-2-oleoyl-SN-glycero-phosphocholine
POPA	1-palmitoyl-2-oleoyl-SN-glycero-3-phosphate
P420	Cytochrome P420
P450	Cytochrome P450
P450ox	P450 oxidised
P450red	P450 reduced
SD	Standard deviation
SDS	Sodium dodecyl sulphate
SDS-PAGE	Sodium dodecyl sulphate polyacrylamide gel electrophoresis
SRS	Simple reconstituted system
TB	Terrific Broth
Tris	Tris(hydroxymethyl)aminomethane
UV	Ultra-violet
vs	Versus
Vis	Visible
v/v	Volume to volume
WT	Wild-type
w/v	Weight to volume
7-BQ	7 -benzyloxyquinoline
7-HQ	7 -hydroxyquinoline

Chapter 1
Introduction

1.0 Introduction

1.1 What are Cytochromes P450?

The cytochromes P450 (abbreviated as CYPs or P450s) are haemoproteins encoded by a gene superfamily that is present in organisms from all kingdoms of life (Degtyarenko and Archakov 1993). All P450 genes have probably evolved from one single ancestral gene over a period of some 3.5 billion years, which would explain why P450 proteins are ubiquitous in the biosphere (Nelson, Koymans, et al. 1996). This diverse enzyme family is thought to have initally evolved as an adaptive reponse to toxic effects of environmental chemicals (Lewis 1996). P450s are involved in biotranformation of endogenous and xenobiotics compounds such as drugs, steroids, vitamins, carcinogens, anesthetics and environmental toxins. They play an important role in biosynthetic pathways of a large variety of primary and secondary metobolites. For example, synthesis of fatty acids, hormones, alkaloids, lignin, glycosides, flavanoids and defence chemicals (Lewis 1996, Ortiz de Montellano 2005).

The discovery of P450s was made in the late 1950s (Klingenberg 1958) in rat liver microsomes and they were named as a result of their unusual spectral properties by Omura and Sato (Omura and Sato 1964). The protein displays a difference absorption maximum at 450 nm when reduced with sodium dithionite and complexed with carbon monoxide (CO); this is still used for estimation of the P450 content (Klingenberg 1958, Omura and Sato 1964), as shown in Figure 1.1. The name stands for the fact these are coloured (chrome) and cellular (cyto) proteins; P for pigment and 450 reflects the absorption peak of the CO complex at 450 nm.

Figure 1.1 Reduced CO difference spectra of detergent solubilised P450 3A4.

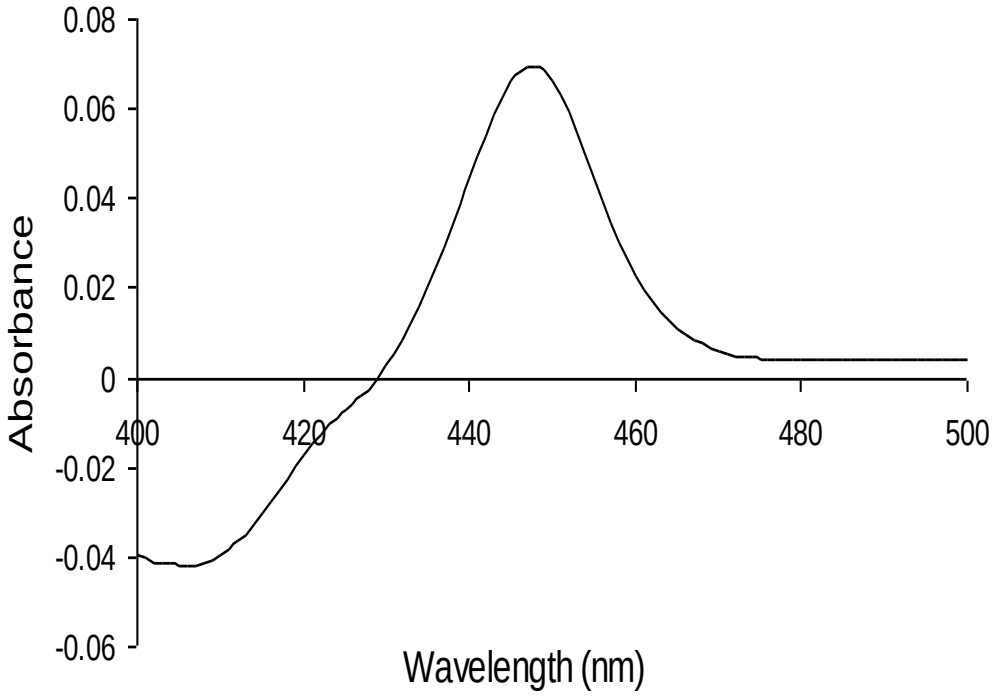

P450 3A4 was diluted in 0.1 M phosphate buffer (KPB) to concentration of 1 μM. The diluted sample was then reduced with few grains of sodium dithionite, divided equally into two cuvettes and the contents of one cuvette were gassed for 30 seconds with CO. The difference spectrum was recorded by using a Cary 300 Bio UV/visible spectrophotometer at 25 ^{o}C.

P450s generally range in molecular weight between 45-62 kDa and contain an iron-protoporphyrin IX haem prosthetic group (b type haem) with a thiolate of a cysteinate residue as the axial fifth iron ligand and water bound at the sixth coordination site. It is the role of thiol (-SH) group from the conserved cysteinate of the protein which sets the P450s apart from other cellular haemoproteins. Most haemoproteins (e.g. cytochrome b_5, peroxidases, and globulin) have nitrogen from the imidazole group of histidine which serves as a ligand to the haem iron (Ruckpaul, Rein, et al. 1989). The thiolate ligand leads to the typical position of the soret absorbance band of the CO-

complex at 450 nm, but also defines the specific catalytic role of P450. P450 ferric (resting) state has five electrons in the iron d-orbitals and depending on the spin paring of these electrons, the enzyme can either exist in the high spin (S=5/2, 5 unpaired electrons) or low spin configuration (S= ½ , 1 unpaired electron). A low spin state is where the least number of electrons are unpaired; this occurs when the energy gap (ΔE) between the e_g and t_{2g} orbitals is larger than the repulsive forces that exists between the coupled electrons (Figure 1.2). When ΔE becomes sufficiently small, the electrons will uncouple and occupy the e_g orbitals, even though they are at a higher energy, because the repulsive force between the electrons is greater. As a result, where there is the greatest number of electrons unpaired, the system is in a high spin state (Shriver and Atkins 2006, Ward 2003).

Figure 1.2 d-orbital splitting in an iron complex

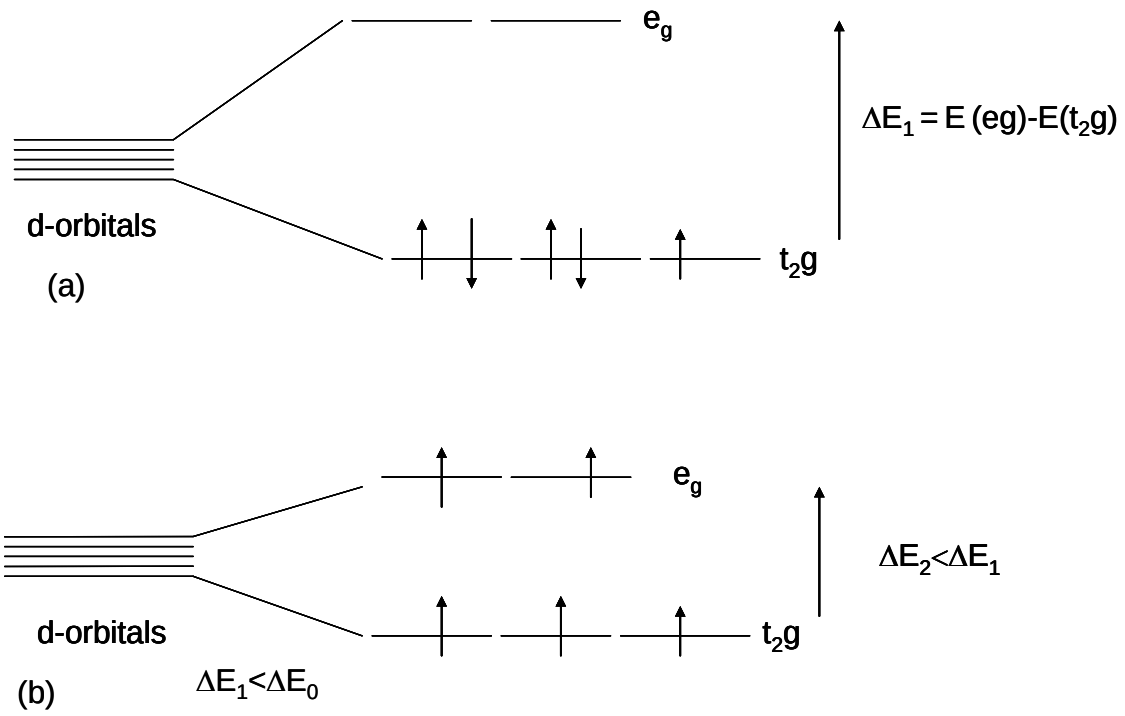

(a) and (b) represent the low and high spin states, respectively, for an iron complex containing 5 d orbital electrons. ΔE_0 and ΔE_1 represent the energy differences between the e_g and t_{2g} states in the low and high spin states, respectively. In the high spin state the energy gap between the e_g and t_{2g} states is sufficiently smaller to make it energetically more favourable for the electrons to uncouple and occupy the e_g orbitals.

1.1.1 What do P450s do?

P450s belong to the class of enzymes called oxygenases. Specifically they are known as monooxygenases or mixed function oxidases, since they catalyse the insertion of a single atom of molecular oxygen into their substrate with the concomitant reduction of the other atom into water. The reducing equivalents (two single-electron steps as we shall see in Figure 1.4) are channeled to the haem of P450 from NAD(P)H by an

associated redox partner enzyme (a flavoprotein or an iron sulfur protein). The overall reaction catalysed by P450s is:

$$RH + O_2 + 2H^+ + 2e^- \longrightarrow ROH + H_2O$$

Where RH is the substrate and ROH is the oxidised product.

P450s catalyse a diverse range of chemical reactions that include hydroxylation, epoxidation, peroxygenation, deamination, desulfuration and dehalogenation, as well as reduction (Sono, Roach, et al. 1996). Their substrates include steroids, fatty acids, prostaglandins, as well as a large number of xenobiotics such as drugs, anesthetics, organic solvents, ethanol, pesticides and carcinogens (Bernhardt 2006). As a result of this diversity of substrates and of reactions catalysed, the study of P450s has become a multidisciplinary field that involves toxicologists, pharmacologists, organic chemists, plant and environmental biologists (Lewis 1996, Ortiz de Montellano 2005).

1.2 P450 nomenclature system

The nomenclature of P450s was originally based on substrate specificity, on spectral properties, or on the source from which the enzymes were isolated (Gonzalez 1990). As different P450s were identified and isolated from various species it became apparent very quickly that it was difficult to discuss such a large number of proteins because a uniform system of nomenclature was lacking. Thus, a new nomenclature system was implemented in 1987 to categorise the growing number of P450s on the basis of their amino acid and gene sequences (Nelson, Koymans, et al. 1996). In this system, P450s are named with root symbol CYP and this is followed by a number for families (proteins that are exhibiting greater than 40% sequence similarity), a capital

letter for subfamilies (proteins with greater than 55% identity) and a number for the gene, for example CYP 3A4. The sequence of the gene has to differ by more than 3% before a new number is assigned. The P450 superfamily at present comprises more than 7700 genes that are categorised into ~800 families (for details see: http://drnelson.utmem.edu/CytochromeP450.html). The numbers of individual P450s in different species differ significantly, showing the highest numbers in plants (Nelson, Zeldin, et al. 2004).

1.3 Electron transfer routes in P450 systems

P450s are commonly separated into two main classes, as shown by Figure 1.3, depending on how electrons from NAD(P)H are delivered to the catalytic centre of P450. The catalytic centre of a P450 is made of haem iron and functions as part of a multi component electron transfer chain in which it acts as terminal oxidase where the activation of molecular oxygen takes place. Interaction of P450 with their electron transfer partners is a necessary prerequisite of P450 catalysis (Paine, Scrutton, et al. 2005). The partner proteins are usually expressed individually, but self-sufficient P450 monooxygenase systems such as P450 BM3 (P450 102A1) of *Bacillus megaterium* have evolved through the fusion of CPR and P450 genes. In recent years, a number of novel fusion P450 systems have rapidly emerged as consequence of large number of genome sequencing projects and are now considered to be categorised separately from class II system, see review by Munro et al for further detail (Munro, Girvan, et al. 2007).

Figure 1.3 Schematic organisation of class I and II P450 systems.

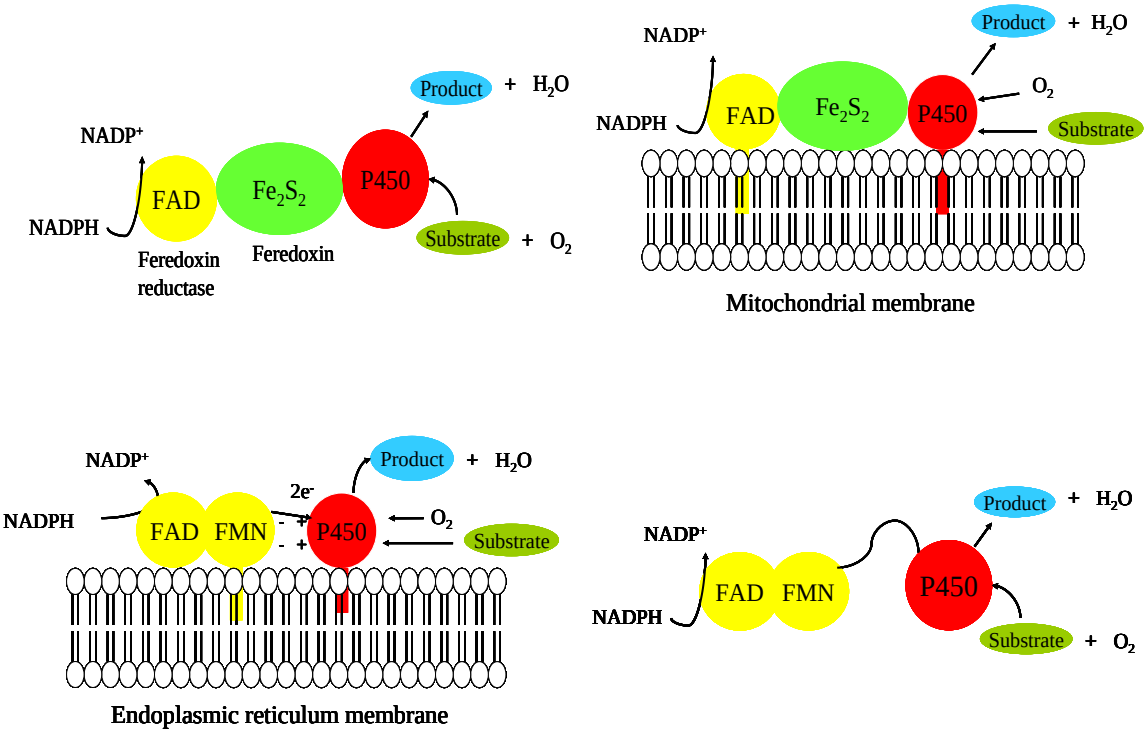

Upper row shows class I systems, bacterial system on the left and mitochondrial on the right. Lower row shows class II system, microsomal system on the left and a class III system, self sufficient P450 BM3 system on the right.

Class I 450 systems are found in the inner mitochondrial membranes of eukaryotes and in most bacteria. In this system electrons from a pyridine nucleotide (NAD(P)H) are transferred via two intermediate proteins, a flavin adenine dinucleotide (FAD) containing ferredoxin reductase and ferredoxin (an iron sulfur protein), which in turn passes electrons onto P450. All three protein components are soluble in bacteria. In eukaryotes only the ferredoxin is soluble, whereas P450 and the reductase are bound to the inner mitochondrial membrane.

Bacterial class I P450s are involved in production of biologically active secondary metabolites such as antibiotics or antifungals, and in oxidation of xenobiotics

and fatty acids. The most extensively characterised class I P450 system is P450 cam (P450 101A1) from *Pseudomonas putida*, which catalyses the 5-*exo*-hydroxylation of D-camphor in the first step of the pathway for breakdown of the compound (McLean, Sabri, et al. 2005), thus enabling its use as a sole source of carbon and energy for growth. P450 cam was the first P450 protein to have its structure determined by X-ray crystallography and more recently crystal structures of its redox partner enzymes have also been solved (Poulos, Finzel, et al. 1985, Sevrioukova, Garcia, et al. 2003, Sevrioukova, Li, et al. 2004).

Eukaryotic class I P450s of mitochondria play an essential role in biosynthesis and metabolism of the cholesterol-derived steroids of vitamin D and bile acids. For example, P450 11A (P450scc) of the adrenal cortex carries out side chain cleavage of cholesterol to form pregnenolone, which constitutes initial and rate limiting step in the synthesis of steroid hormones (Omura 2006). Mitochondrial P450s have been found in diverse animal species including in a number of vertebrates and insects, but none have been observed in plant mitochondria. Although the mitochondrial P450 systems in animal cells are made of same number of protein components as class I bacterial P450s, these P450s do not seem to be of prokaryotic origin. It is thought that during the course of biological evolution of eukaryotic organisms, a microsome-type P450 was translated into mitochondria and presence of microsome type P450s have been found from various tissues including lung, liver, and the brain in the mitochondria (Omura 2006).

The class II P450 system requires a single redox partner protein, known as NADPH-dependent cytochrome P450 reductase (CPR). CPR is an integral membrane bound protein containing two prosthetic groups, flavin adenine dinucleotide (FAD) and flavin mononucleotide (FMN) for the transfer of electrons to one of many P450 isozymes. Microsomal P450s are found on the outer face of endoplasmic reticulum of

eukaryotic organisms where their functions are extremely diverse. Microsomal P450s catalyse the oxidation of xenobiotics such as drugs and environmental pollutants and a further important function is involved in biosynthetic pathways of low-molecular-weight compounds that act as regulators (e.g. steroids, prostaglandins and their derivatives and derivatives of fatty acids). An additional membrane bound protein, cytochrome b_5 (b_5) has been suggested to be involved in electron transfer to some P450s, particularly P450 3A4 (Yamazaki, Nakamura, et al. 2002, Yamazaki, Nakano, et al. 1996, Zhang, Im, et al. 2007).

In plants, class II P450s play an important role in the production of hormones, pigments, fatty acids, and defensive compounds. These P450s are also involved in catabolism of herbicides, insecticides and pollutants (Nielson 2004). Fungal class II P450s carry out synthesis of membrane sterols and mycotoxins, detoxification of phytoalexins and metabolism of lipid carbon sources (Schuler 1996). The class III system is the soluble P450 BM3 (P450 102A1) of *Bacillus megaterium*, a fatty acid ω-hydoxylase which is an interesting natural fusion protein that has a eukaryotic-like CPR and P450 in a single 119-kDa polypeptide. Since being discovered in the 1980s (Narhi and Fulco 1986), P450 BM3 has been the subject of extensive biochemical and structural studies and has served as an important model especially for microsomal P450s. The purified enzyme has very high catalytic efficiency relative to other eukaryotic P450 fatty acid hydroxylases, with turnover numbers of several thousand per minute with various long chain fatty acids (Paine, Scrutton, et al. 2005).

1.4 Catalytic cycle of cytochromes P450

The catalytic cycle of the cytochrome P450s was proposed shortly after their discovery and the currently accepted form is shown in Figure 1.4 (Makris 2005). The

catalytic cycle is multistep and begins in the resting form of the enzyme, a six-coordinate low-spin ferric state (Fe^{III}), with water as the exchangeable distal ligand *trans* to the proximal cysteinate. In the resting state of the enzyme, the reduction potential of the haem iron is relatively low, usually around -400 to -300 mV (Denisov, Makris, et al. 2005, Sono, Roach, et al. 1996). Substrate binding to the enzyme takes place near the distal region of the haem iron (**1**), which causes the distal water molecule to dissociate, resulting in conversion of the haem iron to the pentacoodinate high spin ferric state. The conversion of the ferric iron from low to high spin upon substrate binding results in increase in the redox potential of the haem, thus the high spin form of P450 is much more easily reducible to ferrous form (**2**) by the redox partner protein (Sligar 1976). The stronger the ability of the substrate to perturb the water ligated to the ferric haem, the more pronounced is the resulting shift of the redox potential. In the presence of oxygen or CO the reduction potential of the ferric haem is unchanged as both ligands cannot bind to the ferric state, but are able to bind to ferrous haem (**2**) resulting in the shift of the redox potential towards more positive values than observed under the inert atmosphere.

Figure 1.4 The general catalytic cycle of P450s.

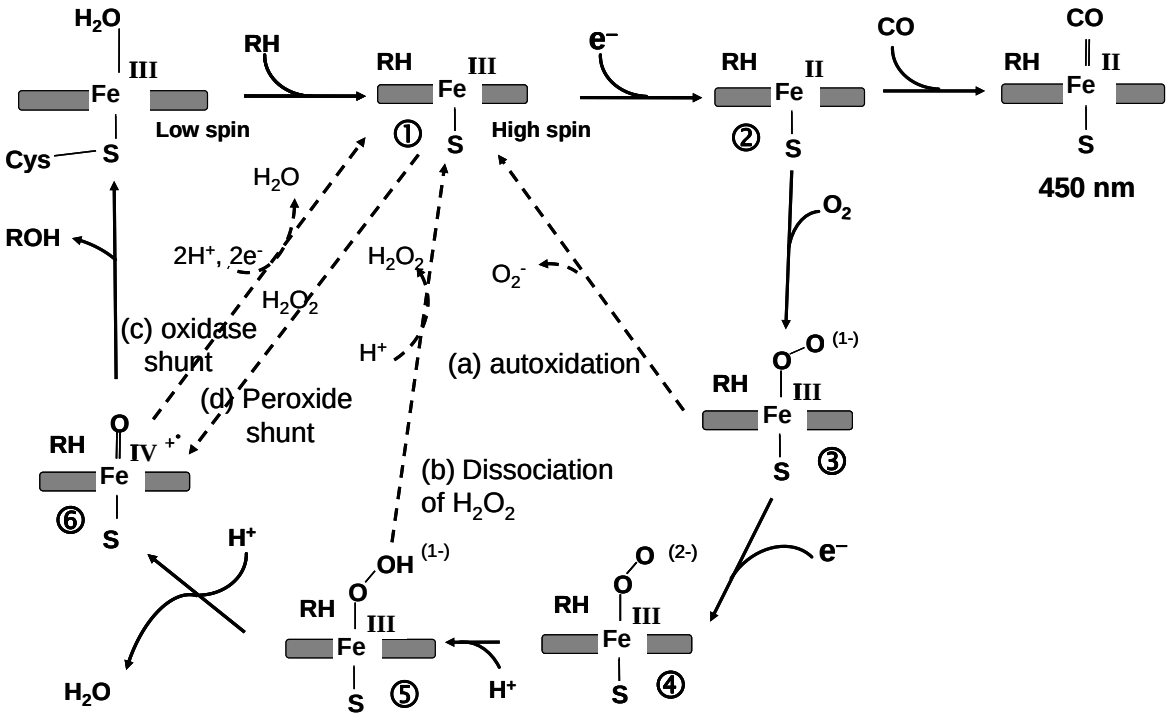

The grey rectangle represents P450 haem; RH represents substrate and ROH as product. The uncoupling side reactions and electron donors for class I and II are shown.

The requirement for substrate to bind before the first electron reduction can proceed is thought to be the physiological gate to the formation of reactive oxygen intermediate (**3**) within P450 otherwise the formation of superoxide and hydrogen peroxide (H_2O_2) from this could lead to enzyme inactivation and be wastage of energy that may be needed for another function. Although substrate binding is observed to be obligatory for first electron reduction in many bacterial P450s, in particular P450 cam and P450 BM3 (Narhi and Fulco 1986, Sligar 1976), this is not the case for all P450 systems. For example, Guengerich and Johnson found microsomal P450 1A2 could be reduced rapidly in the absence of substrate, with rates unaffected by the presence of

substrate (Guengerich and Johnson 1997). These investigators also demonstrated that in the absence of substrate P450 3A4 was reduced at variable rates depending on the system employed, e.g. a purified P450 3A4-CPR fusion protein was reduced at rate 9-12 min^{-1}, in baculovirus microsomes the reduction rate was 2100 min^{-1}, while in a simple reconstituted system (SRS) containing CPR, phospholipids and sodium cholate, the rate was entirely dependent on the presence of b_5, with 700-1200 min^{-1} in its presence and <2 min^{-1} without b_5.

Oxygen binding leads to ferrous dioxygen (Fe^{II}-OO) complex (**4**). Alternatively, CO can bind at this position to form the ferrous carbonmonooxy adduct (Fe^{II}-CO), which has a characteristic absorbance peak near 450 nm. CO binds with high affinity (5.1×10^6 M^{-1} s^{-1}) and prevents the binding and activation of dioxygen, resulting in inhibition of P450 activity (Peterson and Griffin 1972). Crystal structures of ferrous and ferrous-CO P450 cam with its redox partner has been solved and the structures reveal key conformational changes upon binding of the redox partner protein, putidaredoxin (Lee, Wilson, et al. 2010, Nagano, Shimada, et al. 2003, Nagano, Tosha, et al. 2004, Ortiz de Montellano 2010). The oxy-ferrous P450 complex is the last reasonably stable species in the P450 reaction cycle; beyond this stage in the catalytic cycle characterisation of the intermediates is less clear. The structure of the oxy-ferrous P450 intermediate of P450 cam has been solved using cryocrystallography (Schlichting, Berendzen, et al. 2000) and its electronic properties have been characterised using optical absorption, resonance Raman, and Mossbauer spectroscopies (Makris 2005). Recently Denisov et al. have carried out a stopped-flow kinetics on the formation and decay of this intermediate in P450 3A4 as function of temperature in the substrate free and substrate bound form (Denisov, Grinkova, et al. 2006). The oxy-ferrous complex of P450 3A4 was found to decompose extremely rapidly in the absence of substrate.

Saturation with various substrates was found to reduce the rate of autooxidation by almost two orders of magnitude, thus inhibiting the unproductive decomposition of oxy-ferrous complex and production of ROS. The results of the study indicated that the oxy-ferrous complex may be an important route for uncoupling in human liver P450s which is stabilized by the effect of the substrate.

The addition of a second electron at **4,** a reaction step believed to be the rate-limiting in many P450 catalysed reactions, generates a peroxo-ferric species (Guengerich 2002). In microsomal P450s, this electron is donated directly from CPR or in some cases delivered from b_5 (Noshiro, Ullrich, et al. 1981, Pompon and Coon 1984, Yamazaki, Nakano, et al. 1996). Initial protonation of the distal oxygen in the peroxo-ferric complex yields ferric-hydroperoxo intermediate (**5**). Second protonation on the proximal oxygen leads to H_2O_2 formation and hence uncoupling. The subsequent heterolytic cleavage of the O-O bond generates water and high valent ferryl-oxo (π) porphyrin radical or 'compound I' like species (Fe(IV)=O) **(6**), which actually carries out the monooxygenation reaction. This highly active ferryl-oxo intermediate or its electronic equivalent **(6**) has never been directly observed due to being very unstable. Whereas in peroxidases, containing also single haem, this species have been observed (Hosten, Sullivan, et al. 1994). The catalytic cycle is completed by insertion of oxygen atom from a ferryl-oxo intermediate **(6**) to the bound substrate, which is suggested to occur by radical rebound mechanism, shown by Figure 1.5 (He and de Montellano 2004).

The mechanism involves initial hydrogen abstraction from the bound substrate by the ferryl species (Fe(V)=O), formed by P450 catalysed activation of molecular oxygen) to give a carbon radical intermediate ($R^{\cdot}$), the recombination of the resulting

transient hydroxyl (Fe(IV)-OH) and carbon radicals generates the product which subsequently dissociates to leave the enzyme to its initial ferric state (Fe^{III}).

The P450 reaction is essentially 100% coupled (electron transfer to product formation) for substrate specific P450s such as P450 cam, but for less specific P450s, such as P450 3A4, uncoupling can take place at several branch points where multiple side reactions are possible and are known to occur *in vivo*. Uncoupling occurs when (**a**) the oxy-ferrous complex reverts to the ferric state by dissociation of superoxide, (**b**) a molecule of H_2O_2 is formed as a result of protonation on the 'proximal' oxygen atom or (**c**) species **6** is reduced to water instead of oxygenation of the substrate, which takes place by 4-electron reduction of dioxygen with net formation of 2 molecules of water.

Figure 1.5 Schematic representation of the radical rebound mechanism of P450 catalysed hydroxylations.

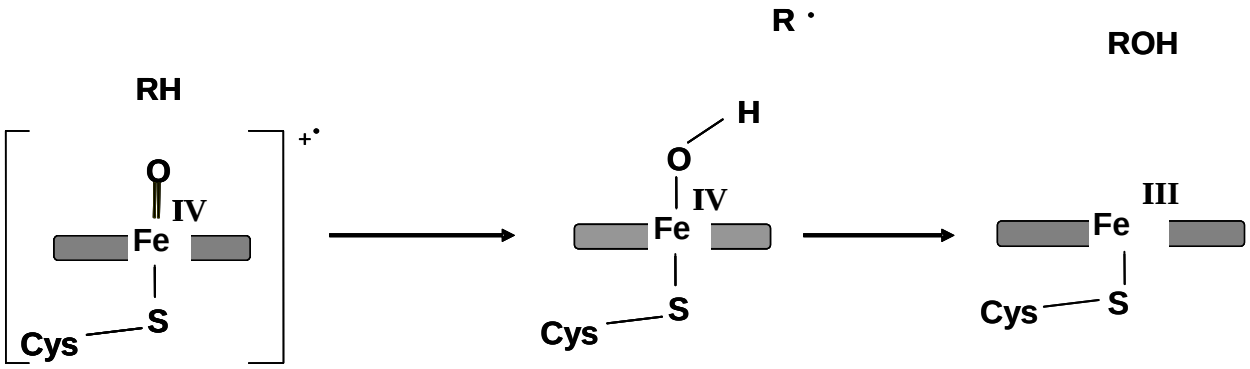

The grey rectangle represents P450 haem; RH the substrate and ROH the product (He and de Montellano 2004).

1.5 Cytochrome P450 reductase

Cytochrome P450 reductase (CPR) is a 78-kDa flavoprotein bound to the endoplasmic reticulum membrane of eukaryotic cells and is an essential component of

the cytochrome P450 electron transport system. The enzyme contains two tightly bound cofactors, one molecule of FAD and one of FMN, which are used to channel electrons from NADPH to haem centre of P450s (Iyanagi and Mason 1973, Yasukochi and Masters 1976). CPR can also donate electrons to other terminal electron acceptors such as haem oxygenases (Schacter, Nelson, et al. 1972) and b_5 (Enoch and Strittmatter 1979). *In vitro,* it is capable of reducing non-physiological electron acceptor cytochrome *c* (Yasukochi and Masters 1976) and anticancer drugs, such as mitomycin *c* (Bligh, Bartoszek, et al. 1990), adriamycin (Bartoszek and Wolf 1992) and the benzotriazine SR4233 (Walton, Wolf, et al. 1992), These drugs are also normally reduced by CPR *in vivo*.

Most organisms contain a single CPR gene, except plants that have two or more. CPR is one of a small family of diflavin reductases which contain both FAD and FMN cofactors. Other mammalian members identified are methionine synthase reductase (Leclerc, Wilson, et al. 1998), isoforms of nitric oxide synthase (Griffith and Stuehr 1995), and NR1 protein (Paine, Garner, et al. 2000). The family also includes bacterial members, such as P450 BM3 and α subunit of bacterial sulfite reductase. Diflavin reductases share a significant sequence homology with two classes of flavoproteins, prokaryotic FMN-containing flavodoxin and FAD-containing ferredoxin reductase. The sequence and structure of CPR suggests that protein has evolved as result of fusion of two ancestral genes encoding proteins related to ferredoxin reductase and flavodoxin (Wang, Roberts, et al. 1997). CPR knockout mice are found to be embroyonically lethal and deletion of the CPR gene in microsomes causes signficant loss of P450 activity, which cannot be compensated by an alternative redox partners such as b_5 (Henderson, Otto, et al. 2003, Shen, O'Leary, et al. 2002).

1.5.1 Structure of cytochrome P450 reductase

Kim and co-workers (Wang, Roberts, et al. 1997) reported the first X-ray crystal structure of an N-terminally truncated CPR from rat liver, Figure 1.6, and this structure has served as a model for solving structures of related diflavin enzymes.

Figure 1.6 Ribbon diagram of the rat liver CPR.

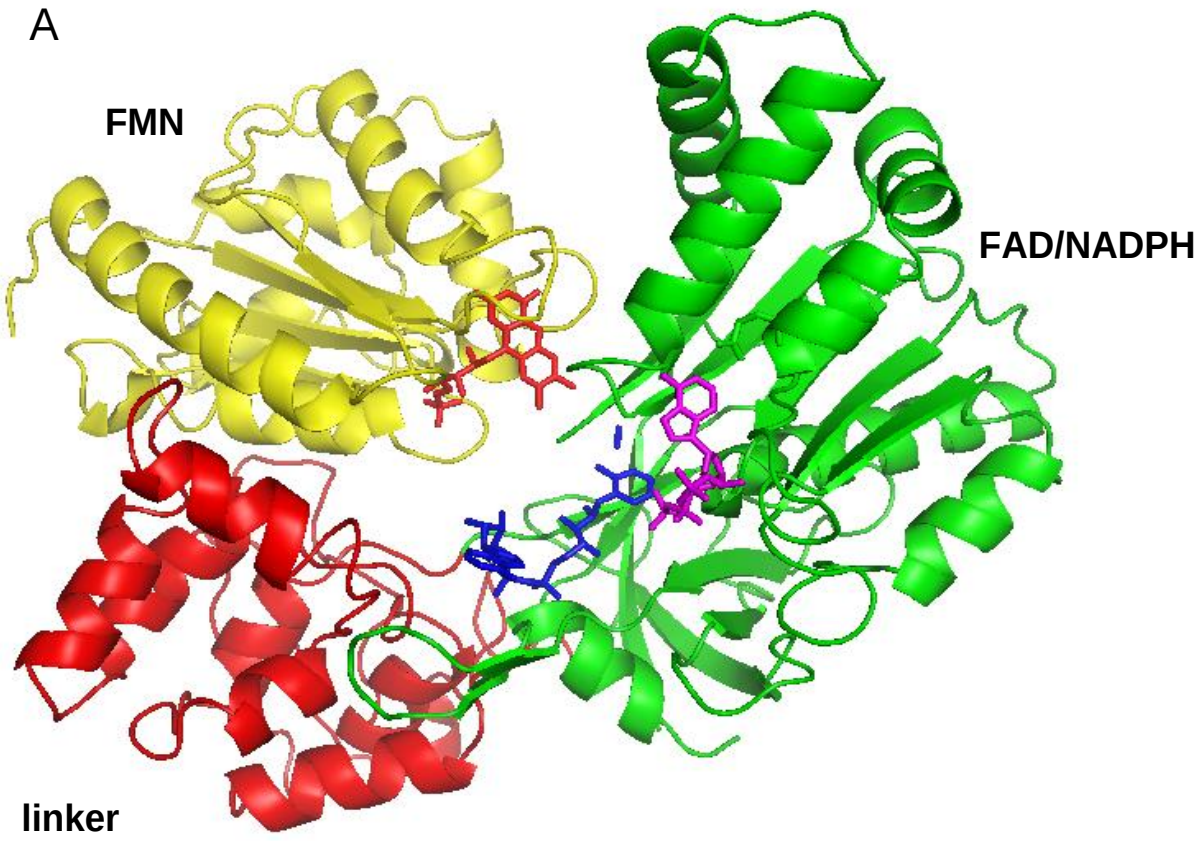

B

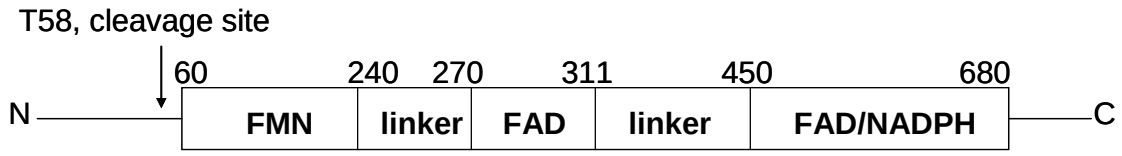

(A) The FMN-binding domain is shown in yellow, linker/connecting domain in red and the FAD/NADPH binding domain is represented in green. Ball-and-stick cofactors are FMN in red, FAD, in blue, and the $NADP^+$, in magenta (PDB file code: 1AMO) (B) Organisation of CPR domains. The numbers on the top show amino acids positions for the corresponding domains in the CPR structure. The linker domain and FAD are intertwined in the linear sequence, but both of the make distinictive structural domains. The cleavage site Threonine (58) in the hydrophobic anchor is also shown.

CPR can be isolated from the endoplasmic membrane by limited proteolysis with steapsin or trypsin. This releases a 72-kDa C-terminal hydrophilic soluble enzyme, which is unable to reduce P450s, but is capable of oxidising NADPH and passing electrons to non-physiological electron acceptors such as cytochrome *c*. Figure 1.7 shows the C-terminal catalytic portion of the enzyme (72-kDa), which binds the cofactors FAD, FMN and NADPH. The 6-kDa N-terminal hydrophobic sequence, which anchors the protein to the membrane, thus ensuring proper spatial interaction is achieved between reductase and P450, is missing from the construct used for the crystal structure determination.

This catalytic fragment of the enzyme consists of three structural domains (Figure 1.6): the FMN-binding domain, the FAD/NADPH-binding domain and the linker domain. The FMN binding domain is structurally homologous to the bacterial flavodoxins, and interacts with P450 for electron transfer (Watenpaugh, Sieker, et al.

1973). In addition to the crystal structure of rat CPR, the structure of the isolated FMN binding domain has been determined by X-ray crystallography and detailed NMR structural studies of the FMN domain have also been carried out (Barsukov, Modi, et al. 1997, Zhao, Smith, et al. 1996).The FAD/NADPH-binding domain has a high sequence similarity to the ferrodoxin reductase (FNR) family of enzymes (Karplus, Daniels, et al. 1991). The CPR crystal structure reveals that tightly bound cofactors FAD and FMN are very close in space with edge-to-edge distance of only 4Å between the two isoalloxazine rings of the flavins, allowing rapid electron transfer between the flavin centres. However, FMN domain in this conformation is too far away from the haem centre and thus it would need to pull out for electron delivery to P450 haem. The linker domain may be involved in positioning the FMN and FAD/NADPH-binding domains with respect to one another.

1.5.2 The electron transfer mechanism in CPR

The kinetic studies in soluble human CPR (lacking the N-terminal hydrophobic membrane anchor) and its component domains have been carried out extensively by steady-state assays with cytochrome *c* and by pre-steady state analysis by stopped-flow spectroscopy and potentiometric methods (Gutierrez, Lian, et al. 2001, Gutierrez, Munro, et al. 2003, Gutierrez, Paine, et al. 2002, Murataliev, Feyereisen, et al. 2004, Sem and Kasper 1994). Early studies have estabilished that physiological electron transfer pathway in mammalian P450 monooxygenase system is from NADPH to FAD to FMN and to haem centre of P450 (Iyanagi and Mason 1973). The reduction potential of the flavins of CPR family have been deterimined and are believed to govern the electron flow in CPR (Munro, Noble, et al. 2001, Vermilion and Coon 1978). The redox states of flavins is shown in Figure 1.7.

Figure 1.7 Structure of flavin redox states.

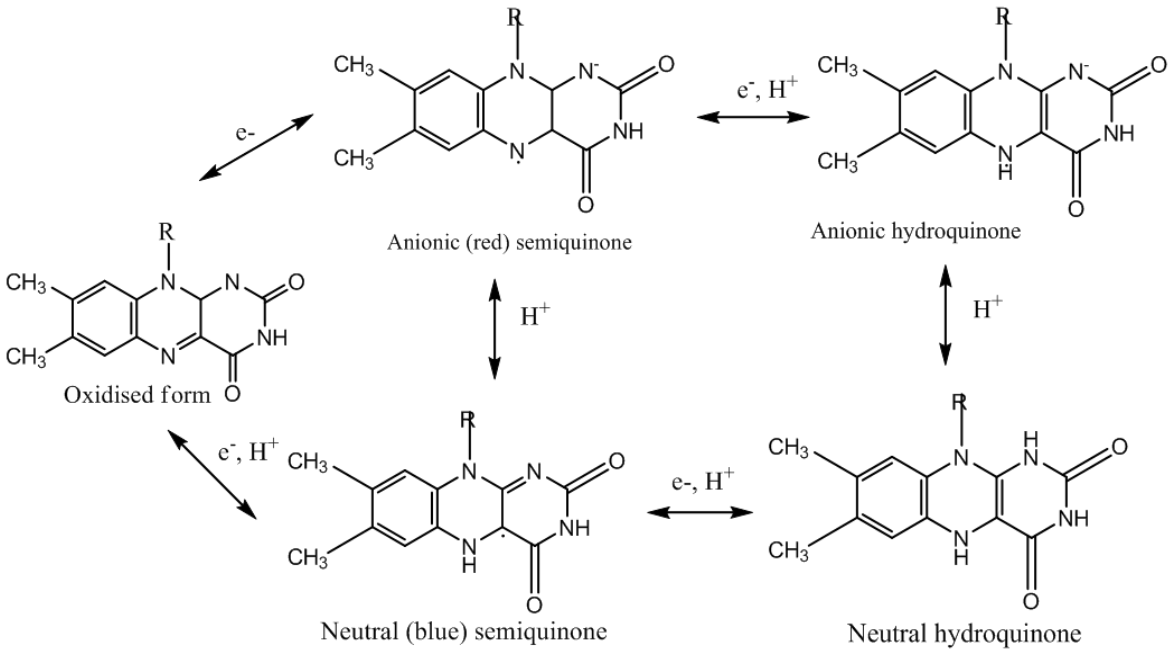

The reduction of the oxidised CPR begins with formation of FAD hydroquinone ($NADP^+$-$FADH_2$-FMN) complex via hydride transfer from enzyme bound NADPH. This is followed by transfer of electrons one by one from FAD hydroquinone ($FADH_2$) to the FMN, yielding the FMN hydroquinone species ($FMNH_2$), which finally passes both electrons sequentially to the haem centre of P450s at two different points in the complex reaction cycle (Figure 1.4). During P450 catalysis, flavins usually cycle between reduction states of 1-3-2-1 or 2-4-3-2 where the numbers refer to the total number of electrons occupied by the flavins (Murataliev, Feyereisen, et al. 2004, Vermilion, Ballou, et al. 1981). Mammalian CPRs can accept up to four electrons, but this species may not be physiologically relevant as it requires the enzyme *in vitro* up to 8 hour of incubation under anaerobic conditions in the presence of excess NADPH. Instead, the enzyme forms an air stable semiquinone species (one electron reduced, FMN_{sq} or $FMNH^{\cdot}$) on the FMN. The interflavin electron transfer of NADPH reduced

human CPR measured by temperature jump relaxation experiments have revealed observed rate of ~55 s^{-1} (Gutierrez, Paine, et al. 2002). Whereas, laser flash photolysis has yielded observed rate of 36 s^{-1} (Bhattacharyya, Hurley, et al. 1994). These observed rates are very slow in comparison to the predicted intrinsic rate of about 10^{10} s^{-1} based on the separation distance between two cofactors in the CPR crystal structure, indicating that electron transfer between the two cofactors may be conformationally gated. Further temperature jump measurements carried out in the presence of glycerol in the sample drastically decreased observed rates of interdomain electron transfer and suggested that reaction is limited by conformational changes (Gutierrez, Paine, et al. 2002). Electron transfer rates for CPR reduced with NADH were found to be 3-fold slower than with NADPH and this difference in observed rates suggested that the coenzyme binding has a significant role in modulating internal electron transfer in CPR. This was later confirmed when electron transfer rates for CPR reduced with dithionite were shown to be ~3-fold slower than for the enzyme reduced by NADPH. Furthermore, addition of 2',5'-ADP to dithionite reduced CPR increased the rate of interdomain electron transfer by 3 fold (Gutierrez, Munro, et al. 2003). It was proposed that the binding of 2'-phosphate group of NADPH in human CPR causes a conformational change involving movement of domains, the rate of which controls the interflavin electron transfer (Gutierrez, Paine, et al. 2002).

1.6 Drug metabolism in man

P450s are major enzymes involved in human drug metabolism and of the 57 human P450s, about one quarter are involved in metabolism of therapeutic drugs (Guengerich 2004). Most drugs are lipophilic and require metabolic processing before they can be eliminated from the body. This occurs in two stages, phase I and II. The first stage involves introduction of small polar groups onto the parent drug which increases

water solubility, so that it can either be excreted directly or conjugated in phase II. The majority of phase I reactions are mediated by P450s, but other enzymes such as reductases and hydrolases also participate as well. The phase II metabolising enzymes which include glucuronsyl transferases, glutathione transferases, N-acetyl transferases and sulphotransferases form conjugates by adding very polar groups such as glucoronide, glutathione, sulphate and acetyl to the modified drug from phase I, thus making it more hydrophilic and easier to excrete from the body.

1.6.1 Drug metabolising P450s

In humans, P450s are distributed in various tissues including heart, lungs, brain and small intestine. P450s of liver play significant role in drug metabolism and mainly belong to families 1-3 (Guengerich 2004). P450s of families 1-3 are responsible for ~80% of all first pass metabolism of therapeutic drugs, as well as other xenobiotic chemicals. The major P450s involved in drug oxidation are summarised below in Table 1.1; P450 3A4, 2D6 and 2C9 can oxidise about 75% of all drugs (Smith and Jones 1992), while all six P450s together can metabolise 90-95% of all drugs.

Table 1.1 Major tissue sites and typical substrates of P450s that are involved in drug metabolism.

P450	Tissue sites	Typical substrates	% of contribution to metabolism of all drugs
2C9	Liver	Anionic and lipophilic e.g.Warfarin, Phenytoin	10
1A2	Liver	Aromatic amines, Caffeine, Tacrine,	2
2D6	Heart, liver, brain	Debrisoquine, codeine	30
2E1	Lymphocytes, lungs, liver	Chlorzoxazone, ethanol, Acetaminophen	4
2C19	Heart, liver	Mephenytoin, diazepam	6
3A4	Liver, small intestine, lung, brain, kidney	Variable structures and usually lipophilic, e.g. Erythromycin, midazolam, testosterone, cyclosporin	>50

The estimated contributions of each human P450 towards metabolism of all drugs is shown, adapted from: (Anzenbacher and Anzenbacherova 2001, Guengerich 2004).

1.6.2 What factors affect P450 function?

1.6.2.1 Genetic polymorphism

The metabolic capacity of each P450 is not equal in all members of a population and can vary between individuals. The main cause of this variability is the genetic polymorphism of these enzymes, which can cause different individuals to express different amounts of P450 proteins. The polymorphism produces three distinct phenotypes, described as poor, extensive, and ultra rapid metabolisers:

1. **Poor metabolisers-** individuals who posses a defective P450 allele. The metabolism and elimination of drugs that are substrates for the deficient enzymes are decreased and the likelihood of drug toxicity is increased. By contrast, some compounds are prescribed as pro-drugs (an inactive molecule which is converted to the active substance in the body) and since therapeutic effect of such a drug depends on its conversion to an active metabolite, in poor metabolisers the drug may be less effective.

2. **Extensive metabolisers-** individuals having normal metabolic activity. They show the predicted responses to therapeutic doses of medication.

3. **Ultra-rapid metabolisers-** individuals with higher than normal metabolic activity due to having more than the normal complement of functional genes or P450 allele.

Genetic polymorphisms have been detected in many drug metabolising P450s, but P450 2C9, P450 2C19 and P450 2D6 are found to be highly polymorphic (Ingelman-Sundberg 2002, Ingelman-Sundberg 2004). P450 2D6 is the most extensively studied

polymorphically expressed drug metabolising enzyme and produces all three phenotypes described. The poor metabolisers are as a result of combinations of any of number of defective alleles, the most common being P450 2D6*4, a splicing defect causing expression of inactive protein. Other less frequent detrimental alleles are the P450 2D6*3 with a frame shift mutation and P450 2D6*5 a gene deletion with the enzyme not being expressed. The ultra rapid metabolisers arise mainly due to gene duplication of allele P450 2D6*2. Population studies of drug metabolism have demonstrated significant inter-population differences in the polymorphic distribution of P450 2D6 activity. Approximately 5-10% Caucasians have deficient function of this enzyme (poor metabolisers), whereas in oriental populations the deficiency is over 50% (Anzenbacher and Anzenbacherova 2001, Ingelman-Sundberg 2004).

1.6.2.2 Induction

Administration of a drug or other xenobiotic may lead to an increase in catalytic activity of the drug metabolising P450 and if stimulation in the activity is due to an increased expression of the enzyme then the process is known as induction. Expression of P450s is tightly regulated, primarily at the transcription level (Schuetz 2001). Because P450 3A family enzymes play extensive role in metabolism of large array of drugs, induction can effect drug-drug interactions. P450 3A members are highly induced by a number of steroids including high doses of glucocorticoids (Heuman, Gallagher, et al. 1982) and by numerous drugs, such as anti-tuberculosis medication rifampicin, the anticonvulsant phenobarbital and some azole antimycotics e.g. clotrimazole (Kocarek, Schuetz, et al. 1995). Therefore, it would be advantageous to develop new drug candidates that are not potent drug inducers to avoid the potential of P450 induction mediated drug-drug interactions in humans.

1.6.2.3 Inhibition

Various drugs and chemicals inhibit P450 activities *in vitro* due to the broad substrate specificity of these enzymes and in clinical practice drug-drug interactions arising from this inhibitory process are quite common (Thummel and Wilkinson 1998). P450s are vulnerable to inhibition at several stages in the catalytic cycle (see Figure 1.3), these include during substrate binding, binding of dioxygen and the catalytic step in which the substrate is oxidised (Correia and Ortiz de Montellano 2004). P450 inhibition can be reversible or irreversible. Reversible inhibition is the most common mechanism and occurs as a result of direct competition between inhibitor and the substrate for occupation of the active site. Competition can be either for the haem iron of P450 or for other regions of the active site. For example ketoconazole is an imidazole-containing compound and a strong P450 3A4 inhibitor, which is able to coordinate directly to the haem moiety and thus as well as blocking the substrate access it prevents dioxygen binding (McGinnity and Riley 2001).

In contrast to the reversible inhibition in which two agents compete for the active sites on the enzyme, irreversible inhibition is caused by reactive metabolites which react covalently with the enzyme or the haem of P450 generated from P450-catalyzed reactions, e.g. furanocoumarins in grapefruit juice are able to inhibit P450 3A4 by this type of mechanism (Guo, Taniguchi, et al. 2000).

1.7 Human cytochrome P450 3A4

Human cytochrome P450 3A4 is one of the four genes belonging to the P450 3A gene family, others identified are P450 3A5, 3A7 and 3A43 (Guengerich 2004). Together, the protein products of P450 3A genes account for the largest portion of P450s in the body. P450 3A4 has a wide substrate spectrum and is involved in the metabolism of 50-60% of all currently used drugs (Guengerich 1999). Human P450

3A4 is the most abundant isoform of P450 3A subfamily and is expressed substantially in liver where on average it constitutes ~30% of the total P450 species, but this can increase up to 60% upon induction by steroids and barbiturates (Thummel and Wilkinson 1998). In small intestinal epithelium, the protein is also expressed in high amounts, about 50% of hepatic levels and 70% of the total P450 protein in this tissue. Extrahepatic tissues such as lung, stomach, colon and brain also contain the enzyme. P450 3A4 has not been found to be expressed in thymus, testis, and prostate or in kidney, but other members of the P450 3A subfamily are. P450 3A4 expression in the fetus is found to be very low and after birth expression levels increase to 50% of that of adult between the age of 6 to 12 months (Guengerich 2004).

1.7.1 Structure of P450 3A4

Due to mammalian P450s being intrinsic membrane proteins and having an inherent tendency to aggregate in solution, it was not until relatively recently that the first mammalian P450 structure, that of rabbit P450 2C5, was determined (Williams, Cosme, et al. 2000). Since 2000, crystal structures of mammalian P450 2C8, 2A6, 2C9, 2B4, 2D6 and 3A4, have also been solved, either ligand free or bound (Otyepka, Skopalik, et al. 2007). Prior to publication of the rabbit P450 2C5 structure, the mammalian P450 structure function studies were mainly based on known structures of bacterial P450s, especially P450 cam (Lee, Wilson, et al. 2010, Poulos, Finzel, et al. 1985) and P450 BM3 (Ravichandran, Boddupalli, et al. 1993).

Figure 1.8 Ribbon structure of the ligand-free P450 3A4.

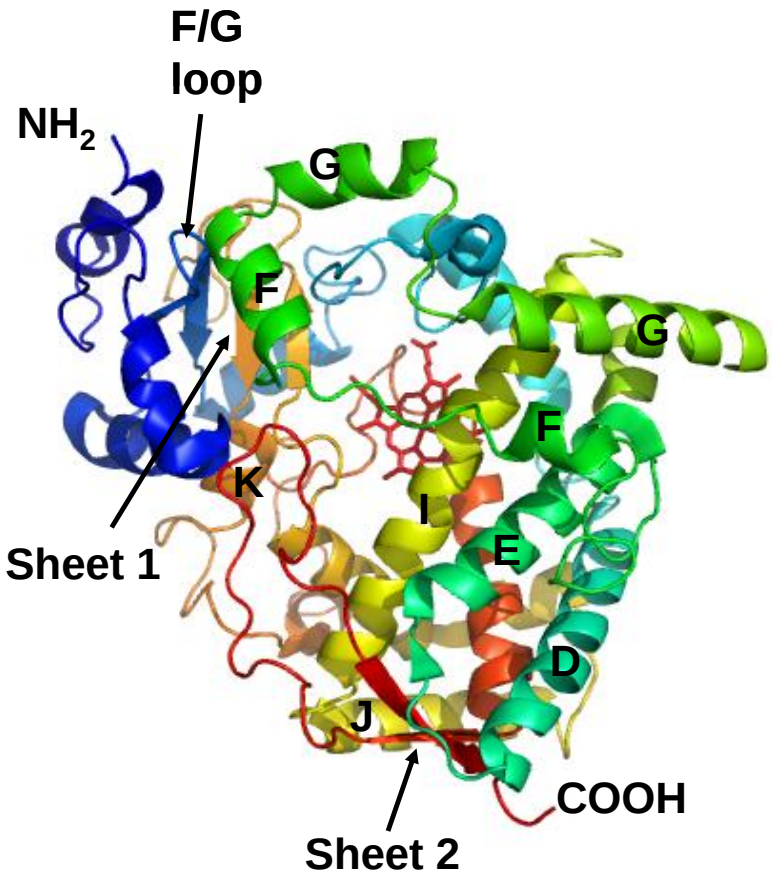

The haem is shown in red sticks and the helices and β sheets are labeled. Diagram was obtained from (Williams, Cosme, et al. 2004) (PDB file code: 1WOE).

The structure of human microsomal P450 3A4, which was determined independently by Williams et al, (Williams, Cosme, et al. 2004) and Yano et al (Yano, Wester, et al. 2004) in 2004 is shown in Figure 1.8. P450 3A4, like all membrane bound P450s presented a unique challenge for crystallisation in that it required to be soluble and monodisperse. This involved truncation of the hydrophobic N-terminal transmembrane leader sequence (amino acid residues 3-24) that helps to anchor the protein to the microsomal membrane. The structure of P450 3A4 shows the common P450 fold, which is a unique feature of the P450 superfamily. The structure is roughly

the shape of a trigonal prism consisting largely of α-helices but with a small β-sheet domain. The helices E, I, J, K and L as well as β sheet 1 are highly conserved among all P450s and form the structural core of the protein. This portion of the structure maintains a conserved binding site for the haem prosthetic group the iron of which is ligated by an absolutely conserved cysteine (Scott and Halpert 2005).

The haem group is confined between helices I and L and forms the base of the active site cavity, which is buried in the core of the protein. The outer surface of the active site cavity is formed by the regions of β sheet 1 and 4, helices F-G, and the loop between helices B and C. The structure bears most resemblance to the structures of mammalian family 2 P450s, which exhibit less than 40% sequence identity with P450 3A4 (Otyepka, Skopalik, et al. 2007). Compared to the family 2 P450s, the F and G helices are notably shorter in P450 3A4, and do not pass over the substrate binding cavity. The F and G helices and F/G loop together with the B/C-loop are thought to control the ligand access to the P450 active site by an open/close motion and also form the membrane interaction domain (Poulos and Johnson 2005, Williams, Cosme, et al. 2000). This segment of the structure is next to the N-terminus of the protein and the amino acids in this region are hydrophobic which makes it more favorable for lipophilic substrates to access this channel for the active site. Epitope mapping by antibodies of the related family 2 P450s have shown that this domain structure is possibly buried in the membrane (Uvarov, Sotnichenko, et al. 1994).

The size of the active site is important as P450 3A4 is known to oxidise several large substrates such as erythromycin (734 Da), and cyclosporine (1203 Da) (Rendic 2002). The two groups report very different volumes of the active site cavity, 1386 Å (Yano, Wester, et al. 2004) and 520 Å (Williams, Cosme, et al. 2004). However, this discrepancy appears to be due to differences in the algorithms used to calculate active

site volumes therefore such numbers cannot be directly compared. Docking studies carried out by Yano and colleagues (Yano, Wester, et al. 2004) have established that the volume of the P450 3A4 active site cavity can accommodate two or more smaller molecules such as testosterone or α-napthoflavone or alternatively can bind a molecule at least large as erythromycin. This is consistent with number of kinetics studies that have reported that P450 3A4 exhibits non-Michaelis-Menten kinetics upon binding of various ligands and displays homo- and heterotropic cooperativity (Atkins 2005, Davydov, Fernando, et al. 2005, Harlow and Halpert 1998, Kapelyukh, Paine, et al. 2008).

In addition to unliganded P450 3A4 structures, structures of several P450 3A4 ligand complexes have also been solved (Ekroos and Sjogren 2006, Williams, Cosme, et al. 2004). The observation that the volume of active site is smaller than expected in the ligand free P450 3A4 structure in comparison to structures from family 2 P450s, led Williams et al. to deterimine two crystal structures of P450 3A4 with progesterone, a substrate and metyrapone, an inhibitor (Williams, Cosme, et al. 2004). However, both structures of P450 complexes achieved very little conformational change in the protein. Whearas, Ekroos and Sjogren (Ekroos and Sjogren 2006) solved crystal structure of P450 complex with erythromycin or ketoconazole and found large conformational changes predominantly in the F and G helices and the intervening loops. The volume of active site was twice that seen in the ligand free structure, suggesting that the protein is highly flexible and can accommodate multiple ligands.

1.7.2 P450 3A4 catalytic selectivity and cooperativity

P450 3A4 is found to be the most catalytically active isoform from P450 3A subfamily enzymes when tested towards all substrates under identical conditions, suggesting that the enzyme is not specific and is capable of hydroxylating a wide array

of unrelated compounds (Williams, Ring, et al. 2002). The enzyme is known to metabolise over 50% of all drugs in current use; for an extensive list refer to Guengerich and Rendic (Guengerich 1999, Rendic 2002). The list of substrates includes not only therapeutic drugs but also pesticides, steroids, non-ionic detergents, carcinogens and other organic chemicals. As a result, P450 3A4 has the broadest catalytic selectivity of any P450 (Guengerich 1999). The enzyme is capable of accommodating smaller molecules such as acetaminophen (151 Da) as well as large molecules like cyclosporin A (1201 Da) in its large active site.

Some, but not all P450 3A4 reactions appear to show cooperativity and the enzyme exhibits both homotropic and heterotropic effects. Positive homotropic cooperativity is observed in either binding or steady state reaction kinetics when a single compound is added to an enzyme typically manifested in a sigmoidal velocity versus substrate concentration curve. Homotropic cooperativity has been shown with several substrates and drugs including testosterone (Harlow and Halpert 1998, Ueng, Kuwabara, et al. 1997), progesterone (Schwab, Raucy, et al. 1988), estradiol (Ueng, Kuwabara, et al. 1997), α-naphthoflavone (Ueng, Kuwabara, et al. 1997), amitriptyline (Schmider, Greenblatt, et al. 1995) and aflatoxin B_1 (Ueng, Kuwabara, et al. 1997). By contrast, positive heterotropic cooperativity is a stimulatory effect on the binding and/or metabolism of one compound produced by another. An example of positive heterotropic cooperativity is the stimulation by the flavonoid α-naphthoflavone of testosterone and progesterone hydroxylation (Harlow and Halpert 1997, Schwab, Raucy, et al. 1988).

Not much is known about the exact mechanism by which cooperativity occurs, but several models have been proposed to explain such behavior. One explanation put forward is related to the ability of the large active site to accommodate more than one substrate molecule simultaneously. Shou and coworkers were among the first to provide

evidence for this theory (Shou, Grogan, et al. 1994). In their study of interactions between α-naphthoflavone and phenanthrene, they observed that P450 3A4 catalyzed oxidation of phenanthrene was stimulated by the presence of α-naphthoflavone without changing the K_m, while phenanthrene partially inhibited α-naphthoflavone metabolism without increasing the K_m. Similarly, in the presence of quinidine, the rates of 5-hydroxylation of declofenac and 10-hydroxylation of R-warfarin were observed to be elevated by several fold (Ngui, Chen, et al. 2001, Ngui, Tang, et al. 2000). This led the authors to speculate that both substrate and the effector (also a substrate in these cases) were simultaneously present in the active site of P450 3A4 as both could access the activated oxy-complex. As a result, investigators proposed a kinetic model involving two binding sites. Further evidence supporting this hypothesis has come from site-directed mutagenesis studies. Harlow and Halpert, in an attempt to identify residues that form or influence the enzyme active site or effector binding site substituted amino acids Leu-211 and Asp-214 of P450 3A4 with larger residues, Phe and Glu respectively. As a consequence of this double mutation, the rate of testosterone metabolism was increased, its kinetics were altered from a sigmoidal to a hyperbolic pattern and the stimulatory effects of α-naphthoflavone were eliminated (Harlow and Halpert 1998). From these results it was concluded that mutations had blocked the separate effector binding site, thus leading to a loss of both homotropic and heterotropic cooperativity during testosterone metabolism. Further work involving mutual effects of different substrates and effectors of P450 3A4 have compelled some authors to suggest that possibly three or more ligand binding sites exist in this enzyme (Galetin, Clarke, et al. 2003, He, Roussel, et al. 2003, Hosea, Miller, et al. 2000). This is supprted by recent work of Kapelyukh et al (Kapelyukh, Paine, et al. 2008) that involved computational docking studies in conjunction with steady-state kinetics on the effect of inhibitors on the Hill

coefficient to provide estimation of number of substrate that can bind to P450 3A4. The study reported that up to 4 or possibly 5 molecules of substrate 7-benzylxyquinoline (7-BQ) can bind simultaneously to P450 3A4.

In addition to the multi-substrate binding model, several groups have suggested that the existence of multiple kinetically distinguishable conformations of P450 3A4, in the presence or absence of various ligands, may contribute to cooperative behaviour. Koley et al used the kinetics of CO re-binding to P450 3A4 after dissociation by flash photolysis to demonstrate that P450 3A4 in the microsomal membrane consists of multiple conformers with different accessibility of the haem for CO and different substrate specificity (Koley, Buters, et al. 1995, Koley, Robinson, et al. 1996). More recently, high pressure spectroscopic studies with P450 3A4 in solution and in membrane have revealed the presence of two conformers with different positions of spin equilibrium and different barotropic properties (Davydov, Halpert, et al. 2003). Evidence has also been presented that P450 conformations change during the course of the catalytic cycle (Schlichting, Berendzen, et al. 2000); for example, it has been found that distinct forms of P450 3A4 (e.g. ferric or ferrous) can differ in their interaction with ligand (Hosea, Miller, et al. 2000).

1.7.3 Measurement of P450 3A4 catalytic activity

P450 catalytic activities can be reconstituted to a greater or lesser extent *in vitro* by mixing purified recombinant P450 and CPR with phospholipids (Lu, Junk, et al. 1969). Purified recombinant P450 3A4 along with other P450 3A subfamily enzymes are found to be particularly sensitive to their environment *in vitro* and effective reconstitution has proved difficult (Guengerich 1999). For example, several investigators have determined that for optimal P450 3A4 catalytic activity a complex phospholipid mixture, particularly one containing negatively charged phospholipids,

(e.g. phosphatidylserine or phosphatidic acid) is required (Imaoka, Imai, et al. 1992, Ingelman-Sundberg, Hagbjork, et al. 1996, Kim, Ahn, et al. 2003). Yamazaki et al. observed that presence of various divalent metal ions (especially Mg^{2+}) can help to stimulate catalysis in P450 3A4 systems (Yamazaki, Ueng, et al. 1995). Further, glutathione and ionic detergent such as sodium cholate have been reported to enhance catalytic rate of P450 3A4 reactions (Gillam, Baba, et al. 1993, Imaoka, Imai, et al. 1992). Specifically, cytochrome b_5 has been found to modulate P450 3A4 activities considerably, for example, Yamazaki et al determined that in their reconstituted system in the presence of either nifedipine or testosterone, the input of the first electron from NADPH to the monooxygenase (ferric to ferrous state) and product formation were negligible in the absence of b_5 (Yamazaki, Ueng, et al. 1995). Subsequent studies by Yamazaki et al. indicated that apo-b_5 (lacking haem cofactor) was as effective as the holo-enzyme in supporting reduction of P450 3A4 and product formation, indicating that the role of the b_5 did not require it to undergo redox changes or to transfer the second electron to P450 3A4 as was originally proposed, but instead may have an allosteric influence on P450 3A4 (Yamazaki, Nakano, et al. 1996, Yamazaki, Shimada, et al. 2001).

1.8 Mechanisms of P450 interactions in microsomal membrane

P450 and CPR seem to be randomly distributed in the microsomal membrane and NADPH supported catalysis of P450 monooxygenase reactions requires P450 and CPR to form a 1:1 functional complex (Miwa and Lu 1984, Miwa, West, et al. 1979). However, P450s are present in the membrane in large excess over CPR, ranging from molar ratio of 10:1 to 25:1 depending on treatment with inducers (Estabrook, Franklin, et al. 1971, Peterson, Ebel, et al. 1976). This stoichiometry and the mutual arrangement of the two enzymes in the membrane clearly have an important implication for electron

transfer from CPR to P450. There are essentially two possible mechanisms for electron transfer in the microsomal membranes: One is the transfer between enzymes forming functional 'clusters' where a stable complex might be formed from one CPR and one or more P450 molecules. The other is by way of random collisions between CPR and P450 diffusing laterally in the microsomal membrane. Evidence supporting both of these models has been presented, but consensus has not yet been reached concerning the mechanism by which these proteins interact functionally in the membrane.

Franklin and Estabrook, based on the kinetics and the extent of P450 reduction in rat liver microsomes proposed that a stable 'cluster' of multiple P450 molecules surround a single CPR molecule in microsomal membrane and electron transfer is unable to take place between different complexes or clusters (Franklin and Estabrook 1971). Later, a similar conclusion was drawn by Peterson et al. from their study on the temperature dependence of the biphasic reduction kinetics of P450 by NADPH in microsomes (Peterson, Ebel, et al. 1976) and by Steir and Sackman from measurements of reduction kinetics of a membrane-soluble, spin labeled fatty acid radical (Stier and Sackmann 1973). On the other hand, analysis of the kinetics of P450 reduction in a reconstituted system, led Taniguchi et al. to suggest that interaction between two proteins is affected by their random collisions caused by their lateral mobility in the plane of membrane (Taniguchi, Imai, et al. 1979). This view was further supported by the work of Yang (Yang 1975), Duppel and Ullrich (Duppel and Ullrich 1976) and Ingelman-sundberg and Johansson (Ingelman-Sundberg and Johansson 1980).

1.9 Characteristics of the cytochrome P450 reduction

The first electron transfer (species 1 to 2, Figure 1.3) can be readily isolated by carrying out the reaction in a CO atmosphere and trapping the reduced P450 in the Fe^{II}-CO complex. The reaction has a unique characteristic in that it usually exhibits biphasic

reduction kinetics, composed of second-order reaction and in some cases the reaction is mutiphasic. This pattern of reduction was first observed in rat liver microsomes and subsequently in the solubilised and purified reconstituted systems. There have been several different explanations put forward as to why P450 reduction takes place biphasically. Peterson et al. have proposed that biphasic reduction kinetics were due to P450 existing as clusters around a limiting concentration of CPR in microsomes and upon addition of reducing equivalents, those P450 molecules in the cluster were reduced rapidly and represented the fast phase of reduction (Peterson, Ebel, et al. 1976). P450s that were not part of the cluster would only be reduced after their initial interaction with CPR, thus displaying slow phase of reduction (Peterson, Ebel, et al. 1976). However, the cluster model was not able to explain the observation of biphasic reduction kinetics of P450 in reconstituted systems at saturating CPR concentrations. Later, Oprian and colleagues proposed that multiple reduction states of CPR may reduce P450s at different rates and since CPR can accommodate maximum of 4 electrons, many CPR subforms may exist, each with their own ability to reduce P450 (Oprian, Vatsis, et al. 1979). This theory was tested by Backes and Reker-Backes (Backes and Reker-Backes 1988) by measuring reduction rates from half and fully reduced CPR. Although completely reduced CPR was found to transfer electrons up to nine times faster than half reduced enzyme, at high NADPH/CPR ratios 98% of CPR existed as completely reduced form. Under these conditions reduction remained biphasic with only 64% of the P450 being reduced in the fast phase, indicating that different reduction states of CPR cannot be the cause of biphasic reduction kinetics for P450 LM2.

The third theory presented for biphasic reduction kinetics was that the spin equilibrium of P450 is a controlling factor for the reduction of the haem protein. According to this model, P450 exists in a pre-equilibrium between low spin ($P450_{LS}$)

and high spin ($P450_{HS}$) forms prior to the addition of reducing equivalents (Backes, Sligar, et al. 1982).

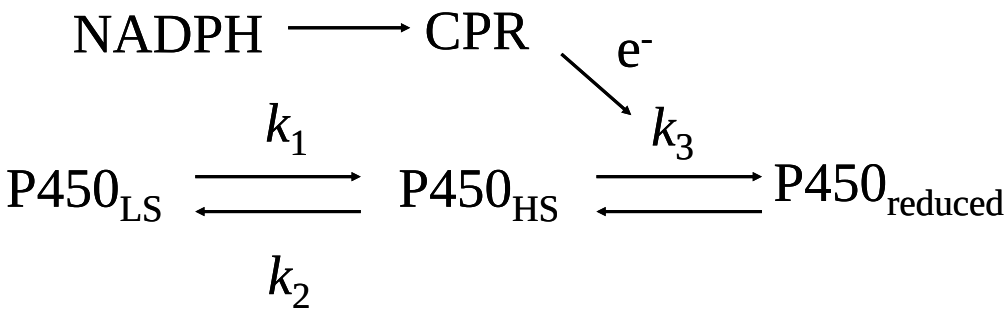

When NADPH is added, firstly high spin P450 is reduced rapidly and the depletion in high spin state perturbs the low to high spin equilibrium. The low spin P450 can then be reduced after passing through high spin stage. If k_1 for the spin-state shift is slow in comparison to reduction rate constant, k_3, then biphasic reaction kinetics would be observed, but if the spin shift is fast then monophasic kinetics would result (Backes and Eyer 1989). For certain P450s this model was found to be valid, for example, Sligar et al. (Sligar, Cinti, et al. 1979) reported that the reduction potential of high spin P450 cam is significantly higher than the low spin enzyme, so making the high spin P450 more readily reducible species. However, Guengerich (Guengerich 1983) working with several rat liver P450s found no general correlation between spin state and reduction potential of haem protein. Kominami and Takemore (Kominami and Takemori 1982) have observed biphasic reduction kinetics for P450 reduction in bovine adrenocortical microsomes and found that substrate was needed for efficient reduction, but they could not find any link between the rate of reduction and high spin content. Furthermore, there was no correlation between the slow phase of P450 reduction and the rate of spin state transition because the latter was predicated to be orders of magnitude faster than the reduction rate (Backes and Eyer 1989). Guengerich and Johnson (Guengerich and

Johnson 1997) in a series of reduction kinetic studies with rabbit and human P450s in various systems, found a negative correlation between haem iron spin state and rate of reduction, some P450s being rapidly reduced in absence of substrate.

Backes and Eyer (Backes and Eyer 1989) put forward an alternative model for P450 reduction to the ones described above. According to their hypothesis, biphasic reduction kinetics is due to CPR and P450 existing in two equilibrium conformations, with one complex being rapidly reduced, while second complex reduced at slower rate. They studied substrate effects on P450 2B4 reduction kinetics and established that both the rate and the affinity of the interaction of P450 2B4 and CPR is strongly dependent on substrate and is also proportional to the rate of P450 2B4 reduction. They suggested that the slow phase of reduction of P450 2B4 could be attributed to the amount of P450 in conformation that was not able to form a functional complex with CPR (i.e. which does not respond to substrate binding). As a result, the slow phase of reduction was dependent on a relatively slow transition to the conformation that would be easily reduced. In the later study, Eyer and Backes (Eyer and Backes 1992) demonstrated that the correlation between rate of reduction and the rate of functional complex formation between two proteins is not simply a feature of P450 2B4 but is a general characteristic of number of different P450s.

In support of this model, Reed and Hollenberg (Reed and Hollenberg 2003) measured the effect of b_5 on the P450 2B4 mediated metabolism of the substrate aminopyrine, and dissociation constant (K_d) values for binding for P450 2B4 and CPR in the presence of substrate. Aminopyrine was chosen as substrate because it was known to reduce the binding affinity between the two proteins, and thus represented an ideal substrate to study conformation-mediated stimulation of P450 2B4 by b_5. In the presence of b_5 metabolism of aminopyrine by P450 2B4 was enhanced and the

measured K_d for CPR and P450 2B4 binding was significantly reduced in the presence of substrate. Additional experiments were also carried out with a redox inactive analogue of b_5 (manganese b_5) to confirm that b_5-mediated stimulation in aminopyrine metabolism was occurring through conformational changes of P450 2B4. Stopped flow measurements of the first electron reduction of P450 2B4 in the presence of manganese b_5 revealed that the rate of first electron delivery to P450 2B4 by CPR is decreased in the presence of b_5 without affecting rate of product formation. The data therefore indicated that b_5 mediated conformational change in P450 2B4 improves coupling in P450 reactions. Reed and Hollenberg ultimately proposed that the progression through P450 catalytic cycle may be limited by conformational equilibrium and mixture of three functionally significant conformation of P450 may exist at each stage of the catalytic cycle (Reed and Hollenberg 2003).

1.10 Interactions between CPR and P450

As the P450:CPR ratio in microsomes is large, rapid association and dissociation of P450 and CPR complexes is needed for the monooxygenase system to work efficiently. Complex formation between CPR and P450 has been reported to take place via two different processes, electrostatic (involving complementary charged residues) or hydrophobic interactions. Voznesensky and Schenkmen (Voznesensky and Schenkman 1992) demonstrated that increasing the ionic strength of the solution from 10 to 100 mM increases the catalytic rate of several P450s, suggesting that hydrophobic interactions are involved in mediating the binding of the proteins. In contrast, several studies have reported that the driving forces involved in complex formation between CPR and P450 are mainly electrostatic interactions between positively charged amino acids on the proximal face of P450 and negatively charged amino acids on the surface of FMN binding domain of CPR (Backes and Kelley 2003). For example, Bernhardt et al.

chemically modified lysine residues on P450 2B4 and showed that the electron transfer from CPR to P450 was inhibited (Bernhardt, Kraft, et al. 1988). Using site directed mutagenesis techniques, a number of lysine and arginine residues have been identified on the proximal surface of P450 2B4 near the haem ligand whose substitution decreases binding to CPR (Bridges, Gruenke, et al. 1998). Further work by Cvrk and Strobel supported the involvement of positively charged lysine residues in the interaction of P450 with CPR (Cvrk and Strobel 2001). They mutated Lys271 and Lys279 on P450 1A1 and found modification of Lys279 resulted in a decrease of reductase-supported monoxygenase activity whereas the hydroperoxide supported reaction was unaffected. Davydov and colleagues measured directly the interaction between P450 2B4 and CPR using fluorescence energy transfer. They demonstrated that increasing the ionic strength of the solution from 0.05 M to 0.5 M resulted in weakening of the CPR-P450 2B4 complex with K_d increasing from 10-90 nM. This result further confirmed that mainly charge pairing is involved in the binding of both proteins and contradicted the earlier findings of Voznesensky and Schenkmen (Davydov, Kariakin, et al. 2000).

In CPR, modification of negatively charged residues of carboxylate groups with water soluble carbodiimide EDC (1-ethyl-3-[3-(dimethylamino)propyl]cabodiimide) caused an increase in K_m values of P450 1A1 and P450 2B1 for 7-ethyoxycoumarin (7-EOC) deethylation and benzphetamine demethylation reactions (Nadler and Strobel 1991, Strobel, Nadler, et al. 1989). It was also demonstrated that neutralising the acidic residues of CPR by EDC inhibits electron transfer to cytochrome *c* or P450. Strobel et al. identified a portion of the FMN domain (residues 109-130) of CPR as a docking surface for P450s (Strobel, Nadler, et al. 1989). This result was supported by experimental work of Shen and Kasper who identified several distinct clusters of acidic amino acids (cluster 1: Asp207-Asp-Asp209; cluster 2: Glu213-Glu-Glu215 and cluster

3, Glu142, Asp144, Asp147) on the FMN binding domain that may interact with cytochrome *c* and P450 (Shen and Kasper 1995). Site directed mutagenesis was carried out on cluster 1 and 2 and was established that cluster 1 does not affect binding of cytochrome *c* but deleting the Asp208 residue alters binding of P450. Modification of cluster 2 residues was found to affect the specific activity of cytochrome *c* without affecting P450 dependent benzphetamine demethylation, but mutatation of cluster 3 resulted in lowering P450 monoxygenase activity. The clusters 1 and 3 are located on the either side of the FMN binding site and these mutagenesis findings indicate that P450 binds at the tip of FMN domain in a way as to shield the FMN cofactor.

1.11 Interactions among P450s and CPR

Although the basic requirements for the interaction of P450 proteins in the microsomal membrane are well known, the organisation of P450s and redox partner enzymes remains to be elucidated. One of the main factors that confound our ability to understand the interactions of the P450 monooxygenase system is the presence of multiple P450s. The multiplicity of P450s in microsomal membrane raises the possibility of both homomeric and heteromeric P450-P450 interactions, which can influence catalytic characteristics of another P450. There have been several lines of supporting evidence presented for such behavior. For example, Cawley et al. demonstrated P450 2B4 dependent 7-pentoxyresorufin-O-dealkylation (PROD) was dramatically inhibited by the addition of P450 1A2 to simple binary reconstituted system (Cawley, Batie, et al. 1995), but the benzphetamine demethylation by P450 2B4 was observed to increase. These results indicated that P450s function differently in the complex reconstituted system when compared to the simple reconstituted system (SRS) containing CPR and a single P450. Later, Yamazaki et al. studied the potential interactions among several human recombinant P450s including P450 3A4. P450 3A4

dependent testosterone 6β-hydroxylation was found to be stimulated by the presence of P450 1A1 and P450 1A2, whereas other P450s were unable to enhance this reaction (Yamazaki, Gillam, et al. 1997). Using chemical cross-linking monoclonal antibody methodology, P450 1A1 was shown to be physically interacting with P450 3A family enzymes in the microsomal membrane and specifically with P450 3A2 (Alston, Robinson, et al. 1991). The authors suggested that complex formation between multiple P450s may exist to stimulate the transfer of drugs and their metabolites. Further work by Cawley and coworkers with P450 2B4 and P450 1A2 revealed that in the presence of certain substrates such as 7-pentoxyresorufin (7-PR), both proteins were capable of forming functionally active heteromeric complexes (Backes, Batie, et al. 1998). As the CPR concentration in a ternary reconstituted system of CPR, P450 1A2 and 2B4 in the presence of 7-PR was increased, P450 1A2 was exclusively found to bind to CPR with high affinity causing CPR to be drawn away from P450 2B4 (CPR-1A2-2B4). Thus, a dramatic inhibition of PROD activity was found, but at saturating concentrations where CPR binding sites of P450 1A2 become fully occupied, and CPR binds to P450 2B4 resulting formation of quaternary complex (CPR-1A2-2B4-CPR), then an increase of PROD activity was observed. The study supported the idea that the presence of one P450 can influence the catalytic activity of another through formation of heteromeric complexes. Later, it was demonstrated that the heteromeric 1A2:P450 2B4 complex is formed through charge pairing interactions, which can be disrupted by changes in ionic strength. PROD activity was found to be inhibited at high ionic strength both in the simple and mixed reconstituted system.

1.12 Aims and objectives

The aim of this research project was to study the kinetics of electron transfer between the recombinant human enzymes, CPR and P450 3A4, in a reconstituted system by stopped-flow experiments in order to establish the mechanism by which electron transfer takes place between two redox enzymes.

The thesis is divided into five Chapters. The present Chapter has given an overview of knowledge of P450s with particular emphasis on human drug metabolizing P450s and examines the published experimental findings in relation to the work carried out in this thesis. Chapter 2 outlines the materials and methods employed in the experiments described in subsequent Chapters. It gives a detailed account of the major practical strategies and techniques used in this study. Chapter 3 deals with the approaches developed for the expression and purification of CPR and P450 3A4 and their reconstitution into liposomes. Purified proteoliposomes are characterised by electron microscopy and optical difference specroscopy. Chapter 4 describes stopped-flow absorption studies of the first electron transfer between CPR and P450 3A4 in the purified proteoliposomes. The effects of varying CPR:P450 molar ratio on the rate of first electron transfer and on the steady state kinetics of NADPH oxidation and testosterone hydroxylation have been investigated. Finally, Chapter 5 ties in all the results and conclusions from previous Chapters and future experiments are discussed.

Chapter 2
Materials and Methods

2.0 Materials and Methods

2.1 Materials

Chromatography columns – DEAE-Sepharose, 2',5'-ADP-Sepharose-4B, Hi-Trap chelating Sepharose, Superose 6 HR 10/30, Superose 6 prepgrade, Superdex 200 PC 3.2/30, HiLoad 26/60 and pre-packed PD-10 columns – were obtained from Amersham Biosciences, UK. High molecular weight (HMW) gel filtration calibration kit was obtained from Amersham Biosciences, UK. Quick-Change® XL mutagenesis kit was from Stratagene, UK. Vivaspin 20 centrifugal concentrators were purchased from VWR, UK. NuPAGE 4-12% Bis-Tris gels, NuPAGE (x4) loading buffer and NuPAGE MOPS SDS running buffer (x20) were obtained from Invitrogen, UK. Competent cells, *E. coli* JM109, BL21 (DE3) pLysS and XL-1 Blue were purchased from Stratagene, UK. The Avanti® mini extruder was obtained from Avanti Polar Lipids, USA. The Xcell Surelock Novex mini cell and BenchMark™ and Protein Ladder were obtained from Invitrogen, UK.

2.1.1 Chemicals

Growth media tryptone, peptone, yeast extract and bacteriological agar were purchased from Oxoid, UK. Isopropyl β-D-1-thiogalactopyranoside (IPTG), ampicillin, Tris-HCl, DTT, EDTA, CHAPS, Triton X-100, β-Nicotinamide adenine dinucleotide phosphate (NADPH), horse cytochrome *c*, δ-aminolevulinic acid (δ-ALA), and riboflavin were from Sigma-Aldrich, UK. Buffer constituents, potassium dihydrogen orthophosphate (KH_2PO_4), dipotassium hydrogen orthophosphate (K_2HPO_4), 2′,3′ adenosine monophosphate (AMP), potassium chloride, sodium chloride, potassium hexacyanoferrate (III), ferric chloride hexahydrate ($FeCl_3$ $6H_2O$), ammonium thiocyanate (NH_4SCN) and glycerol were from Fisher Chemicals, UK. Complete™

protease inhibitor cocktail tablets were obtained from Roche, UK. The phospholipids, 1-palmitoyl-2-oleoyl-*SN*-glycero-phosphocholine (POPC) and 1-palmitoyl-2-oleoyl-*SN*-glycero-3-phosphate (POPA) were obtained from Avanti Polar Lipids, USA.

2.1.2 P450 substrates and metabolites

7-Benzyloxyquinoline (7-BQ), and 7-hydroxyquinoline (7-HQ) were from BD Biosciences, UK. Testosterone, erythromycin, 2β-hydroxytestosterone and 6β-hydroxytestosterone were obtained from Sigma-Aldrich, UK. All other reagents were of the highest available purity.

2.1.3 *E. coli* expression vectors

The P450 3A4 plasmid expression construct (pB84) was made using the vector pCWOri+, and contained P450 3A4 cDNA with an ompA (+2) leader sequence and a six-histidine tag on the N-terminus, Figure 2.1. The cDNA of P450 is inserted between the cloining sites NdeI and XbaI; the plasmid has ampicillin resistance gene, pBR origin of replication, Lac I gene and uses tac promoter to drive expression. The plasmid is ~5500 base pairs in size. In bacteria, the ompA signal peptide plays a role in protein export, directing the polypeptide chain to the inner membrane. During translocation of the protein across the inner membrane, this signal peptide is removed to leave only the native protein. The presence of the two additional amino acids (alanine and proline) between the ompA leader sequence and the methionine start codon are needed for efficient cleavage by the appropriate bacterial proteases. In our laboratory, N-terminal sequencing was carried out on the purified P450 samples generated from this construct and it was confirmed that the purified P450 3A4 samples were of the full-length unmodified form, i.e. the ompA leader sequence had been completely removed (Ward 2003).

Figure 2.1 Diagram of expression vector, pB84.

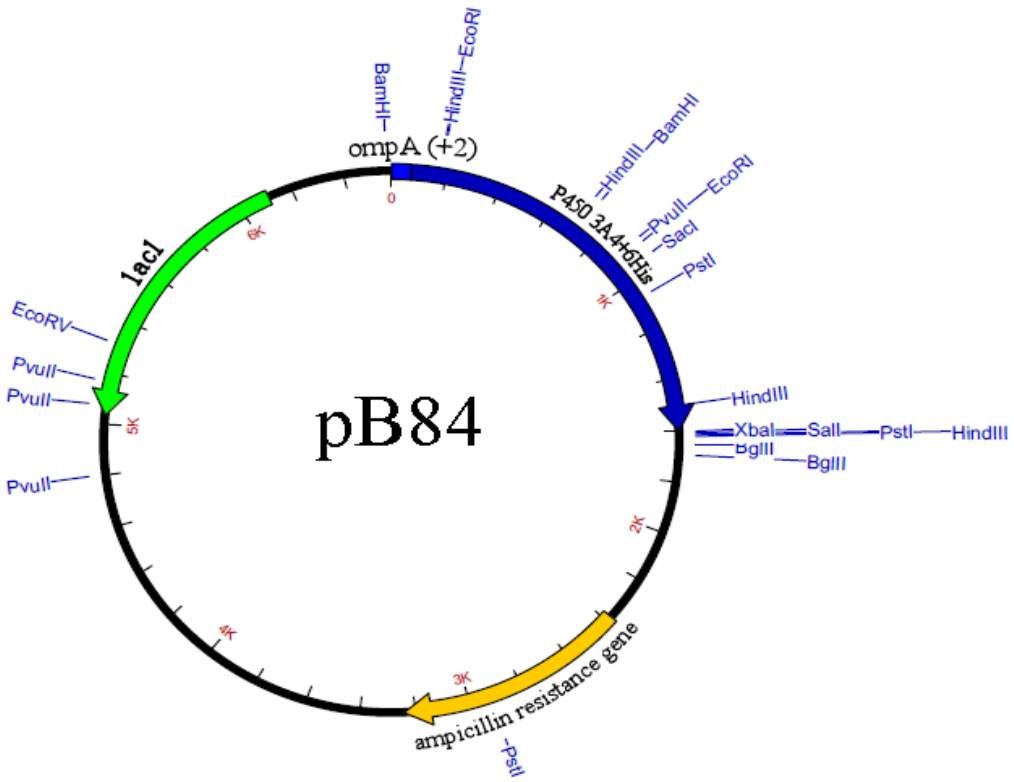

The full-length CPR expression construct (pB209) was made using the vector pCW, Figure 2.2. The cDNA of CPR with pelB leader sequence is inserted between the restriction sites NdeI and SacI; the plasmid has ampicillin resistance gene, pBR origin of replication, Lac I gene and uses tac promoter to drive expression. The pB209 plasmid is ~7100 base pairs in size. Both constructs were a generous gift from Dr. Mark Paine, Biomedical Research Centre, University of Dundee, UK.

Figure 2.2 Diagram of expression vector, pB209.

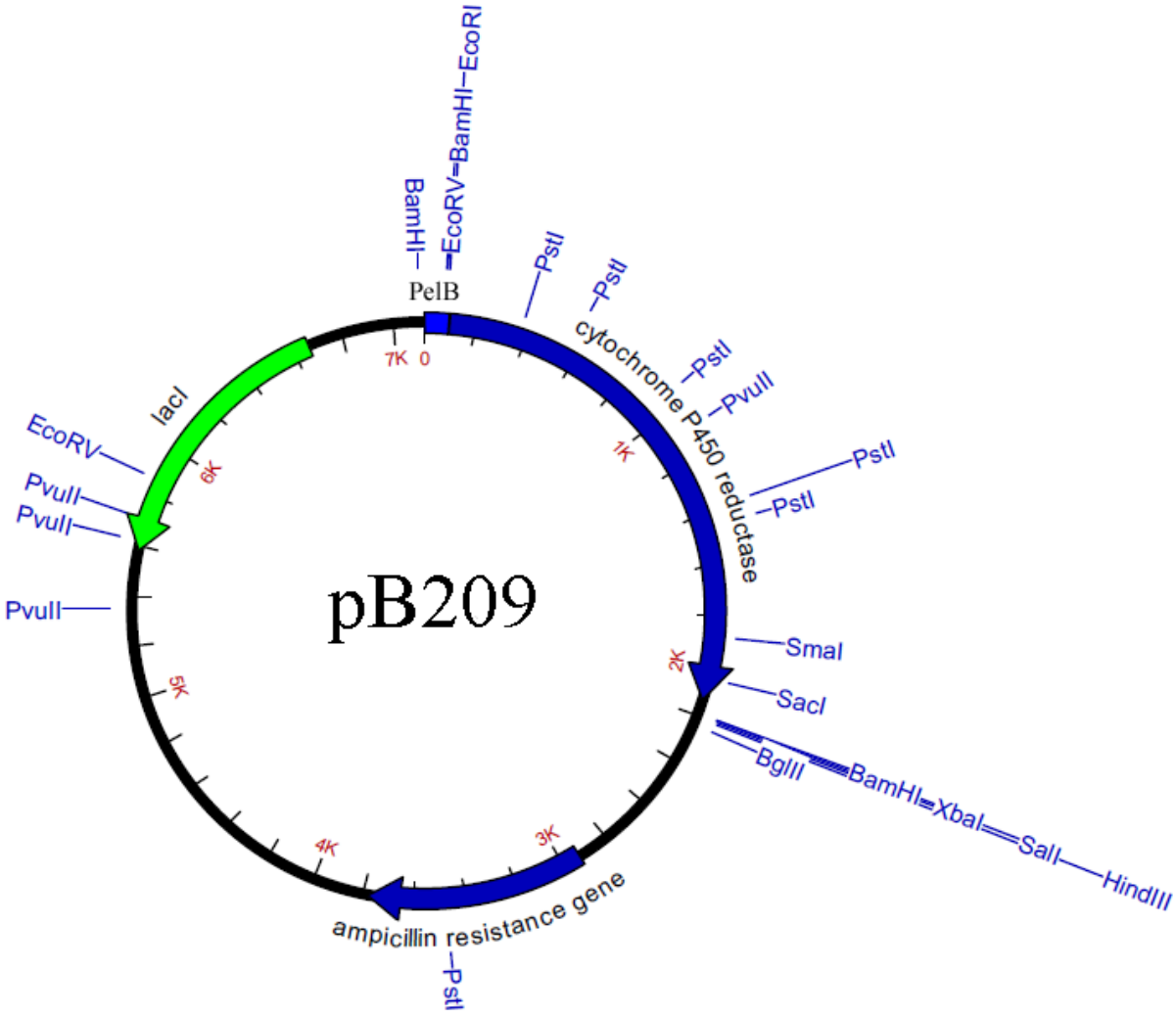

2.2 Methods

2.2.1 Preparation of stock solutions and media

Stock solutions of 0.5 M IPTG, 50 mg/mL ampicillin, 1 mg/mL riboflavin, 1 M thiamine and 0.5 M δ-ALA were prepared by dissolving in double distilled water (ddH_2O) and filter sterilizing using 0.2 µM Acrodisc® syringe filter. Chloramphenicol was dissolved in ethanol to final concentration of 50 mg/mL. Trace elements were

prepared by adding 24.4 g/L iron (III) citrate, 1.72 g/L zinc chloride, 2 g/L cobalt chloride hexahydrate, 2 g/L sodium molybdate, 1 g/L calcium chloride, 1.28 g/L copper chloride, 0.52 g/L boric acid, and 10% v/v concentrated HCl, and was filter sterilized.

Luria-Bertani (LB_{amp}) broth was prepared by dissolving 2.5 g yeast extract, 5 g tryptone and 5 g NaCl in 0.5 L ddH_2O. The medium was autoclaved at 120 ℃ for 30 minutes and allowed to cool below 50 ℃ before adding 50 μg/mL ampicillin. If LB_{amp} agar was desired, 10 g bacteriological agar was included in the same volume. Terrific Broth (TB) was usually prepared by mixing 12 g tryptone, 24 g yeast extract, 2 g peptone and 4 mL glycerol in 0.9 L ddH_2O. TB media was sterilized by autoclaving in a 2 L flask. Potassium phosphate buffer (KPB), pH 7.40, containing 23.1 g/L KH_2PO_4, and 125.4 g/L K_2HPO_4, was autoclaved separately and added to the medium after cooling below 50 ℃.

2.2.2 Transformation of plasmid DNA

A 200 μL aliquot of competent JM109 cells (efficiency of ≥ 1 x 10^8 cfu/μg) was thawed on ice and divided equally into two sterile eppendorf tubes. 5 μL of plasmid DNA (~150 ng of pB209) was added to one aliquot of competent cells and to other 1 μL of pUC18-control DNA (50 ng) was added. Cells were left on ice for 30 minutes, and heat pulsed for 45 seconds precisely at 42 ℃ and placed back on the ice for further 2 minutes. 900 μL of LB_{amp} broth was added to each aliquot, which were incubated at 37 ℃ for 1 hour. The cells were pipetted onto LB_{amp} agar plates, which were incubated at 37 ℃ overnight.

2.2.3 Method A: Expression and purification of human CPR

A single colony was taken from an LB_{amp} agar plate to inoculate 5 mL of LB_{amp} broth, which was grown at 37 ℃ to an OD_{600} of ~1. The 5 mL culture was then poured

into a flask containing 200 mL LB_{amp} broth , which was grown overnight at 37 ℃. 10 mL of this starter culture was taken to inoculate 0.5 L of TB medium containing 50 μg/mL ampicillin and 1 μg/mL riboflavin. TB medium was grown at 30 ℃ with shaking speed of 200 rpm to an OD_{600} of ~1. The cells were induced with 0.5 mM IPTG and grown for 16-20 hours at 30 ℃. The culture was harvested by centrifugation using a Beckman JA-10 rotor at 6500 rpm for 7 minutes at 4 ℃. The supernatant was discarded and cells were frozen at -80 ℃ until processed for purification.

The following buffers were used for the purification of CPR:

***Buffer A*:** 50 mM Tris-HCl, 10% v/v glycerol, 0.5 mM EDTA, 0.5 mM DTT, pH 7.80.

***Buffer B*:** 30 mM Tris-HCl, 0.1% v/v Triton X-100, 10% v/v glycerol, 1 M NaCl, 0.1 mM DTT, 0.1 mM EDTA , pH 7.6.

***Buffer C*:** 30 mM Tris-HCl, 0.1% v/v Triton X-100, 10% v/v glycerol, 0.15 M NaCl, 0.1 mM DTT, 0.1 mM EDTA , pH 7.6.

***Buffer D*:** 100 mM KPB, 0.1% v/v Triton X-100, 10% v/v glycerol, pH 7.4.

The frozen pellets were thawed at room temperature and resuspended in buffer A containing 1 mM PMSF (5 mL buffer added per gram of cells). The suspension was stirred for 15 minutes at 4 ℃ and cell lysis was done by sonicating for 6 x 20 second bursts using a Soniprep 150 apparatus with the large probe (19 mm tip diameter) at an amplitude of 10 microns. In between each burst the cells were chilled on ice water for

90 seconds to prevent protein being denatured by heat. The sonicated suspension was solubilised by adding 0.1% v/v Triton X-100 and stirring for 15 minutes at 4 ℃. Insoluble material was removed by centrifuging using Beckman JA-30.5 rotor at 25000 rpm for 50 minutes at 4 ℃. The supernatant was collected and stored at 4 ℃, for up to 1 hour. The supernatant was loaded onto a DEAE Sepharose anion exchange column (2.6 x 10 cm), which had been pre-equilibrated with 2 column volumes (CV) of buffer A. The column was washed with 2 CV of 15% buffer B with 85% buffer A and protein was eluted in a linear gradient of 15-50% buffer B with buffer A. Eluted protein suspension was loaded onto a 2′,5′-ADP Sepharose column (2.6 x 5 cm) that was pre-equilibrated with 2 CV of buffer A. Impurities were removed by washing the column with 2 CV of 15% buffer B with 85% buffer A. 0.5 CV of buffer C containing 1 mM potassium hexacyanoferrate was used to oxidize the flavoprotein and excess potassium hexacyanoferrate was removed by washing the column with 2 CV of buffer C. Finally, protein was eluted using buffer C containing 5 mM 2′,3′ AMP and ~5 µg of sample was run on the SDS-PAGE gel to asses the purity.

Eluted protein was dialysed overnight against buffer D using dialysis tubing with a 12-kDa molecular weight cut-off (MWCO), changing the buffer least once. The protein was concentrated using 20 mL Vivaspin centrifugal concentrator with a 30 kDa MWCO. The final stock concentration typically was between 50-100 µM and was stored at 4 ℃ for immediate usage or at -20 ℃ after addition of 50% v/v glycerol for a longer period. A PD-10 desalting column was used for buffer exchanging the protein stock solutions stored at -20 ℃. This column was equilibrated with 25 mL of Buffer D and a 2.5 mL sample was applied to the column. Once the protein was run into the column bed, it was eluted with 3.5 mL of buffer D.

2.2.4 Protein concentration determination

CPR concentration was determined spectrophotometrically using a Cary 300 Bio UV/visible spectrophotometer (Varian, UK). Buffer D was split equally between two cuvettes and baseline reading was taken. Protein was diluted in the sample cuvette and a scan was run from 300 nm to 600 nm (Figure 2.3). Protein concentration was calculated using an extinction coefficient of 21.4 mM^{-1} cm^{-1} at 456 nm for the oxidised enzyme (French and Coon 1979).

Figure 2.3 The absorbance spectrum of the purified recombinant oxidised CPR.

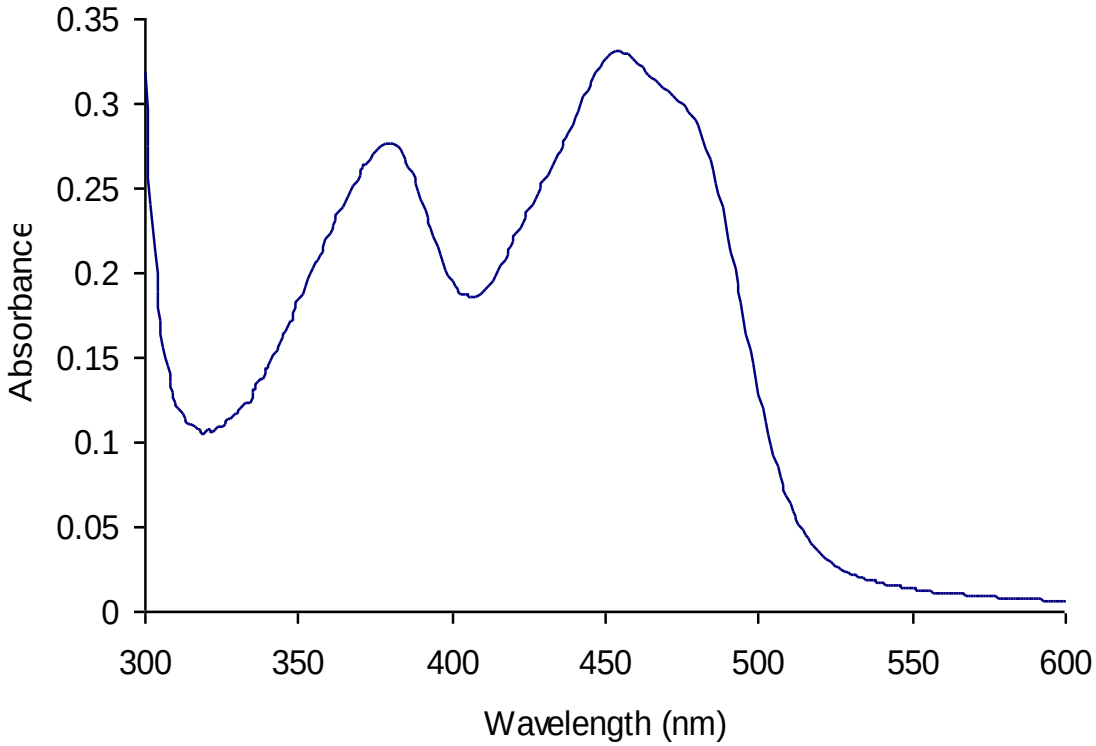

2.2.5 Method B: Optimization of expression and purification of CPR

The following changes were made to method A in order to improve stability of the full-length CPR;

- The expression strain, *E. coli* JM109 was replaced with BL21 (DE3) pLysS and overnight culture contained 50 μg/mL chloramphenicol in addition to 50 μg/mL ampicillin.
- The temperature of the cell cultures post induction was adjusted from 30 ℃ to 28 ℃.
- The cell culture time to harvesting was shortened from 20 to 10 hours.
- PMSF was replaced by a cocktail of complete™ protease inhibitors, 1 tablet being added to every 50 mL of cell suspension.
- 10 mM CHAPS was added to the sonicated suspension and 0.1% v/v Triton X-100 was removed from all buffer solutions. The protein was dialyzed in buffer D containing 2 mM CHAPS.

2.2.6 Assay of CPR catalytic activity

The catalytic activity of CPR was measured using cytochrome *c* assay (Masters et al., 1967) on the Cary 300 BIO spectrophotometer with Peltier temperature controller set at 30 °C. The reaction mixture consisted of 50 μM cytochrome *c*, 2 nM CPR in 0.3 M KPB (pH 7.7), 10% v/v glycerol and 0.1% v/v CHAPS or Triton X-100. The solution was equilibrated in the spectrophotometer at 30 ℃ for 3 minutes and the reaction initiated by adding NADPH solution (50 μM final concentration). The rate of cytochrome *c* reduction was calculated using a difference extinction coefficient of $\Delta\varepsilon_{550nm}$ = 21.1 mM^{-1} cm^{-1}. Rates were linear with respect to time and CPR concentration. The activities are expressed as nanomoles of cytochrome *c* reduced in 1 minute per 1 mg of protein.

2.2.7 N-Terminal sequencing of the CPR

5 μg of purified CPR was run on SDS-PAGE gel and the gel was rinsed thoroughly with ddH_2O and immediately given to Protein and Nucleic Acid Chemistry Laboratory (PNACL) at the University Leicester for N-terminal sequencing.

2.2.8 Site directed mutagenesis of CPR

For each desired mutation, individual oligonucleotide primers (Invitrogen, UK) were designed in the forward (F) and reverse (R) directions, as shown in Table 2.1.

Table 2.1 Sequence of primers for mutations, mutated nucleotide bases is underlined.

Mutant	Primer sequence
T58A: F	5'-gagttcaccaaaattcaggcattgacctcctctgt-3'
T58A: R	5'-acagaggaggtcaatgcctgaattttggtgaactc-3'
K55Q: F	5'-gtccccgagttcacccaaattcagacattgacctc-3'
K55Q: R	5'-gaggtcaatgtctgaatttgggtgaactcggggac-3'
K55QT58A: F	5'-gagttcacccaaattcaggcattgacctcctctgt-3'
K55QT58A: R	5'-acagaggaggtcaatgcctgaatttgggtgaactc-3'

Site-directed mutagenesis was carried out using Quick-Change® XL mutagenesis kit, Stratagene, UK. Oligonucleotide primers were incorporated into wild-type pB209 plasmid (Figure 2.2) and amplified using *pfuTurbo*® DNA polymerase by polymerase chain reaction (PCR). Sample and control reactions were set up for amplification as follows:

Sample reaction: 5 µL of 10x reaction buffer, 1.40 µL (92 ng/µL) of each of the forward and reverse direction primers, 1.5 µL of 10 ng DNA template, 1 µL dNTP mix, 3 µL Quick solution and 36.7 µL ddH_2O to bring the final reaction volume to 50 µL.

Control reaction: 5 µL of 10x reaction buffer, 1.25 µL (125 ng/µL) of each of the forward and reverse direction primers, 2 µL of 10 ng control DNA template (plasmid 4.5 kb), 1 µL dNTP mix, 3 µL Quick Solution and 36.5 µL ddH_2O to bring the final reaction volume to 50 µL.

1.25 µL (2.5 U/µL) of pfuTurbo® DNA polymerase was added to both tubes and the reaction mixture was overlayed with 30 µL of mineral oil to prevent evaporation. Cycling parameters for the reaction mixture were 90 ^oC for 1 minute followed by 18 cycles at 95 ^oC for 50 seconds, 60 ^oC for 50 seconds and 68 ^oC for 8 minutes (for pB209 vector). Following the temperature cycling, the reaction tubes were cooled to 37 ^oC for 2 minutes and 1 µL DpnI restriction enzyme was added. The tubes were left at 37 ^oC for an hour to allow digestion of the parental template DNA. Plasmid pB209 containing mutations were transformed into *E. coli* XL-1 Blue cells and transformed colonies were grown on LB_{amp} agar plates. Small scale plasmid preparations were done using Promega's Wizard® Plus Minipreps-DNA purification kit. In order to confirm the desired mutations and verify the absence of unintended mutations, all plasmid constructs were sequenced at PNACL. The sequencing primers used are shown in Table 2.2.

Table 2.2 List of primers used for sequencing CPR mutant proteins.

Primer	Sequence
CPR F1	5'-tcagagagagcagctttgtgg-3'
CPR F2	5'-gagatgggccggctgaagagc-3'
CPR F3	5'-aactctgtgcacatcrgtgcg-3'
CPR R1	5'-ccacacgtccaggagtagcg-3'
CPR R2	5'-gtactccacaaccaccgcaca-3'
CPR R3	5'-actgcagccaggaccggattc-3'
CPR R4	5'-accagggcgttgtcgatctcc-3'

2.3 Expression and purification of human P450 3A4

Plasmid pB84 was transformed into *E. coli* JM109 using the method described in section 2.2.2, P450 was expressed essentially using the same protocol as described for CPR except riboflavin was substituted by trace elements (0.125 mL of the stock solution was added to 0.5 L of TB media) and 0.5 mM δ-ALA and 1 mM thiamine were added to TB media. The following buffers were used for P450 purification;

***Buffer A1*:** 50 mM KPB, 0.5 M KCl, 20% v/v glycerol, pH 7.40.

***Buffer A2*:** 50 mM KPB, 5 mM CHAPS, 1 M imidazole and 10% v/v glycerol, pH 7.40.

Buffer A3: 100 mM KPB, 0.1 mM DTT, 0.1 mM EDTA, 5 mM CHAPS, and 20% v/v glycerol, pH 7.40.

The cell pellets were resuspended in buffer A1 containing Complete™ protease inhibitor cocktail tablets (1 tablet was added for each 50 mL cell suspension). The cell suspension was stirred for 15 minutes at 4 ℃ until it became homogeneous and then sonicated at amplitude of 10 microns using the large probe (19 mm tip diameter) for 5 x 20 seconds. In between each burst the cells were kept on ice water for 90 seconds. 10 mM CHAPS was added to the sonicated cell suspension, which was stirred for 30 minutes at 4 ℃ and cell debris was removed by centrifugation using Beckman JA-30.5 rotor at 25000 rpm for 50 minutes at 4 ℃. The supernatant was collected and stored at 4 ℃ for up to 1 hour until the nickel affinity column was ready.

A Hi-Trap Sepharose chelating column (2.6 cm x 5 cm) was charged with 0.1 M nickel sulphate solution and equilibrated with 2 CV buffer A1. The supernatant was loaded onto a column and washed with following step gradient of imidazole using buffer A1 and A2: a) 0 mM (100 mL), b) 100 mM (25 mL), c) 125 mM (75 mL), d) 150 mM (75 mL), e) 400 mM (50 ml)**.** Protein was eluted in the final step and purity was determined by SDS-PAGE. The protein was dialysed against buffer A3 using dialysis tubing with a 12 kDa MWCO, changing the dialysis buffer at least once. The protein was concentrated using a 20 mL Vivaspin protein concentrator that had 10 kDa MWCO; the stock concentration was usually between 75-150 µM. Protein was stored at 4 ℃ for a week and at –20 ℃ after addition of 50% v/v glycerol for not immediate usage.

2.3.1 Analysis of P450 content

P450 3A4 concentration was determined using a Cary BIO 300 UV/visible spectrophotometer, following the method of Omura and Sato (Omura and Sato 1964). Protein was diluted into 0.1 M KPB (pH 7.40) containing 10% v/v glycerol and 0.1% w/v CHAPS and samples were split equally between two cuvettes. A few grains of sodium dithionite were added to both cuvettes to reduce the protein and the baseline was recorded between 350 nm to 500 nm. The sample cuvette was then bubbled with CO for 30 seconds and the reduced-CO versus oxidised CO-difference spectrum was recorded. The difference extinction coefficient ($\Delta\varepsilon$ 450-490 nm) of 91 mM^{-1} cm^{-1} (Omura and Sato 1964) was used to calculate the concentration of P450.

For NADPH-reduced CO-difference spectra of P450 3A4, the method was essentially as described by Kim et al (Kim, Ahn, et al. 2003). SRS was prepared by mixing 2 μM P450 3A4, 1 μM CPR, 40 μM liposomes, 100 μM testosterone (final concentration of methanol <2% v/v) or 7-BQ (final concentration of ethanol <2% v/v) in 0.1 M KPB (pH 7.4) containing 10% v/v glycerol and 0.1% w/v CHAPS or 0.1% v/v Triton X-100. A 2 mL sample was split between quartz cuvettes (1 cm path length) and CO was bubbled into sample cuvette for 30 seconds and baseline was taken between 400 nm to 500 nm. After incubation at 25 ℃ for 3 minutes, 0.2 mM NADPH was added to the sample cuvette and the difference spectrum was immediately measured. Finally, sodium dithionite was added to both cuvettes and the difference spectrum was again measured. CO-difference spectra were also recorded in the absence of liposomes and substrate in the SRS and spectra shown are average of at least three experiments. *E. coli* membranes co-expressing equimolar amounts of human CPR and human P450 3A4 were a generous gift of Dr. Richard Ward in our laboratory.

2.3.2 Preparation of spheroplasts and E. coli membranes co-expressing equimolar amounts of human CPR and P450 3A4

Cell cultures were chilled on ice for about 10 minutes and then cells were pelleted by centrifugation at 3000 rpm (2800g) for 20 minutes at 4 ^{o}C. The supernant was discarded and cell pellets were resuspended in ice-cold 2 x TSE buffer (50mM Tris-acetate, 250mM sucrose, and 0.25mM EDTA), then an equal volume of ice cold ddH_2O was added. Then 20 mg/mL lysozyme (prepared in ddH_2O) was added to the resuspended cells to final concentration of 0.25mg/mL. The cells were gently shaken at 4 ^{o}C for 30-60 minutes. Spheroplasts were centrifuged at 3000 rpm for 20 minutes and supernant was discarded and 4mL resuspension buffer (100mM KPB, pH7.60, 6 mM magnesium acetate, 20% glycerol and 0.1mM DTT) (per a pellet derived from 100 mL cell culture) was added. The spheroplasrs were then stored at -70 ^{o}C. Spheroplasts were thawed on ice and 1 μg/mL of protease inhibitors, aprotinin and leupeptin and 1 mM PMSF were added. Spheroplasts were then sonicated for 3 x bursts of 30 s. Then the cell suspension was centrifuged at 12000 g for 15 minutes. The supernatant was ultracentrifuged for 60 minutes at 180000 g at 4 ^{o}C. Supernantant was then discarded and membranes were resuspended in ice cold 1 x TSE buffer and were stored at -70 ^{o}C.

2.4 Reconstitution of enzymes into liposomes

Purified enzymes were reconstituted into liposomes made up of a binary mixture of equal amounts of the phospholipids POPC and POPA. These phospholipids were particularly chosen in view of the evidence that long unsaturated POPC with mixture of anionic POPA exert a significant stimulatory effect on the catalytic activity of P450 3A4 in reconstituted systems (Kim, Ahn, et al. 2003, Taniguchi, Imai, et al. 1979). Tanguchi et al (Taniguchi, Imai, et al. 1984) have reported that there is correlation between the net negative charge of the vesicles and the P450 catalytic activity in a

reconstituted system and lipids such as POPA is efficient for catalytic activities of P450 because it has a high net negative charge.

The method was essentially as described by Kim et al (Kim, Ahn, et al. 2003). 10 mg/mL of POPC and 9 mg/mL of POPA (50:50 POPA:POPC mol%) were dissolved in dichloromethane and the solvent was evaporated under a gentle stream of nitrogen gas; the sample was then stored under vacuum for ~2 hours to remove any residual solvent. The dry lipid film was suspended in 25 mM Tris-HCl buffer solution, pH 7.40, containing 0.1 M NaCl and 0.5 mM EDTA. The lipid suspension was thoroughly mixed by vortex. The lipid dispersion was sonicated at amplitude of 10 microns (using the small probe, tip diameter 3 mm) for 30 seconds and frozen and thawed five times. After the freeze and thaw cycles, the lipid dispersion was placed into 0.5 mL gas tight syringes, which were fixed onto the Avanti® mini extruder. Phospholipids were pushed continually (25 times) through two 100 nm pore size polycarbonate membranes to obtain homogenous large uniform vesicles (liposomes). The prepared liposomes were kept at 4 ℃ for up to 3 days and the required aliquots were taken for protein reconstitution.

The simple reconstituted system (SRS) was obtained by simply mixing the desired amounts of CPR, P450 3A4 and preformed liposomes followed by dilution in 0.1 M KPB (pH 7.40) containing 10% v/v glycerol and 0.1% w/v CHAPS and incubating for 10 minutes at room temperature prior to assay.

2.5 Assay of P450 catalytic activity

Fluorescence experiments were carried out on a Perkin-Elmer LS 50B Luminescence spectrometer (Perkin-Elmer, UK). The assay mixture was prepared with 0.5 μM P450 3A4 in 0.1 M KPB, pH 7.40 containing 10 % v/v glycerol, to which 10 μL

of 7-BQ (0.1 mM final concentration) was added (final concentration of ethanol was less than 0.5 % v/v). The solution was equilibrated at 25 ℃ for 3 minutes in the fluorimeter and the reaction initiated by addition of cumene hydroperoxide (0.5 mM final concentration from 50 mM stock solution in acetone). The fluorescence at 530 nm (slit width 20 nm) was observed when excited at 409 nm (slit width 2.5 nm) using a 1 cm path length cuvette. The reaction was followed for 5 minutes and rates (arbitrary units s^{-1}) were derived from the linear part of the curve. Turnover rates are average of at least three experiments and were converted to units of [7-HQ] formed/min/nmol P450 using a 7-HQ standard curve produced using an authentic standard of 7-HQ.

For measurement of P450 activity in the SRS, the incubation mixture was prepared by mixing 0.5 μM P450, 1 μM CPR (purified either using method A or B), 0.1 mM 7-BQ, 40 μM liposomes in 0.1 mM KPB, pH 7.40, containing 10% v/v glycerol, 0.1% w/v CHAPS. The reaction was initiated with 0.5 mM NADPH or cumene hydroperoxide.

2.6 Stopped-flow kinetics

All kinetic experiments were at 25 ℃ using an SX.18 MV-R stopped-flow spectrometer (Applied Photophysics, UK) with a dead time of ~1.5 ms. The sample-handling unit of the stopped flow instrument was contained within a customized glovebox (Belle Technology, UK) and the temperature of the mixing chamber was controlled by a circulating water bath. 0.1 M KPB (pH 7.40) containing 10% v/v glycerol, and 0.1% w/v CHAPS was made anaerobic by bubbling nitrogen gas for about 2 hours prior to placing in the anaerobic glovebox. NADPH was taken as powder form to the glovebox and dissolved in anaerobic 0.1 M KPB. Protein samples were kept on ice at all times in the glovebox, any trace of oxygen was removed by buffer exchange in

0.1 M KPB using a PD-10 column. SRS was prepared by mixing 8 μM P450 3A4, 4 μM CPR, 160 μM liposomes in 0.1 M KPB (pH 7.40). If substrate was desired, 0.5 mM testosterone was added to the SRS and to the NADPH solution. The SRS and 0.4 mM NADPH solution were transferred into gas tight syringes and slowly bubbled with CO gas (1 mL sample bubbled for 1 minute) under a fume-hood. Samples were then introduced anaerobically into the sample-handling unit of the stopped-flow and equilibrated at 25 ℃ for 3 minutes. To initiate the reaction, equal volumes of SRS and 0.4 mM NADPH solution were mixed from the two syringes and the reaction was monitored by an increase in absorbance at 448 nm due to the formation of the ferrous-CO complex of P450. Mixing in the stopped-flow apparatus dilutes both substrate and the enzymes by twofold. The data from three or more shots was averaged and fitted using the manufacturer's software with a single (equation 2.1) or double exponential function (equation 2.2) to obtain the observed rate constants and amplitudes.

Kinetic studies with purified proteoliposomes were carried out on a stopped-flow apparatus that was not maintained within an anaerobic glovebox. In order to achieve anaerobic conditions, gas tight syringes were attached to the cell block by Luer fittings and adapters. The cell was made anaerobic by washing with concentrated solution of sodium dithionite (~15 mM) followed by extensive flushing with anaerobic 0.1 M KPB (pH 7.40). Proteoliposomes and NADPH solution (with or without substrate) were prepared in gas tight syringes in anaerobic glovebox and both samples were taken out of the glovebox to bubble with CO gas under a fume hood. The samples were introduced into anaerobic sampling handling unit of the stopped-flow apparatus. Data were collected using a 'logarithmic mode' which collects a minimum of 1000 data points per trace and the traces shown are average of three to six individual reactions.

Averaged traces were fitted with a single or double exponential equation (equation 2.1 and 2.2) using the manufacture's software.

$$A_{448} = Ce^{-k_{obs}t} + b$$

Equation 2.1

Where A is the absorbance change, k_{obs} is the observed rate constant, C is the constant related to the initial amplitude and b is an offset value to account for a non-zero baseline.

$$A_{448} = C_1{}^{-k_{obs}t} C_2{}^{-k_{obs2}t} + b$$

Equation 2.2

Where A is the absorbance change, k_{obs} and k_{obs2} are the observed rate constants for the fast and slow phases. C_1 and C_2 are relative amplitude values for the two phases, and b is an offset value to account for a non-zero base line.

2.7 Glycerol density gradient centrifugation

0.2 mL of the SRS containing 10 µM P450 3A4, 10 µM CPR and 0.4 mM liposomes in 0.1 M KPB (pH 7.40) was layered on 3 mL 30% v/v glycerol in the reconstitution buffer, which was itself layered on a 0.5 mL cushion of 50% v/v glycerol in the same buffer. The preparation was centrifuged at 100,000 g at 4 ^{o}C for 2 hours in a Beckman JA-30.5 rotor. 0.2 mL fractions were taken from the bottom of the tube and from 30% v/v glycerol/buffer interface. SDS-PAGE gel was carried out for analysis in

the fractions. In this gradient, proteoliposomes are found in the 30% v/v glycerol/buffer layer and unbound proteins are concentrated in the lower layer.

2.8 Gel filtration chromatography experiments

2.8.1 Preparation of SRS for gel filtration

SRS was prepared mixing 10 μM P450 3A4, 10 μM CPR and 10 mM of liposomes in 0.1 M KPB (pH 7.40) containing 0.1% w/v CHAPS and 10% v/v glycerol. The final sample volume for loading was 5 mL and was incubated for 10 minutes at room temperature prior to subjecting to chromatography. Upto 5 mL proteoliposome sample was eluted in the void volume of superose 6 prepgrade column and this was enough for about 10-15 stopped-flow or steady state kinetic experiments.

2.8.2 Superdex 200 PC 3.2/30 column

Gel filtration chromatography was carried out on the AKTA™ purifier system (Amersham Biosciences, UK). Analytical gel filtration experiments were carried out using Superdex 200 PC 3.2/30 column (0.32 x 30 cm), which was previously calibrated using a set of molecular weight standards obtained from Sigma-Aldrich, UK, Table 2.3. The column was equilibrated with 2 CV of 0.1 M KPB (pH 7.40) and 50 μL samples of either CPR, P450, liposomes or SRS were injected on the column and run at flow rate of 0.1 mL/min with 0.1 M KPB (pH 7.40). Fractions of 0.2 mL were collected for SDS-PAGE analysis.

Table 2.3 Calibration data for Superdex 200 PC 3.2/30 column.

Protein standard	**Molecular Weight (kDa)**	**Retention Volume (mL)**
Carbonic anhydrase	29	1.78
Bovine serum albumin	67	1.60
Alcohol Dehydrogenase	150	1.47
β –Amylase	200	1.38
Apoferritin	443	1.25
Thyroglobulin	669	1.12
Blue dextran	2000	0.94

The void volume (V_e) of the column was determined to be 0.94 mL using blue dextran.

The Superdex HiLoad 26/60 (2.6 x 60 cm) was equilibrated with 2 CV of 0.1 M KPB (pH 7.40) and 2 mL samples of SRS and protein reconstitution mixture was applied on the column. The column was eluated at 2 mL/min with 0.1 M KPB (pH 7.40) and 2 mL peak fractions were collected. The column had previously been calibrated using set of molecular weight standards purchased from Sigma-Aldrich, UK, Table 2.4.

Table 2.4 Calibration data for Superdex 26/60 column.

Protein Standard	**Molecular Weight (kDa)**	**Retention volume (mL)**
Carbonic anhydrase	29	234
Bovine serum albumin	67	199
Alcohol Dehydrogenase	150	176
β-Amylase	200	161
Apoferritin	443	142
Thyroglobulin	669	126
Blue dextran	2000	115

The void volume (V_e) of the column was determined to be 115 mL using blue dextran.

2.8.3 Superose 6 chromatography

Superose 6 HR 10/30 (1.0 x 30 cm) was equilibrated with 2 CV of 0.1 M KPB (pH 7.40) and 0.24 mL of SRS or protein mixture without liposomes was applied on the column. The column was run at 0.4 mL/min with 0.1 M KPB (pH 7.40) and 1 mL peak fractions were collected. The Superose 6 HR 10/30 column was calibrated using a set of molecular weight markers purchased from Amersham Biosciences, UK, Table 2.5.

Table 2.5 Calibration data for Superose 6 HR 10/30 column.

Protein standard	**Molecular weight (kDa)**	**Retention volume (mL)**
Bovine serum albumin	67	17.21
β-amylase	200	15.61
Apoferritin	443	15.00
Thyroglobulin	669	13.03
Blue dextran	2000	7.40

The void volume (V_e) of the column was determined to be 7.40 mL using blue dextran.

The Superose 6 prep grade column (2.6 x 34 cm) was run in a similar fashion except that 5 mL of SRS was loaded on the column and 2 mL peak fractions were collected. The void volume fractions of the column were considered to contain only the proteins physically incorporated into liposomes.

Protein concentration was adjusted in the initial reconstitution mixture to obtain the desired molar ratios of P450 and CPR in liposomes. All chromatographic runs were monitored by UV/visible detector on the AKTA™ purifier. The elution profile of haem protein at absorbance of 420 nm, of flavins at 450 nm and of liposomes or SRS at 280 nm. The void volume fractions were pooled and activity assays were done immediately to quantitate the total amount of P450 and CPR in the proteoliposomes. P450 recovery was quantitated by CO-difference spectroscopy (Omura and Sato 1964) and of CPR

using cytochrome *c* reductase activity (Yasukochi and Masters 1976). Typically, a proteoliposome sample contained ~0.1 μM of each CPR and P450. SDS-PAGE gel analysis was also carried with each chromatographic run to estimate visually the proportions of CPR:P450 incorporated into liposomes.

2.9 Lipid assay

The concentration of liposomes in the void volume fractions of Superose 6 column was determined by a colorimetric method based on complex formation of ammonium ferrothiocyanate with phospholipids (Stewart 1980). 0.1 mL of aliquots of void volume fractions were lyophilized (Thermo Savant Modulyo D freeze dryer, USA) at -50 ^{o}C for 24 hours, the dry extract was dissolved in 2 mL of chloroform and 2 mL of ammonium ferrothiocyanate solution (prepared by dissolving 27.03 g of $FeCl_3 6H_2O$ and 30.4 g NH_4SCN in ddH_2O) was added. The mixture was vigorously vortex for 1 minute and centrifuged at 1000 rpm for 5 minutes. Following phase separation, the lower chloroform layer was removed with a Pasteur pipette and an OD reading was determined at 488 nm in a cuvette. Three OD readings were averaged and concentration of liposomes was determined by comparing with a standard curve obtained using known amounts of POPC and POPA.

2.9.1 Transmission electron microscopy of liposomes and proteoliposomes

A sample of liposomes and SRS was run on the Superose 6 column and 0.2 mL of the void volume eluates were given to the Electron Microscope Laboratory at the University of Leicester (All EM work was carried out by Mr. S.C. Hyman). For negative staining, 5 μL of sample was applied to the surface of a carbon coated copper grid, which was suspended in the neck of a bottle of 25% glutaraldehyde for 3 minutes

to fix the sample to the carbon surface. Excess sample was removed by touching the grid with a filter paper and immediately a droplet of 2% uranyl acetate was applied. Excess stain was taken off with a filter paper and the sample was air dried for ~10 minutes before placing it in the Jeol 1220 transmission electron microscope (Jeol Ltd, UK).

2.10 Optical measurements of substrate binding to P450 3A4

Testosterone and erythromycin binding to P450 3A4 in proteoliposomes was determined spectrophotmetrically by using a Cary 300 Bio UV/visible spectrophotometer with a Peltier temperature control unit maintaining the temperature at 25 ℃ (Varian, UK). 0.98 mL of proteoliposomes was equally divided between quartz cuvettes (1 cm path length) and baseline was scanned between 350-500 nm. Substrates were dissolved in methanol to a final stock concentration of 40 mM and added in 0.25 µL aliquots to sample cuvette and an equal volume of methanol was added to the reference cuvette (final concentration of methanol was ≤2% v/v). The spectra were recorded between 350-500 nm on the addition of increasing concentration of substrate, all spectra being corrected for any dilution effects. The difference in absorbance, ΔA(390 nm - 420 nm) was plotted versus increasing substrate concentration to estimate apparent dissociation constant (K_d) and maximal absorption change (A_{max}) for the transition using non-linear regression analysis with Microcal OriginPro software, version 7.5. The data was fitted either to a rectangular hyperbolic binding equation (equation 2.3) or to a Hill equation (equation 2.4) where the data appeared sigmoidal.

$$\Delta A = \frac{A_{\max}[S]}{K_d + [S]}$$ **Equation 2.3**

$$\Delta A = \frac{A_{\max}[S]^n}{K_d + [S]^n}$$ **Equation 2.4**

Where ΔA is the absorbance difference, A_{max} is the maximal absorbance difference, and *S* is the substrate concentration, K_d, is the apparent dissociation constant, is the substrate concentration giving absorbance change of 50% A_{max} and *n* is the Hill coefficient, the measure of cooperativity. An *n* value of one indicates a single binding site. The degree of spin equilibrium transition of P450 haem iron (i.e. low to high form) upon substrate binding at 25 ºC was calculated using difference extinction coefficient (390-420 nm), of 126 $mM^{-1} \cdot cm^{-1}$ (Gibson, Cinti, et al. 1980, Schenkman, Remmer, et al. 1967).

2.11 NADPH consumption assay

The rate of NADPH oxidation was determined at 25 ^{o}C by monitoring absorption changes at 340 nm using a Cary Bio 300 UV/visible spectrophotometer. A sample of 480 µL proteoliposomes was preincubated for 3 minutes at 25 ^{o}C with or without 0.5 mM testosterone (final concentration of methanol 2% v/v). The reaction was initiated by addition of 20 µL of NADPH solution (100 µM final concentration) and the decrease in absorbance at 340 nm was monitored for either 5, 10, or 30 minutes (reaction progress being linear over all these time points), the reaction being linear over this time period. The rate was calculated using a molar extinction coefficient of 6.22

mM^{-1} cm^{-1} for NADPH at 340 nm and the values shown are the average of a minimum of three experiments.

2.12 Measurement of testosterone metabolism

To measure the rate of 6β-hydroxy-testosterone (6β-OH) formation, 480 µL of purified proteoliposomes containing 0.5 mM testosterone was preincubated at 25 ^{o}C for 3 minutes and reaction was started by addition of 20 µL of NADPH solutions (final concentration 100 µM). After, 5, 10 or 30 minutes (reaction progress was linear over these time periods), 0.25 mL of ice cold methanol was added to stop the reaction and the sample was placed on ice for 10 minutes. Then spiked with 0.1 µM 2β-OH as internal standard and centrifuged at 13,000 rpm for 8 minutes. 0.25 mL of supernatant was removed for HPLC analysis and 10 µL volumes were loaded onto a Thermo-Hypersil 5 µm ODS (C_{18}) HPLC column (4.0 x 250 mm, Thermo Scientific, UK) connected to an Agilent 1100 series HPLC instrument (Agilent Technology, UK) equipped with diode array UV/visible detection. Elution was carried out using a gradient of methanol: water: acetonitrile from 42.5:55:2.5 to 72.5:22:2.5 at a flow rate of 1 ml/min over 19 minutes, at 35 ^{o}C. The peaks corresponding to testosterone and its metabolites were monitored at 240 nm and quantification of metabolites was done by comparing the peak area of the metabolite with that of the internal standard. Rates were calculated using a 6β-OH testosterone calibration curve. The data presented are the average of 3 experiments.

Chapter 3
Characterisation of a reconstituted cytochrome P450 reductase and cytochrome P450 3A4 system

3.0 Introduction

3.1 The importance of studying membrane proteins

The various genome analyses suggest that up to 30% of the proteins expressed in eukaryotic cells are membrane proteins (Nilsson, Persson, et al. 2005, Wallin and von Heijne 1998). Membrane proteins and their complexes play an essential role in many cellular and physiological processes. These include, among others, molecular transport, signal transduction, cellular adhesion and energy conversion. However, there is considerable lack of information about their three dimensional structure, stability and the nature of behaviour within the membrane compared to their water soluble counterparts. As of 1st July 2009, ~54 000 protein structures are deposited in the Protein Databank (http://www.pdb.org), and of which membrane proteins represent <1% of the structures. This is particularly important because membrane proteins represent the largest group of current or future drug targets. The hydrophobic character of membrane proteins makes their isolation and purification process extremely challenging. Most membrane proteins cannot be readily extracted in sufficient quantities from their native environment and are therefore overexpressed in organisms like yeast or bacteria, and once the membrane protein has been overexpressed in appropriate host, detergents have to be used for solubilisation and purification, Figure 3.1 shows common types of detergents used in solubilisation of membrane proteins. Detergents are amphiphillic molecules that form micelles in water. Protein solubilisation takes place by binding of these molecules to the hydrophobic parts of the proteins on one side and interacting with the aqueous phase on the other side.

Figure 3.1 Structure of common type of detergents used in purification of membrane proteins.

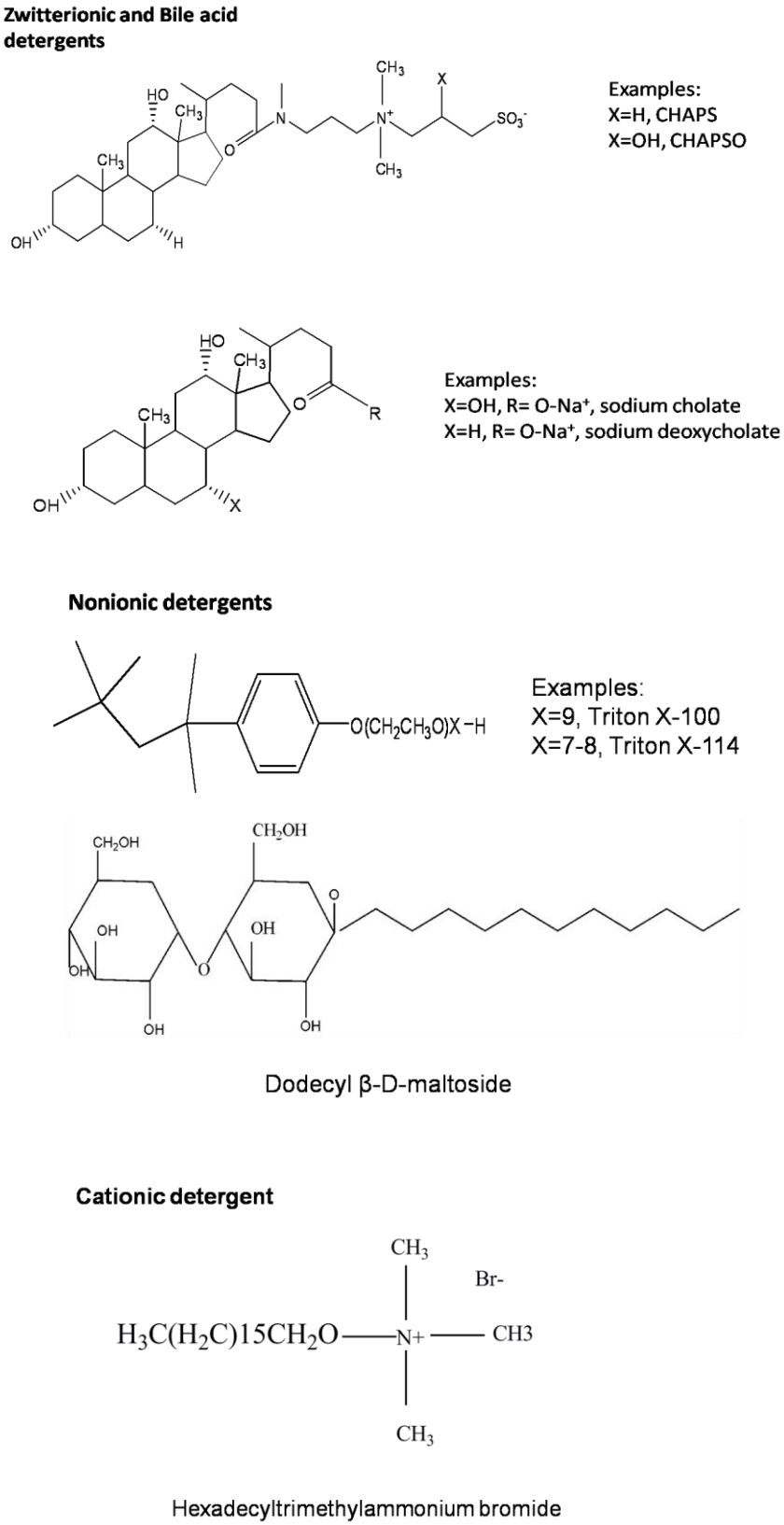

There are often drawbacks in using detergents as these compounds are a poor mimic of the native membrane in which these proteins reside. An inappropriately chosen detergent can destabilize the membrane protein and lead to loss of activity over time. Once the membrane protein has been isolated and purified, although it is often possible to determine its structure in the presence of detergent, studying its structure-function relationship *in vitro* requires it to be reconstituted into an artificial or native membrane. Many membrane proteins only fully express their activity once correctly oriented and inserted into phospholipid bilayer. The reconstitution of membrane proteins allows detailed spectroscopic and kinetic characterization of the purified protein using techniques such as stopped-flow spectroscopy.

A number of methods exist for reconstitution of membrane proteins into the bilayer of lipid vesicles (liposomes) and are described below briefly with each having their own limitations (Rigaud and Levy 2003). For vesicle formation (Figure 3.2), the lipid is first solubilised in a solvent and dried in order to create a lipid film. The addition of water or buffer causes the lipid to swell and form bilayers, with vigorous vortexing multilamellar large vesicles (MLVs) are formed. MLVs can be extruded through filters of appropriate diameter to form large unilamellar vesicles (LUVs) or sonicated by bath or probe tip sonicator to form small unilamellar vesicles (SUVs).

Figure 3.2 Diagram of lipid vesicle formation.

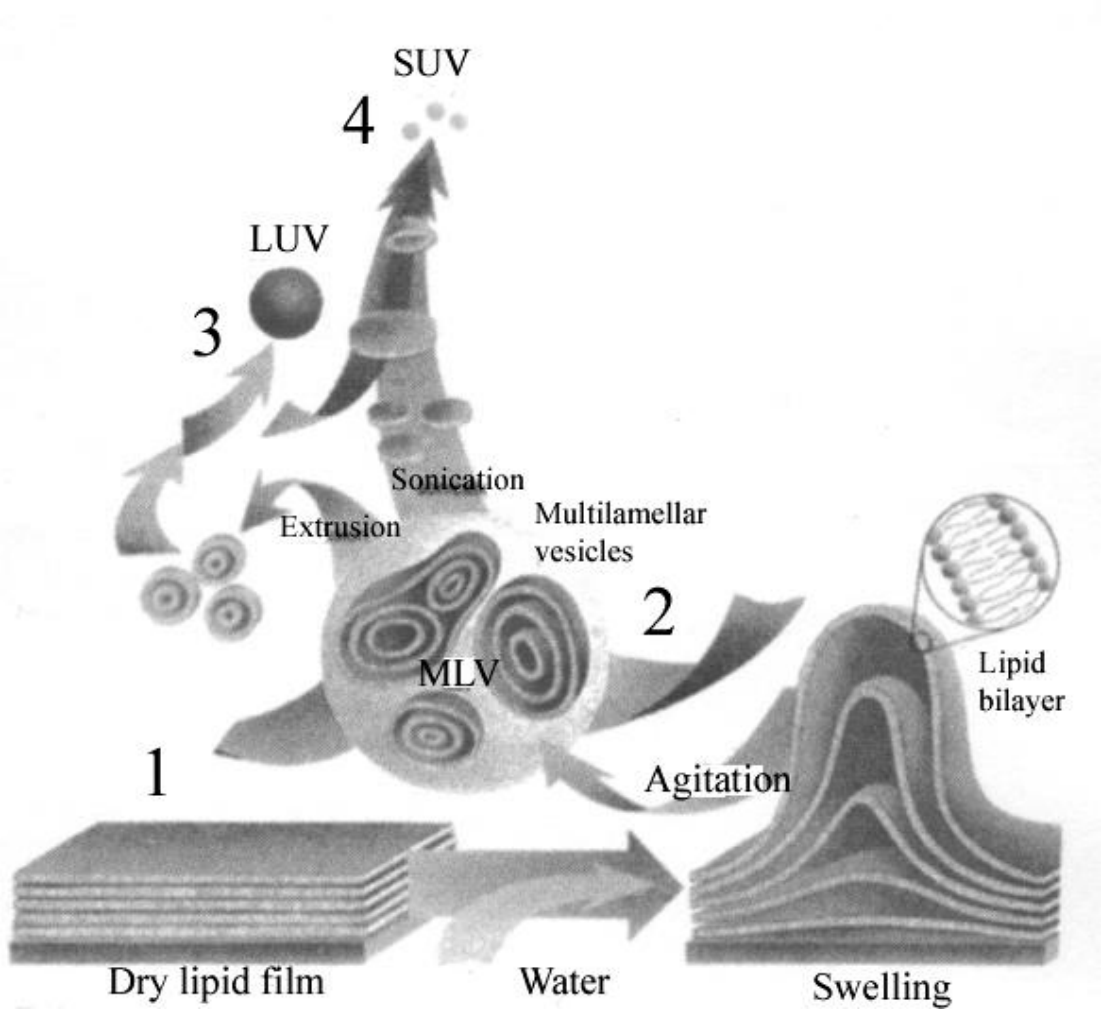

(1) Start of vesicle formation with a lipid film. (2) Addition of water causes the lipid to swell and agitation results MLV (3), extrusion of MLVs forms LUVs (4) or sonication results a homogenous population of SUVs adapted from, (Lasic 1997).

The insertion of a membrane protein into preformed vesicles can be done by the following methods of reconstitution:

Mechanical reconstitution: This procedure involves sonication of a mixed suspension of lipid and isolated proteins. The method has the disadvantage in that local probe

heating can lead to degradation and denaturation of membrane proteins and small size proteoliposomes are formed.

Direct reconstitution: This is one of the earliest approaches of reconstitution of membrane proteins into vesicles. It is carried out by simply mixing protein of interest with liposomes with or without appropriate detergent.

Organic solvent mediated reconstitution: The procedure involves mixing lipid vesicles with protein and using reverse phase evaporation method. However the organic solvents can alter the native structure of the protein by disrupting hydrophobic core of the protein that deterimines overall conformation.

Detergent mediated reconstitution of membrane protein: This is the most widely used method for reconstitution of membrane proteins into vesicles. The method involves solubilisation and purification of the membrane protein by the chosen detergent. The purified protein is supplemented with an excess lipid film and detergent, leading to a solution of MLVs containing protein, lipid and detergent. Next, the detergent is removed by various strategies including the use of dialysis, gel filtration, dilution or polystyrene beads. This results in incorporation of membrane protein into closed phospholipid bilayers.

Figure 3.3 illustrates how liposomes can be prepared using a mini extruder and a diagram of the componets used to make up the SRS.

Figure 3.3 (A) A flow diagram of preparation of liposomes and (B) a schematic of components used for preparing the SRS.

A

Phospholipid suspension
loaded into gas tight syringe

carefully place syringe into one end of the mini-extruder.

Place the device on the heat block and gently push the plunger of the filled syringe until the lipid solution is completely transferred to the alternate syringe.

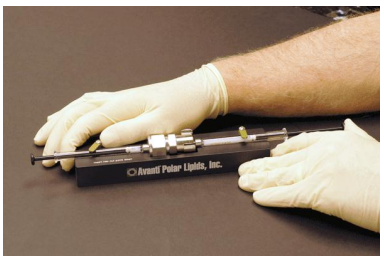

Repeat the above step up to 25 times, until the lipid suspension becomes clear.

Store lipid solution at 4ºC

Pictures shown were adapted from Avanti-Polar lipids website (http://avantilipids.com).

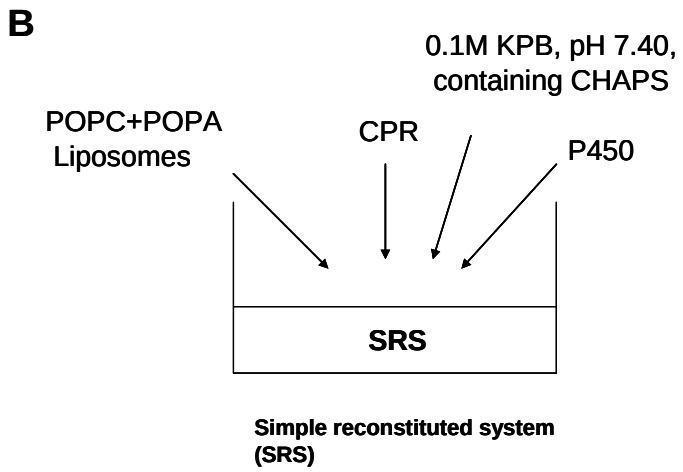

This Chapter describes the approaches developed for the expression and purification of CPR and P450 3A4 and their reconstitution into phospholipid bilayers.

3.2 Optimisation of the expression, solubilisation and purification of CPR

The ~6-kDa N-terminal domain of CPR serves to anchor the flavoprotein to the endoplasmic reticulum membrane and is necessary requirement for electron transfer interaction with P450. During the bacterial expression, purification, or long storage of CPR, bacterial proteases can easily cleave this 60 residue hydrophobic segment to form the truncated, water-soluble species, see Figure 1.6b (Bonina, Gilep, et al. 2005). Initially, full-length CPR was expressed and purified using method A, which was adapted in our laboratory from published methods (Smith, Tew, et al. 1994, Yasukochi and Masters 1976), see Figure 3.4 for flow diagram for the preparation of CPR. Method A resulted in ~70% of full-length flavoprotein (78-kDa) being proteolysed to soluble form (72-kDa), as shown in Figure 3.5.

Figure 3.4 Flow diagram showing some of the key steps in CPR preparation by method A.

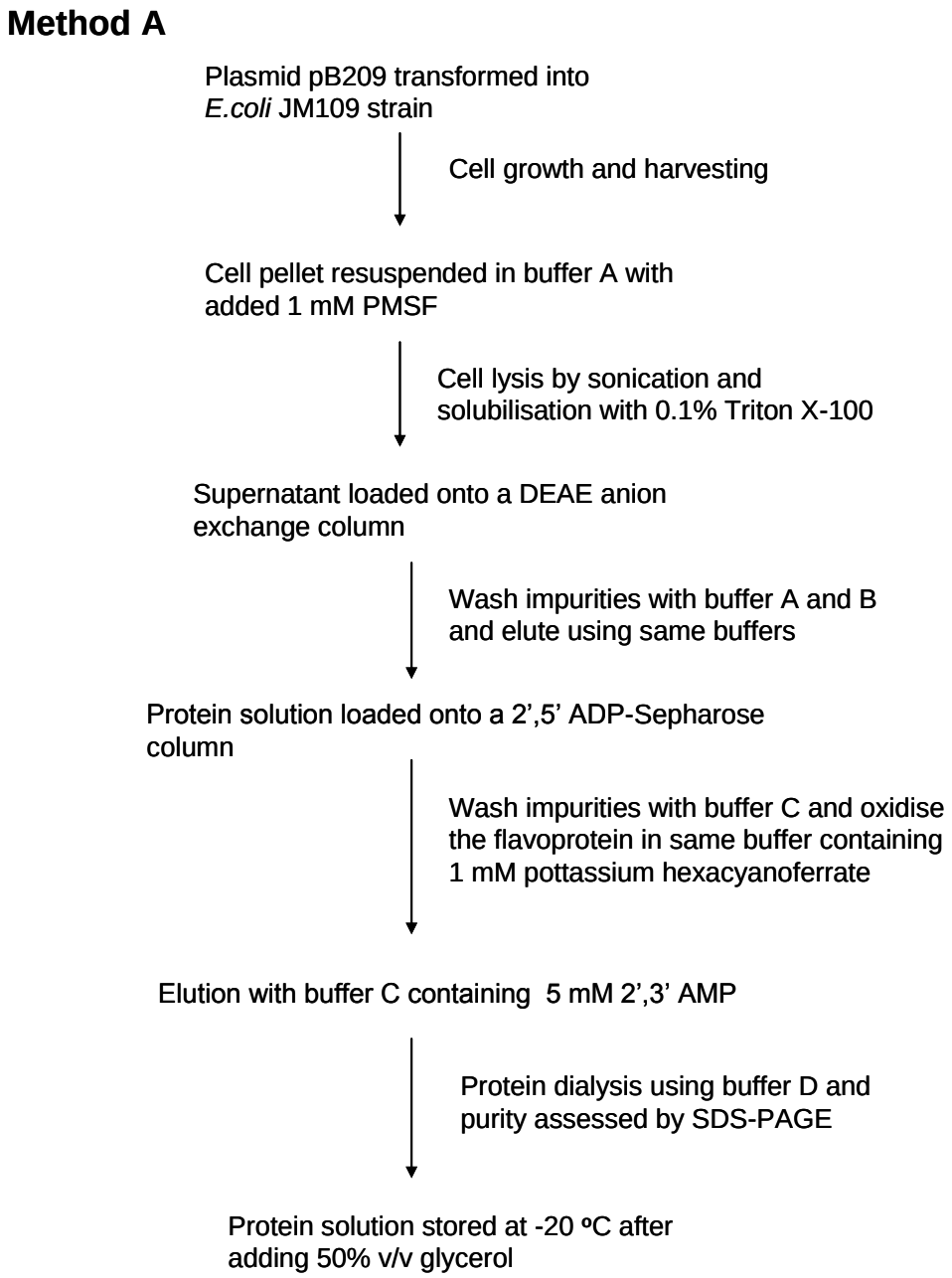

Buffer A contained 50 mM Tris-HCl, 10% v/v glycerol, 0.5 mM EDTA, 0.5 mM DTT, pH 7.80. Buffer B contains 30 mM Tris-HCl, 0.1% v/v Triton X-100, 10% v/v glycerol, 1 M NaCl, 0.1 mM DTT, 0.1 mM EDTA, pH 7.50. Buffer C contained 30 mM Tris-HCl, 0.1% v/v Triton X-100, 10% v/v glycerol, 0.15 M NaCl, 0.1 mM DTT, 0.1 mM EDTA, pH 7.50. Buffer D contained 100 mM KPB, 0.1% v/v Triton X-100, 10% v/v glycerol, pH 7.40.

Figure 3.5 SDS-PAGE gels of wild-type CPR purification.

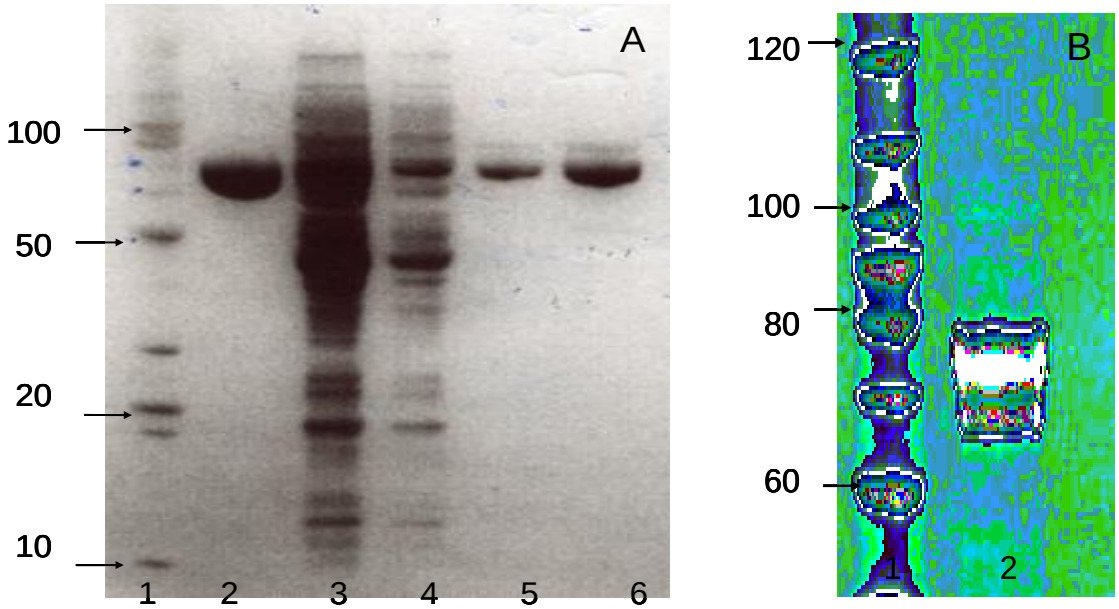

(A) Method A. Lane 1: Protein standards (kDa). Lane 2: Purified soluble CPR (72 kDa), Lane 3: 25000 RPM supernatant, Lane 4: Fractions from DEAE Sepharose, Lanes 5 and 6: Purified CPR, upper band as full length, (78-kDa) and lower band as soluble (72-kDa). (B) Method B Lane 1: Protein standards (kDa), Lane 2: Purified CPR upper band as full length (78-kDa) and lower band as soluble (72-kDa).

The flow diagram for preparation of the CPR using optimized method (method B) is shown in Figure 3.6. The modifications to method A considerably improved stability of the flavoprotein, with ~90% full-length content routinely achieved, judging visually from SDS-PAGE gel, Figure 3.4. All purified protein samples were stable for up to two weeks at 4 ℃, confirmed by SDS-PAGE analysis, and method B typically yielded 10-15 mg of purified full-length CPR per liter of cell culture. All purified CPR samples were assayed by their ability to reduce cytochrome *c*. The method relies on the absorbance difference at 550 nm of the reduced against oxidised cytochrome *c*. Specific activities were found in the range of 45-52 µmol/min/mg CPR, which are consistent

with the published values for purified soluble CPRs, 50-60-µmol/min/mg protein (Lamb, Warrilow, et al. 2001, Shen, Porter, et al. 1989, Yamazaki, Nakamura, et al. 2002).

Figure 3.6 Flow diagram showing some of the key steps in CPR preparation by method B.

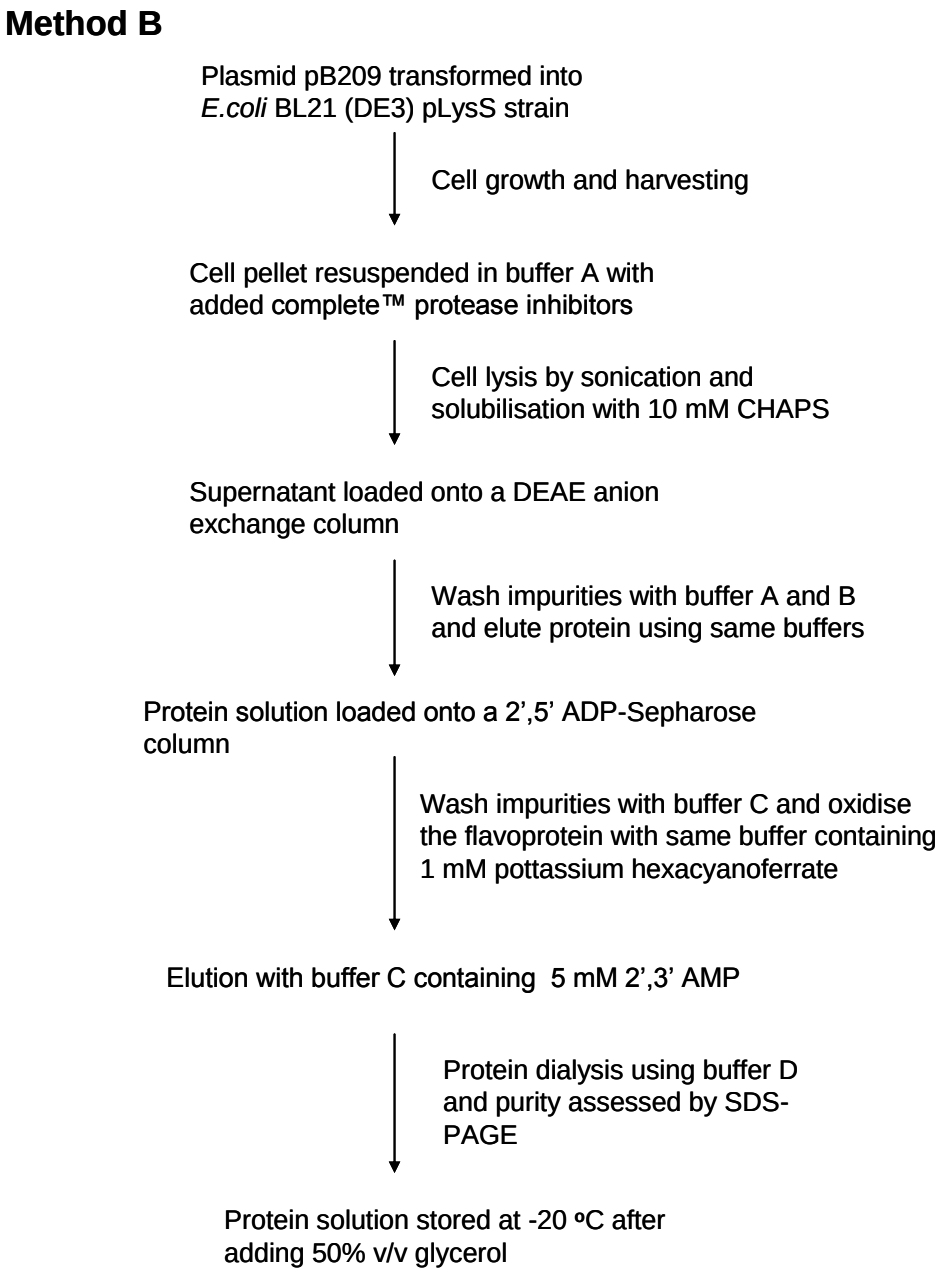

Buffer A contained 50 mM Tris-HCl, 10% v/v glycerol, 0.5 mM EDTA, 0.5 mM DTT, pH 7.80. Buffer B contained 30 mM Tris-HCl, 0.1% v/v Triton X-100, 10% v/v glycerol, 1 M NaCl, 0.1 mM DTT, 0.1 mM EDTA, pH 7.50. Buffer C contained 30 mM Tris-HCl, 0.1% v/v Triton X-100, 10% v/v glycerol, 0.15 M NaCl, 0.1 mM DTT, 0.1 mM EDTA, pH 7.50. Buffer D contained 100 mM KPB, 0.1% v/v Triton X-100, 10% v/v glycerol, pH 7.40.

3.2.1 Site directed mutagenesis of CPR

While method B yielded ~90% full-length CPR, proteolysis of the membrane binding segment was not eliminated completely. Site-directed mutagenesis was therefore carried out in an attempt to engineer a CPR stable to endogenous bacterial proteases. The protease sensitive site was identified by N-terminal sequencing of the purified protein, carried out from an SDS-PAGE gel at the Protein and Nucleic Acid Chemistry Laboratory (PNACL) at the University of Leicester. The site for proteolytic digestion of CPR was identified as threonine 58, and this residue was substituted to alanine (T58A) using the Quick-change™ site directed mutagenesis kit. In addition, a further two mutants were generated based on the study of Bonina et al (Bonina, Gilep, et al. 2005) where it was found that replacing conserved lysine 55 with glutamine in rat liver CPR stabilizes the flavoprotein to protease attack. Lysine 55 of the human enzyme was replaced by glutamine (K55Q), and the double mutant K55QT58A was also generated. DNA sequencing confirmed all three mutants were produced successfully, and these were expressed and purified by both methods. SDS PAGE analysis of mutants (Figure 3.7) show a slight improvement to the stability of the protein, particularly when purified by method B, but all mutants failed to yield protein that was completely stable to proteolysis.

Figure 3.7 SDS-PAGE of purified wild-type CPR and site-directed mutants.

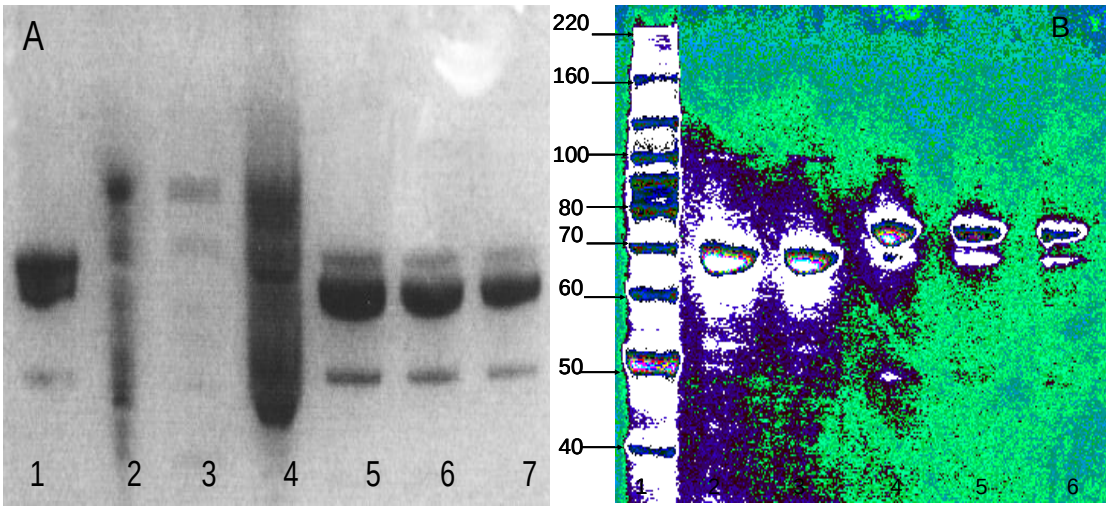

(A) Method A. Lane 1: Soluble wildtype CPR (72 kDa) Lane 2 and 3: DEAE anion flowthrough fractions, Lane 4: 2',5' ADP-Sepharose flowthrough fractions, Lane 5: CPR T58A, Lane 6, CPR K55Q and Lane 7, CPR K55QT58A (Upper bands 78 kDa and Lower bands 72 kDa). (B) Method B. Lane 1: Protein molecular weight standards (kDa). Lane 2 and 3: Soluble wild-type CPR (72 kDa), Lane 4, CPR T58A, Lane 5, CPR K55Q and Lane 6, CPR K55QT58A (Upper bands 78 kDa and Lower bands 72 kDa).

3.3 Expression and purification of P450 3A4

Catalytically active mammalian P450s with unmodified cDNAs have proved notoriously difficult to express in *E. coli* and usually require modifications in the amino–terminal region of the enzyme to obtain a high level of protein expression (Gonzalez and Korzekwa 1995). However, it was found in Professor Wolf's laboratory in Dundee that an increased level of P450 expression in *E. coli* was possible by fusing a bacterial leader sequence to the amino-terminus of the P450, thus avoiding the need to make mutations in the amino-terminal sequence of the P450 itself (Pritchard, Ossetian, et al. 1997). In this study, we used the expression construct (pB84) kindly provided by Professor Wolf, which was engineered to contain an amino-terminal ompA leader sequence. The protocol for expression and purification of P450 3A4 was developed in

our laboratory by Dr. Richard Ward (Ward 2003). The only modification here is the use of 5 mM instead of 2 mM CHAPS in purification buffers A1 and A2. Figure 3.7 shows a flow diagram of the expression and purification of P450 3A4, which was purified to essentially a single protein band on the SDS PAGE gel using Nickle HiTrap™ chelating column (Figure 3.8b); typical yields obtained averaged between 15-20 mg/L of cell culture.

Figure 3.8 Flow diagram showing some of the key steps in P450 3A4 preparation.

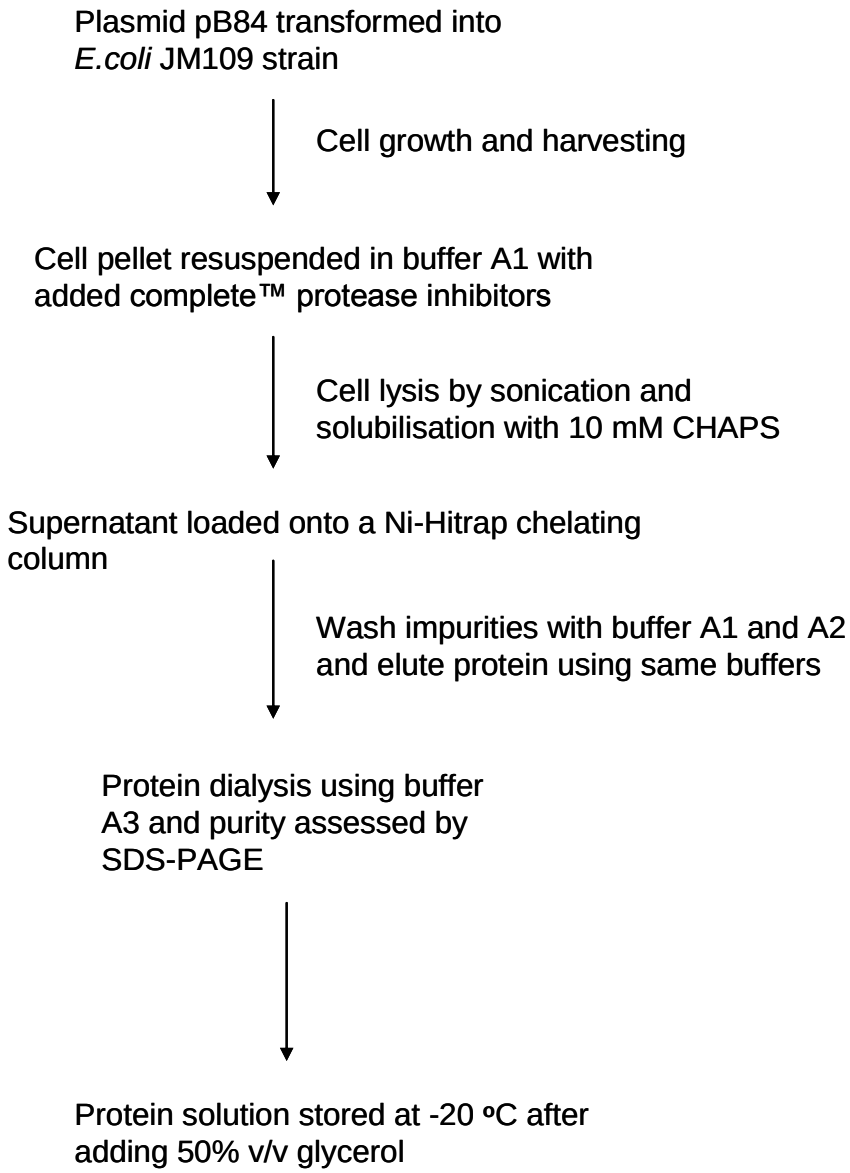

Buffer A1 contained 50 mM KPB, 0.5 M KCl, 20% v/v glycerol, pH 7.40. Buffer A2 contained 50 mM KPB, 5 mM CHAPS, 1 M imidazole and 10% v/v glycerol, pH 7.40. Buffer A3 contained 100 mM KPB, 0.1 mM DTT, 0.1 mM EDTA, 5 mM CHAPS, and 20% v/v glycerol, pH 7.40.

Figure 3.9 shows the absolute optical absorption spectrum and the reduced CO-difference spectrum of the purified P450. As is evident from the difference spectrum, protein samples were generally found to contain very little or no P420.

Figure 3.9 UV-visible spectra and SDS-PAGE gel of purified recombinant P450 3A4.

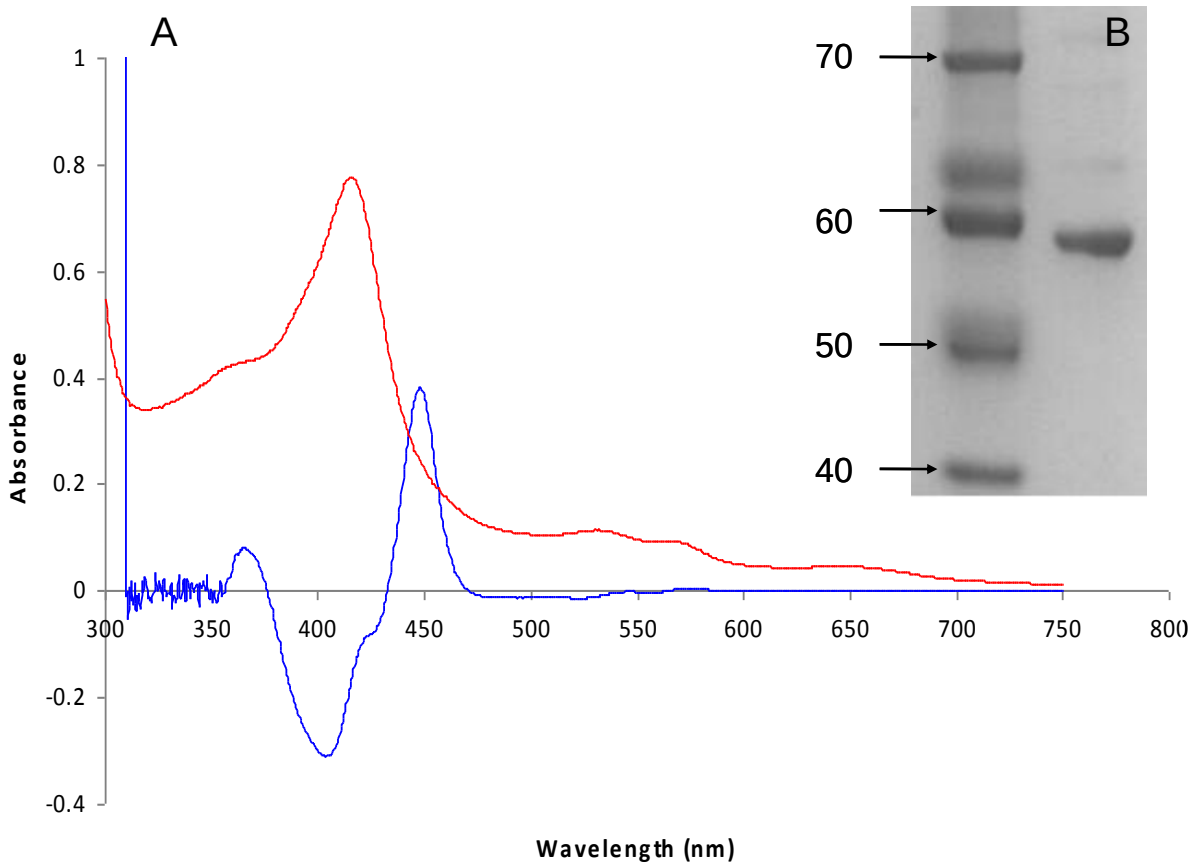

(A) Absorption spectrum of oxidised (Fe^{III}) (red) and sodium dithionite reduced (Fe^{II})-CO-difference spectrum (blue). (B) Lane 1: Protein molecular weight standards (kDa). Lane 2: purifiedP450 3A4 (~55 kDa).

P450 3A4 catalytic activity was measured using the fluorescent substrate 7-benzyloxyquinoline (7-BQ). P450 3A4 debenzylates 7-BQ to a highly fluorescent product, 7-hydroxyquinoline (7-HQ), and thus the course of the reaction can be followed fluorometrically, Figure 3.10.

Figure 3.10 Reaction scheme of metabolism of 7-BQ by P450 3A4.

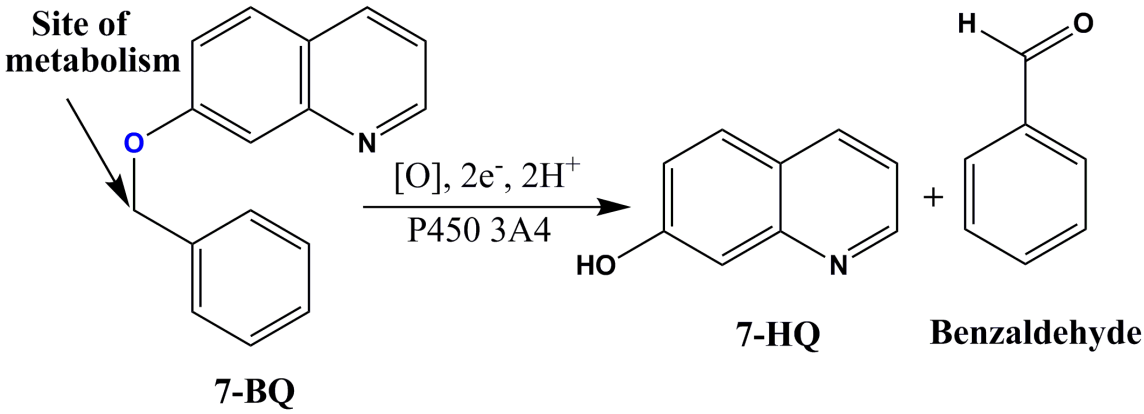

The 7-BQ assay has the advantages that it offers high sensitivity, is homogenous and simpler to conduct than assays requiring HPLC; it can be carried out with the enzyme in solution or in the membranous system. When P450 is in solution, organic peroxides, such as cumene hydroperoxide can provide both electrons and oxygen directly for substrate turnover without the need of molecular oxygen, NADPH and CPR, Figure 3.11. Electrons enter the substrate binding pocket of P450 ferric (resting state) and convert P450 active site directly to the catalytic active species (Ferryl-oxo-intermediate), as shown by Figure 3.12.

Figure 3.11 Reaction scheme of cumene hydroperoxide (CuOOH) supported 7-BQ oxidation by P450 3A4.

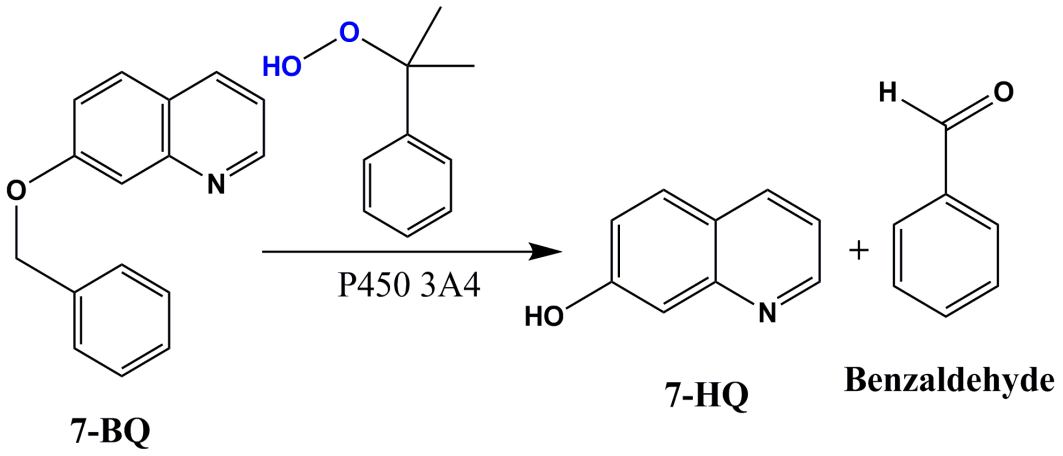

The cleavage of the O-O bond of CuOOH molecule can either occur homolytically or heterolytically.

Figure 3.12 Formation of active oxygen intermediate by cumene hydroperoxide.

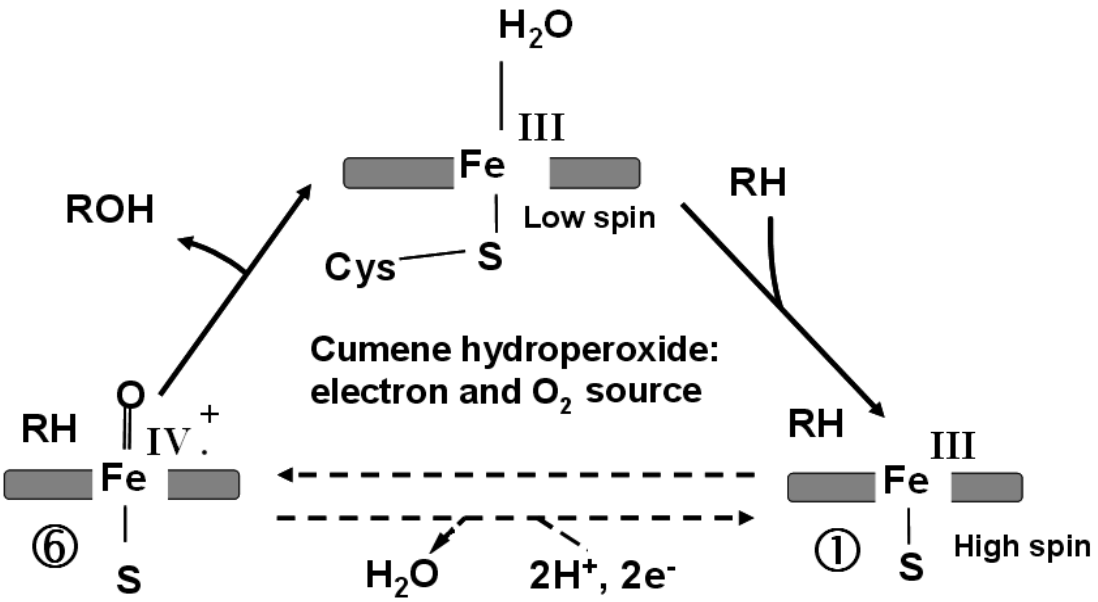

Intermediates 1 and 6 show substrate bound and active forms of P450, respectively. RH is the substrate and ROH is the yielded product.

There are two possible mechanisms for peroxide reduction of the P450, involving either heterolytic or homolytic scission of peroxide O-O bond, (Barr, Martin, et al. 1996, Rota, Barr, et al. 1997). In the heterolytic mechanism, first two electron reduction of the peroxide is followed by heterolysis of O-O bond cleavage that forms peroxyl radicals completely independent of oxygen (reaction 3.1 and 3.2). Thompson and Wand (Thompson and Wand 1985) with ^{18}O labeled experiments have shown that the peroxide oxygen is incorporated in the substrate during the hydroxylation reaction.

$$P450\text{-}Fe^{III} + ROOH \xrightarrow{\text{Heterolytic}} P450^{\cdot+}(Fe^{IV}=O) + ROH$$

$$P450^{\cdot+}(Fe^{IV}=O) + ROOH \longrightarrow P450(Fe^{IV}=O) + ROO^{\cdot}$$

Reaction 3.1-2

Where ROOH is the hydroperoxide. Alternatively, homolytic scission of O-O bond can result to form the initial alkoxyl radical, reaction 3.3.

$$P450\text{-}Fe^{III} + ROOH \xrightarrow{\text{Homolytic}} P450^{\cdot+}(Fe^{IV}=O) + RO^{\cdot} + H^{+}$$

Reaction 3.3

The subsequent β-scission of the alkoxyl radical yields peroxyl radical by indirect mechanism, reaction 3.4 and 5.

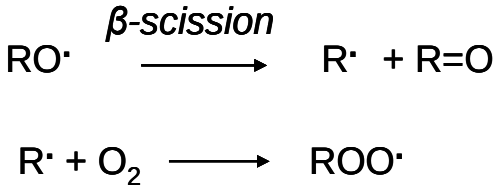

Reaction 3.4-5

Or peroxyl radical can also result from direct oxidation of the hydroperoxide by Fe^{III} ion or P450, reaction 3.6.

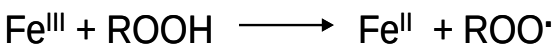

Reaction 3.6

The data in Table 3.1 shows 7-BQ turnover rates of P450 3A4 in solution. In order to investigate the effect of each detergent on the P450 activity, 0.1 % v/v Triton X-100 or 0.1 % w/v CHAPS were added to the assay buffer containing 0.5 μM P450 3A4. The 7-BQ turnover rates were decreased by 20 fold with Triton X-100 and were halved in the presence of CHAPS. These findings indicate that excess amount of detergent can lead to inhibition of P450 catalytic activity.

Table 3.1 7-BQ Assay in solution.

Sample condition	**Electron source**	**7-HQ formation rate nmol/min/nmol P450**
No detergent	Cumene hydroperoxide	2.0 ± 0.15
0.1% w/v CHAPS	Cumene hydroperoxide	1.0 ± 0.2
0.1% v/v Triton X-100	Cumene hydroperoxide	0.1 ± 0.15

The assay conditions were 0.5 μM P450 3A4 and 0.1 mM 7-BQ in 0.1M KPB, pH 7.40 containing 10% v/v glycerol. The reaction was initiated by 0.5 mM Cumene hydroperoxide. All values are average of +/- SD of three experiments.

Non-ionic detergents such as Triton X-100 were commonly employed in early P450 purification work, because they produced purer protein samples than could be achieved by using other compounds like sodium cholate, an anionic bile salt related to CHAPS. Triton X-100 was found to inhibit P450 reactions in a concentration dependent manner; at low concentrations the rate of metabolism of substrate aminopyrine was competitively inhibited (Denk, Schenkman, et al. 1971) and at higher concentration (near or at critical micelle concentration (CMC) the P450s ability to bind to the substrate was found to be diminished (Denk, Schenkman, et al. 1971, Wagner, Dean, et al. 1984, Wagner, Dean, et al. 1987). Hosea and Guengerich (Hosea and Guengerich 1998) studied the effect of range of detergents on the catalytic activity of P450 either in human liver microsomes or in a recombinant human reconstituted system. They found

that in particular, Triton N-101, which is structurally similar to Triton X-100, produced a marked inhibition in comparison to using sodium cholate (Lu, Levin, et al. 1974) and that both detergents are substrates of P450 3A4, which can competitively as well as non-competitively inhibit P450 activity.

3.3.1 Reconstitution of CPR and P450 3A4

For NADPH-dependent P450 catalytic assays, a simple reconstituted system (SRS) was prepared by mixing the desired amounts of CPR (purified by method A or B) and P450 3A4 with preformed liposomes with final dilution into 0.1 M KPB, pH 7.40, containing 10% v/v glycerol and 0.1% w/v CHAPS and incubating for 10 minutes at room temperature prior to assay. The 7-BQ assay was then conducted and data is shown in Table 3.2. Noticeably, rates of 7-HQ formation are slower with Triton X-100 CPR, which strongly suggests that Triton X-100 is inhibiting P450 catalytic activity in the reconstituted system.

Table 3.2 7-BQ debenzylation by P450 3A4 in the SRS.

Sample condition	**Electron source**	**7-HQ formation rate nmol/min/nmol P450**
SRS contained CHAPS purified CPR	Cumene hydroperoxide	1.95 ± 0.12
SRS contained Triton purified CPR	Cumene hydroperoxide	0.80 ± 0.1
SRS contained CHAPS purified CPR	NADPH	1.65 ± 0.05
SRS contained Triton purified CPR	NADPH	1.09 ± 0.2

SRS was prepared mixing CHAPS or Triton X-100 purified CPR (1 μM), 0.5 μM P450 3A4, 0.1 mM 7-BQ and 40 μM liposomes in 0.1 M KPB, pH 7.40, containing 10% v/v glycerol and 0.1% w/v CHAPS. The reaction was initiated by 0.5 mM Cumene hydroperoxide or NADPH. All rate values are the average +/- SD of three or more experiments.

3.3.2 NADPH-dependent reduction of P450 3A4

In the SRS, NADPH reduced CO-difference spectral studies were carried out to measure the total amount of P450 interacting with CPR. The reduction of P450 with NADPH was compared to the total amount of P450 reduced by sodium dithionite. The assay was also carried out in the absence of liposomes and in the presence of testosterone or 7-BQ. Figure 3.13 shows CO-difference spectra of P450 3A4 in the presence of various components of SRS and in *E. coli* membranes coexpressiong equimolar CPR and P450 3A4, reduced by NADPH or sodium dithionite, all the data are summarised in Table 3.3.

P450 reduction by sodium dithionite is shown in panel A of Figure 3.12, the spectrum shows very little P420 formation and at least 80% of the total amount of P450 was reduced. Panel B shows reduction of P450 3A4 by NADPH, with Triton X-100 solubilised CPR (method A), all the CO-difference spectra show a large amount of P420 formation. Spectrum 1 and 2 is in the absence and presence of liposomes, and almost identical amount of P450 is reduced. Addition of testosterone and 7-BQ has increased reduction to 11% and 15.4%. In presence of CHAPS CPR (panel C), reduction with or without liposomes is about 4 fold less than observed with Triton X-100 CPR in the SRS and ~40-50% P450 appeared to be converted into its denatured form, P420. With addition of testosterone and 7-BQ, P450 reduction has 3 fold increase and very little P420 have formed. In *E. coli* membranes (panel D), co-expressing equimolar quantities of P450 3A4 and CPR, reduction is ~2 fold higher of Triton CPR and ~8 fold higher than CHAPS CPR. There is notable stimulation of P450 reduction in the presence of substrate and all spectra are without P420.

Figure 3.13 Effect of various components of the SRS on the CO-difference spectra of P450 3A4 reduced with 0.2 mM NADPH.

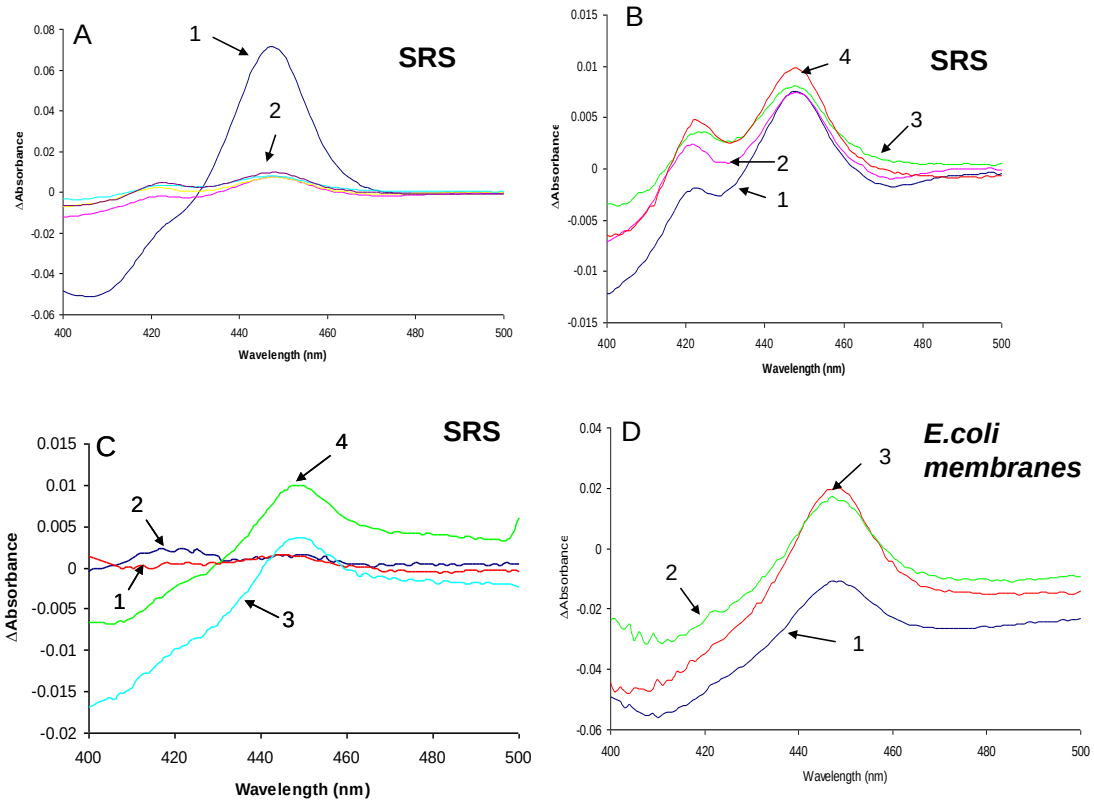

(A) CO-difference spectra of P450 3A4 reduced with few grains of sodium dithionite (1) and 0.2 mM NADPH (2). (B) Enlarged version of CO-difference spectra of P450 3A4 reduced by NADPH (as shown as 2 in A); with Triton-X-100 solubilised CPR in the SRS, 1, no liposomes; 2, with liposomes; 3, with testosterone; 4, with 7-BQ. (C) Same as B, except with CHAPS solubilised CPR in the SRS. (D) CO-difference spectra of P450 3A4 in E. coli membranes, reduced by NADPH; 1, no substrate; 2, with testosterone and 3, with 7-BQ. The SRS contained 1 μM P450 3A4, either 2 μM Triton X-100 or CHAPS solubilised CPR, 40 μM liposomes, 100 μM testosterone or 7-BQ in 0.1 M KPB (pH 7.40) containing 10% v/v glycerol, 0.1 % CHAPS or Triton X-100. E. coli membranes contained equimolar P450 3A4 and CPR.

Table 3.3 P450 3A4 reduction by NADPH in various reconstitution premixes and in E. coli membranes co-expressing equimolar of CPR and P450.

Sample condition	% of P450 reduction (No substrate)	% of P450 reduction (+Testosterone)	% of P450 reduction (+7-BQ)
1 μM P450 3A4, and 2 μM *CHAPS CPR* in 0.1 M KPB, pH 7.40, containing 10% v/v glycerol and 0.1% w/v CHAPS.	1.90 ±0.2		
1 μM P450 3A4, and 2 μM *Triton CPR* in 0.1 M KPB, pH 7.40, containing 10% v/v glycerol and 0.1% w/v CHAPS.	8.2 ±1.2		
1 μM P450 3A4, 2 μM *CHAPS CPR* and 40 μM *liposomes* in 0.1 M KPB, pH 7.40, containing 10% v/v glycerol and 0.1% w/v CHAPS.	2.20 ±0.6	6.26 ±0.8	7.0 ±2.2
1 μM P450 3A4, 2 μM *Triton CPR* and 40 μM *liposomes* in 0.1 M KPB, pH 7.40, containing 10% v/v glycerol and 0.1% w/v CHAPS	8.70 ±1.4	11 ±0.9	15.4 ±1.30
E. coli membranes co-expressing equimolar amounts of P450 3A4 and CPR	15.4 ±2	32 ±4.3	37 ±3.1

The differences in conditions are shown in itailics and 0.2 mM NADPH comcrntration was used to reduce the enzyme. All rate values are the means +/- SD of at least three experiments

There is a negligible effect of liposomes on the amount of P450 reduced in the SRS, which indicates that the proteins are not incorporating into liposomes but are probably forming large aggregates. Numerous publications report that these enzymes have a tendency to aggregate both in solution and in the microsomal membrane. Early studies by Bendt and Gray (Dean and Gray 1982, Myasoedova and Berndt 1990) suggested that P450 2B4 and P450 1A2 exist in solution as hexamers or heptamers. The aggregation state of these enzymes was decreased by using the non-ionic detergent, n-octylglucoside, but adding enough detergent to completely abolish aggregation resulted in the total loss of CPR supported monooxygenase activity. Kawato and colleagues (Gut, Richter, et al. 1982, Kawato, Gut, et al. 1982) carried out rotational diffusional studies and observed that some fraction of P450 was immobilised both in the reconstituted system and in microsomes. This immobilisation of P450 was attributed to the formation of large P450 aggregates and a decline in the fraction of immobile P450 was brought about by including CPR or b_5 in the membrane or increasing the lipid:P450 molar ratio.

In the present study, the standard lipid-to-protein (L:P) molar ratio used to prepare SRS was 40:1. By comparison, Kim and co-workers have used L:P ratio of 100:1 for their reconstituted system containing P450 3A4, CPR and liposomes. Taniguchi et al have prepared a reconstituted system containing CPR, P450 2B4 and lipid vesicles at molar ratio of 1:1:400 (Taniguchi, Imai, et al. 1987). Guengerich and co-workers have reconstituted P450 3A4, CPR, b_5 and lipid vesicles at ratio of 1:3:2:100 (Yamazaki, Johnson, et al. 1996). We increased the L:P ratio by 10-fold in an attempt to incorporate more proteins in the liposomes, but there was no significant change observed in the amount of P450 reduced by NADPH. This implies that the

proteins remained highly aggregated and may require adding detergent for dissociation and incorporation into liposomes.

Notwithstanding the low level of protein incorporation in the SRS, the P450 reduction is distinctly stimulated by the presence of substrate and the values obtained in the presence of testosterone are in good agreement with those of Kim et al (Kim, Ahn, et al. 2003), who reported 6.5-7.0% reduction measured from their CO-difference experiments with P450 3A4 in a reconstituted system. Interestingly, there is a clear difference in the reduction of P450 in the absence or presence of liposomes depending on which detergent was used to purify CPR, which suggests that the detergent has not been removed from CPR by dialysis. There is clearly a large amount of P420 formation in the presence of Triton X-100 solubilised CPR in the SRS, which strongly indicates that this detergent is deleterious to P450. This may be a result of Triton X-100 reaching its CMC (0.01% v/v), so the P450 that is being reduced is likely incorporated into a mixture of detergent/lipid micelles. As Triton-X-100 has a low CMC (0.01% v/v), it cannot be separated from protein samples using common methods like dialysis or gel filtration. CHAPS, on the other hand, has the advantage of having a high CMC (0.6% w/v) allowing these methods to be used.

These findings, taken together with the results of 7-BQ assay, demonstrate that Triton X-100 has a strong inhibitory effect on the P450 activity, and due to its difficulty of removing from purified CPR samples, it was replaced by CHAPS for routine preparation of CPR.

3.3.3 Kinetics of P450 3A4 reduction by CPR in SRS

In order to analyse the first electron transfer (species 1 to 2, Chapter 1) from CPR to ferric P450 in SRS, single wavelength stopped-flow absorption studies were performed under an anaerobic CO atmosphere. The formation of the CO complex of the

reduced P450 was monitored at 448 nm and transients were collected over a timescale from 0.2 to 50 s. Figure 3.14 shows kinetics of P450 reduction in the presence of testosterone. There is an initial rapid decrease in absorbance which corresponds to flavin reduction, followed by an increase in absorbance that represents the reduction of the haem protein. The reduction of P450 in the presence of testosterone exhibits biphasic kinetics and the reaction trace is best fitted to the sum of two first order reactions, ~70% of the total P450 is reduced at $k_1 = 0.32\ s^{-1}$ and ~30% at $k_2 = 0.03\ s^{-1}$. In the absence of substrate, P450 reduction rate was very slow. The electron transfer rate measured in the presence of testosterone is about 10-fold faster than that previously reported for P450 3A4 in SRS containing P450 3A4, CPR, phosphatidylcholine, phosphatidylserine and sodium cholate (Yamazaki, Johnson, et al. 1996). The increase in rate of reduction is because the substrate raises the redox potential of the haem, which increases the theromodynamic driving force of the reaction (Das, Grinkova, et al. 2007, Sligar, Cinti, et al. 1979).

Guengerich and co-workers have reported that reduction of ferric P450 3A4 by CPR in their reconstituted system is entirely dependent on the presence of cytochrome b_5, with rate of $<0.03\ s^{-1}$ without cytochrome b_5 as compared to 12-20 s^{-1} in its presence (Guengerich and Johnson 1997, Yamazaki, Johnson, et al. 1996, Yamazaki, Ueng, et al. 1995). In other systems, the rate of reduction of P450 3A4 was found to be variable, for example in baculovirus microsomes, the rate was 36.5 s^{-1} without substrate and 38 s^{-1} with testosterone, indicating that rapid reduction of P450 in this system does not require substrate binding. Reduction of P450 3A4 in human liver microsomes was observed to be up to 50-fold slower than in baculovirus microsomes.

Figure 3.14 Time course of P450 3A4 reduction monitored at 448 nm by formation of the Fe^{II}-CO complex in a stopped-flow spectrophotometer at 25 ^{o}C.

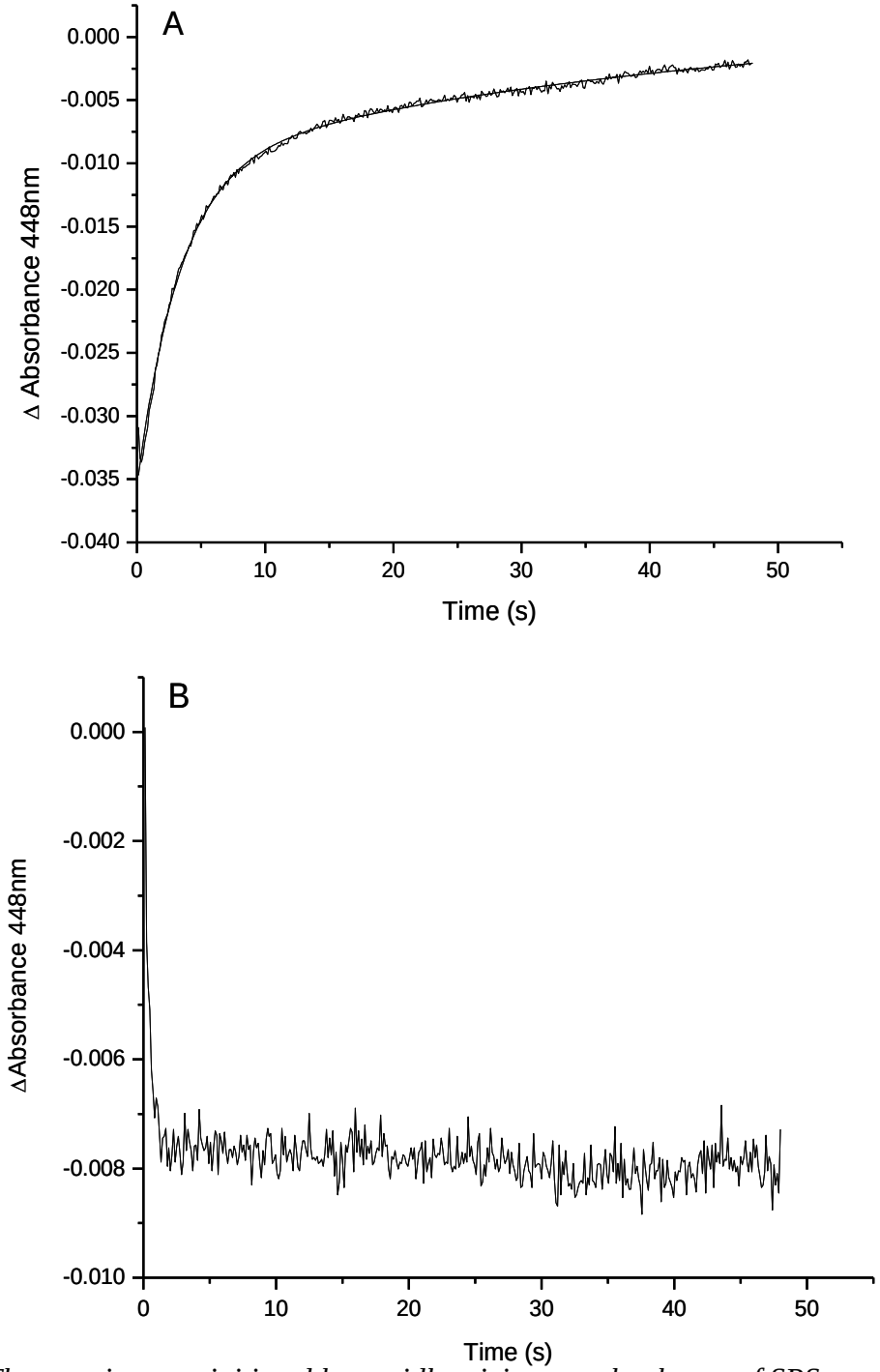

(A) The reaction was initiated by rapidly mixing equal volumes of SRS containing 8 μM P450 3A4, 4 μM CHAPS purified CPR, 160 μM liposomes, 0.5 mM testosterone in 0.1 M KPB, pH 7.40, containing 10% v/v glycerol and 0.1% w/v CHAPS, with 0.4 mM NADPH, 0.5 mM testosterone in the same buffer. (B) Reaction without testosterone.

3.4 Separation of proteoliposomes from protein aggregates

The main purpose of charactersing SRS was to obtain a well defined and controllable system that would allow us to carry out accurate measurements by kinetic studies. The charactertised SRS (or proteoliposomes) would be detergent and aggregate free containing only the anchored proteins in the liposomes. The lipid environment would be also stimulated providing a highly functional system.

3.4.1 Glycerol density centrifugation

As an initial approach, glycerol density gradient centrifugation was carried out to separate proteins incorporated into liposomes from unbound proteins. Analysis of the purified SRS by SDS-PAGE showed only full-length CPR and P450 3A4 in the 30% v/v glycerol/buffer interface and purified SRS was fully reducible by NADPH CO-difference spectroscopy, Figure 3.15. Isolation of proteoliposomes from unbound proteins has the advantage of preventing P420 formation as the proteins that remain would be fully inserted into liposomes and that the truncated CPR would also be removed from the SRS sample. However, the more practical method of gel filtration chromatography was employed to purify SRS. The gel filtration technique can be used to investigate the oligomeric state of individual proteins as well as removing detergent, which leaves behind detergent-free physically incorporated proteins in the liposomes.

Figure 3.15 Analysis of proteoliposomes by CO-difference spectroscopy and SDS-PAGE.

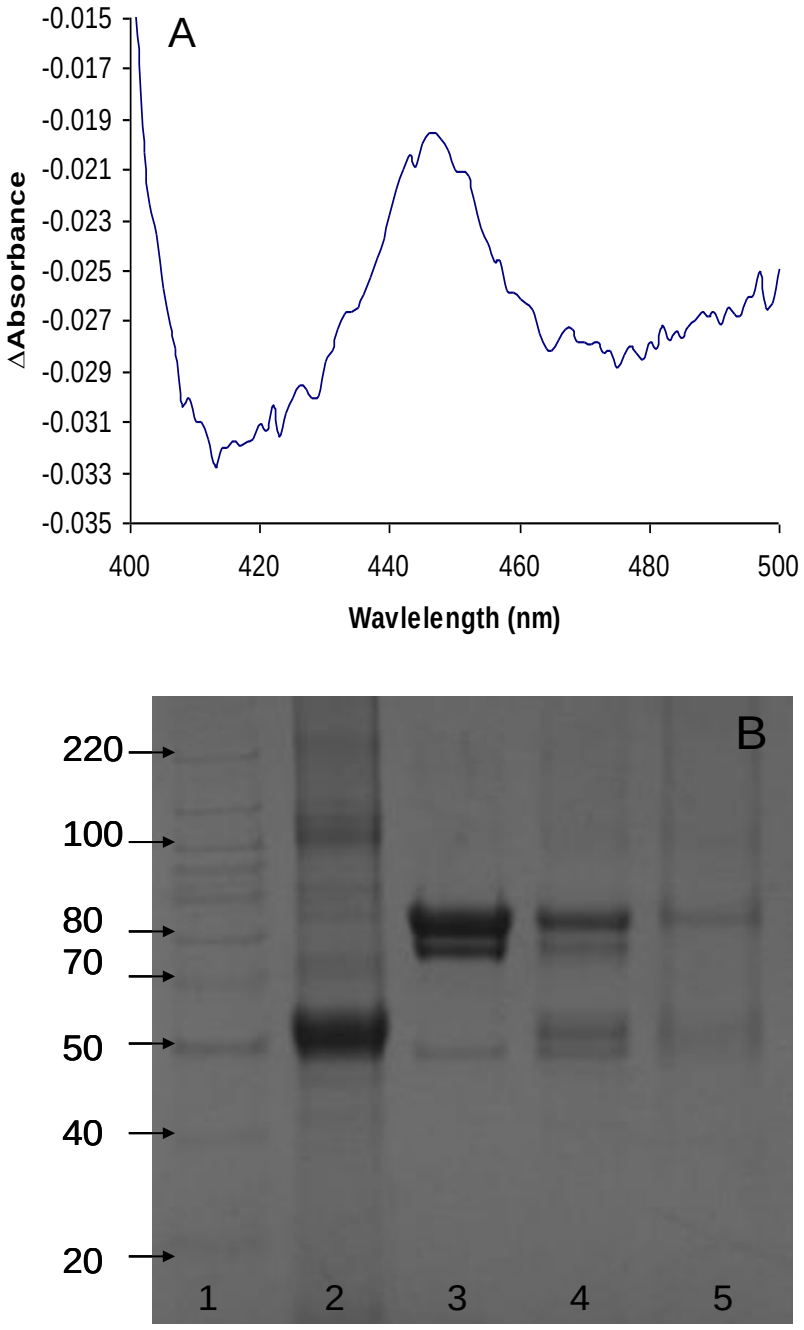

(A) NADPH reduced CO-difference spectrum of P450 3A4 in SRS purified on a discontinuous glycerol gradient, in the presence of 0.5 mM testosterone and (B) SDS-PAGE analysis of the purified SRS, Lane 1: Protein standards; Lane 2: purified P450 3A4; Lane 3: Purified CPR; Lane 4: SRS prior to purification; Lane 5: SRS post purification.

3.5 Characterisation of SRS using size exclusion chromatography

SRS was subjected to gel filtration in order to determine the oligomeric state of P450 and CPR and to purify SRS from aggregates. Initially, individual components were characterised by chromatography on a Superdex 200 PC 3.2/30 column, as shown in Figure 3.16.

Figure 3.16 Superdex 200 PC 3.2/30 chromatography of SRS components and SDS-PAGE analysis of CPR.

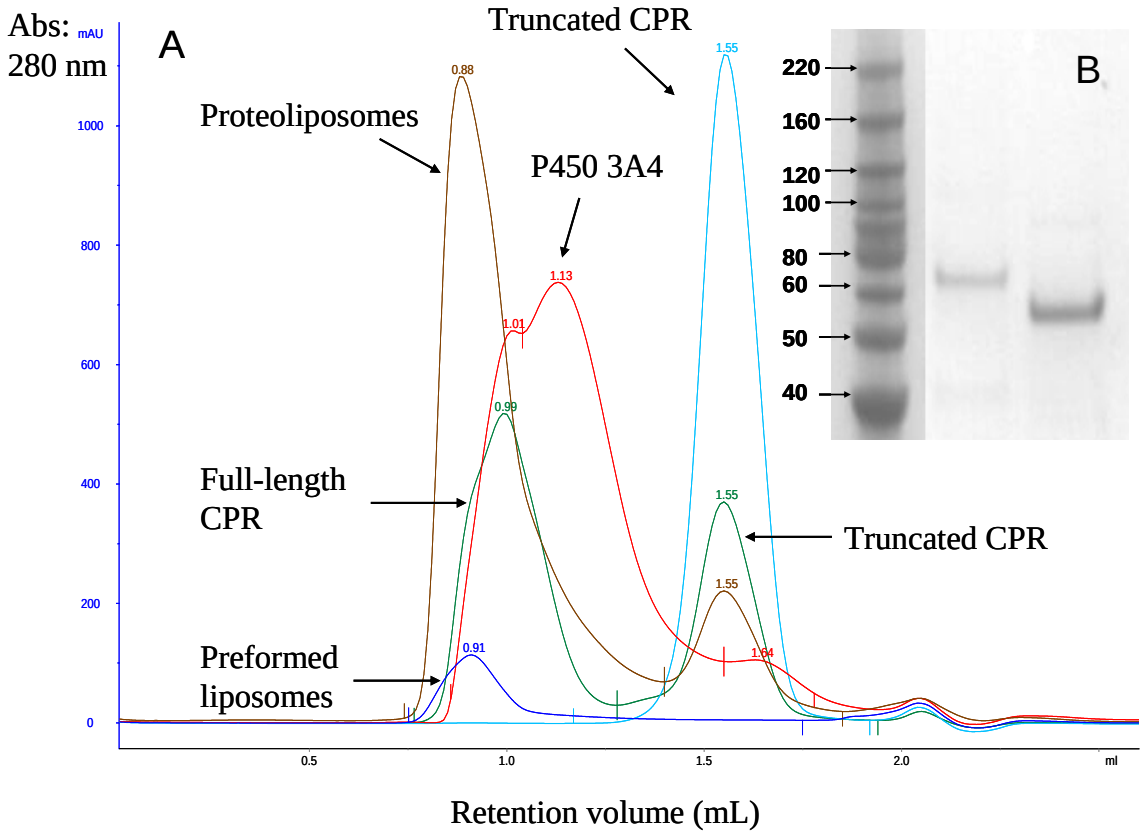

(A) Elution profiles of the SRS components were followed by monitoring absorbance at 280 nm. (B) SDS-PAGE gel of wildtype CPR eluates from Superdex 200 PC 3.2/30 column. Lane 1, full-length CPR (78 kDa) and Lane 2, proteolysed CPR (72 kDa).

The CPR elutes as two species, a peak at 0.99 mL, indicative of large aggregates of having molecular weight over 669 kDa, and second peak at the same position as soluble CPR, 1.55 mL, corresponding to the monomer. The fractions under the peaks were analysed by SDS-PAGE gel (Figure 3.16b); the first peak is comprised of intact species (Lane 1) and second was truncated CPR (Lane 2). The presence of the hydrophobic N-terminal sequence thus leads to aggregation. The P450 chromatogram has a shoulder peak eluting at 1.01 mL with the main elution peak at 1.13 mL, both species corresponding to aggregates of >669 kDa, and a species eluting at 1.64 mL which is a monomer. The liposomes elute as a single species in the void volume, whereas the proteoliposome preparation shows two peaks (Figure 3.17), a broad peak eluting in the void volume which contains both P450 and intact CPR, and a much smaller peak corresponding to proteolysed CPR.

Figure 3.17 Elution profile of SRS on Superdex 200 PC 3.2/30 column.

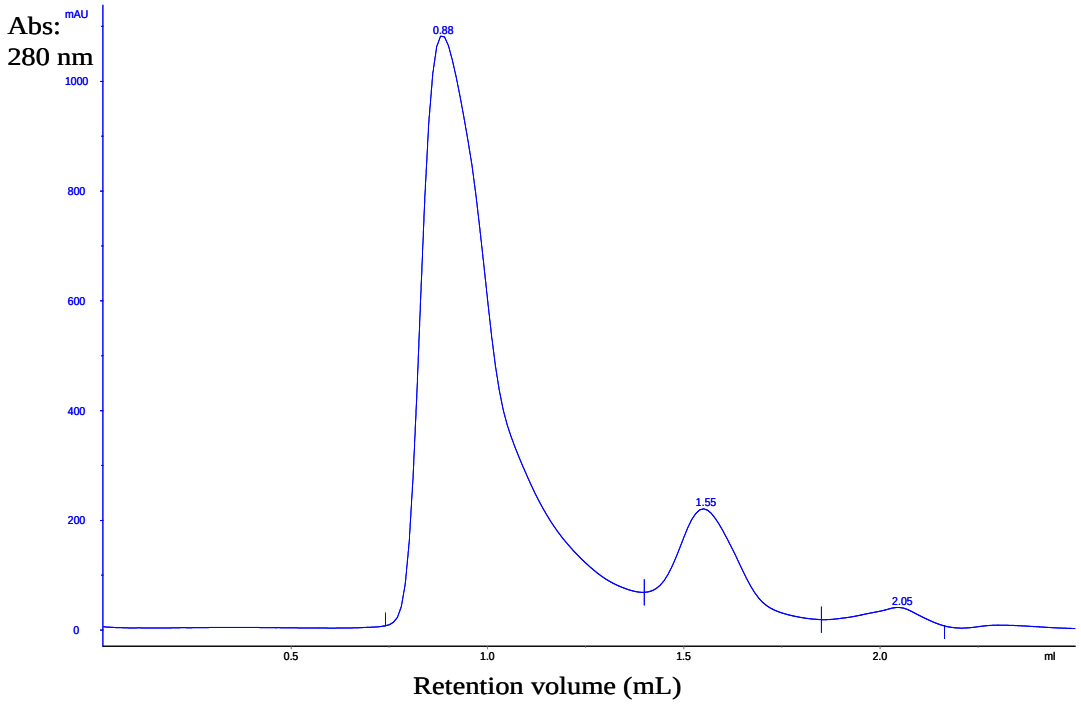

Elution was followed by monitoring absorbance at 280 nm.

As a larger volume of proteoliposomes was needed for kinetic and spectroscopic studies, the analytical Superdex 200 PC 3.2/30 column was replaced by a Hiload Superdex 26/60 column.

Figure 3.18 Superdex Hiload 26/60 eluates of the SRS and reconstituted protein mixture.

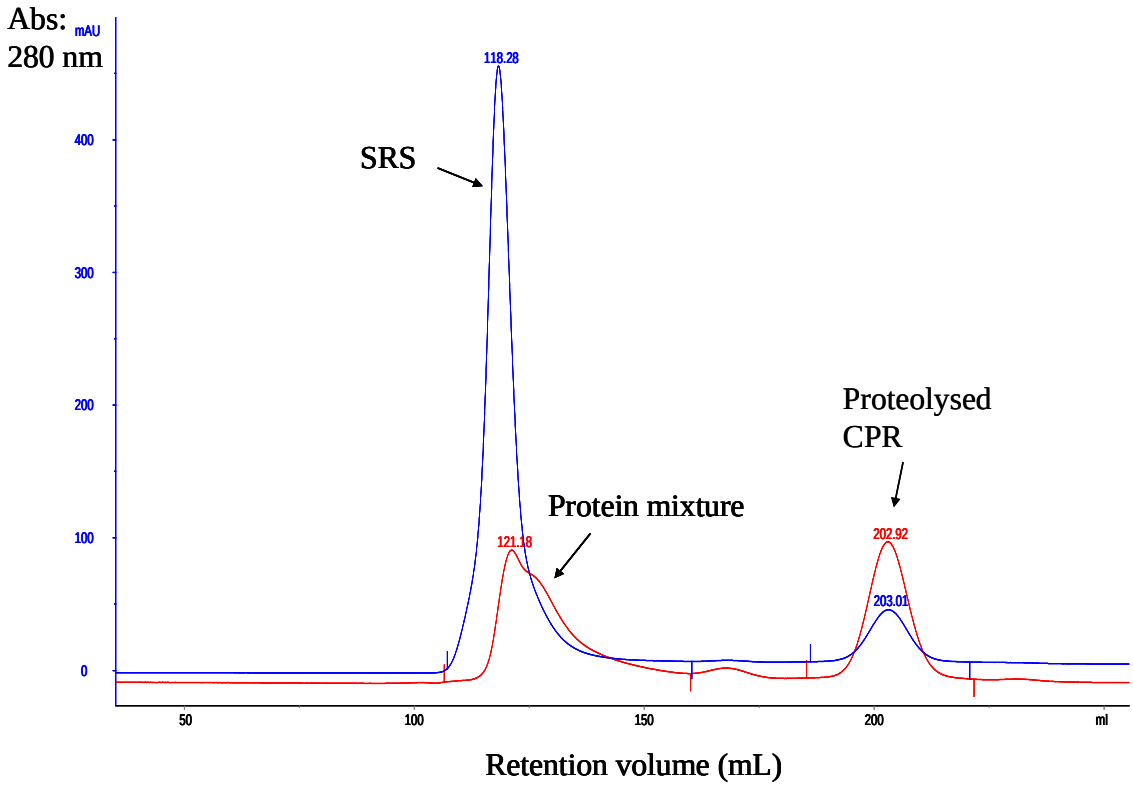

Elution profile was followed at 280 nm.

Samples of SRS and of the lipid free system were injected on the column; as seen in Figure 3.19, separation of proteoliposomes from the large protein aggregates was not achieved with Superdex Hiload 26/60 column as both samples had eluted in the void volume. A column with larger exclusion limit of 600 kDa was required to obtain adequate separation and thus a Superose 6 HR 10/30 column, which had an exclusion limit of about 6000 kDa, was employed.

Figure 3.19 Superose 6 HR 10/30 column chromatograpy of SRS and protein mixture and SDS-PAGE analysis of fraction of SRS.

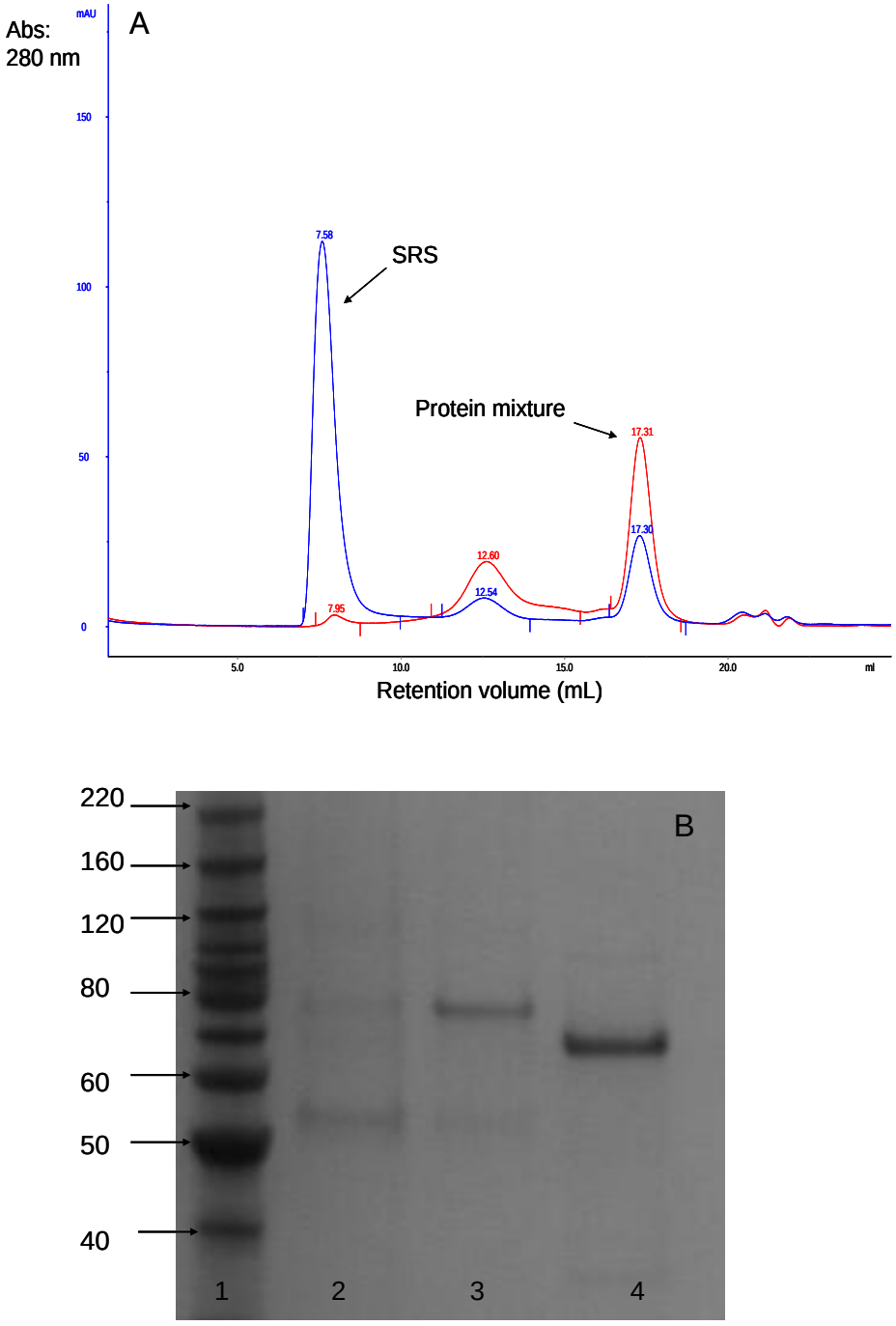

(A) Superose 6 HR 10/30 eluates of the proteoliposomes and protein mixture monitored at 280 nm. (B) SDS-PAGE of fractions from peak 1, 2 and 3 of the proteoliposomes. Lane 1: Protein standards. Lane 2: Pooled samples from void volume identified as full-length CPR and P450 3A4; Lane 3: Aggregated P450 and CPR and Lane 4: Proteolysed CPR.

The elution profiles of the proteoliposomes and of the protein mixture in the absence of lipids on the Superose 6 10/30 column are shown in Figure 3.19. Proteoliposomes elute as a broad peak in the void volume; a smaller peak at 12.60 mL contains protein oligomers that have molecular weight over 669 kDa. The later peak eluting at 17 mL was found to contain only the cleaved CPR, see Figure 3.18. The chromatogram of the reconstituted proteins (without liposomes) also shows three different peaks: a minor peak in the void volume and a peak at 12.60 mL both correspond to large aggregates of molecular weight over 669 kDa, while the third peak is the elution of the cleaved CPR. Figure 3.20 shows elution profile of proteoliposomes on Superose 6 prepgrade column monitored at wavelengths 280, 420 and 450 nm.

Figure 3.20 Superose 6 column chromatograpy of SRS.

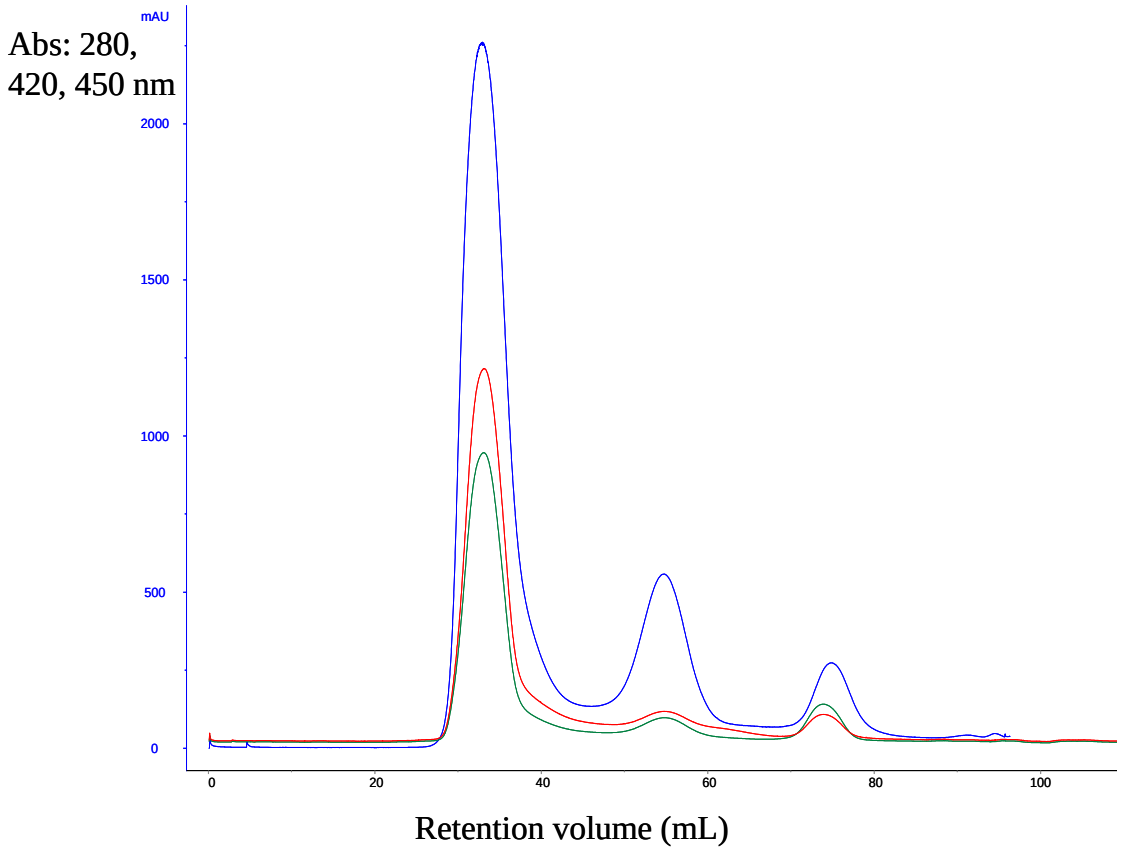

(A) Elution profile of proteoliposomes on a Superose 6 column monitored at absorbance, 280 nm (blue), 420 nm (red for P450) and 450 nm (green for CPR). SRS was prepared mixing 10 µM of each P450 3A4 and CPR and 10 mM liposomes in 0.1 M KPB (pH 7.40) containing 0.1% w/v CHAPS and 10% v/v glycerol and 5 mL sample was injected on the column.

3.6 Characterisation of the purified proteoliposomes

3.6.1 CO-difference spectroscopy

The evidence in the preceding section shows that fractions collected from the void volume of Superose 6 column contained only full-length CPR and P450 which are physically incorporated in the liposomes. At an L:P molar ratio of 40:1, less than 10% of the total amount of protein was incorporated into liposomes. The L:P ratio was varied from 40:1 to 2000:1 in order to obtain maximum amount of protein into liposomes; at the optimal ratio of 1000:1 between 20-30% of the total proteins were found to be incorporated. We also increased the CHAPS concentration from 0.1-1% w/v in the reconstitution buffer, but there was no increase in the amount of protein incorporated. CHAPS was then substituted by 0.1% v/w sodium cholate in the reconstitution buffer; this led to an increase in the amount of protein incorporated in the liposomes, but this detergent also caused a substantial amount of P420 formation, which indicated that sodium cholate had not been removed by Superose 6 chromatography.

The extent of reduction of P450 by NADPH in the presence of 0.5 mM testosterone was at least 10 fold higher in the purified proteoliposomes than observed in SRS. P450 was 10 (± 2)% reducible without substrate and 75 (±4)% reducible in the presence of testosterone. This implies that the Superose 6 chromatography efficiently yields preparations in which the enzymes are fully incorporated into liposomes. Figure 3.21 shows a typical NADPH and dithionite reduced CO-difference spectrum of P450 3A4 in proteoliposomes. The dithionite CO-reduced spectrum has a P420 peak which may be a result of excess dithionite used to reduce such a small quantity of P450. By contrast, the NADPH-reduced spectrum is completely free from P420.

Figure 3.21 Typical CO-difference spectra of P450 3A4 in proteoliposomes.

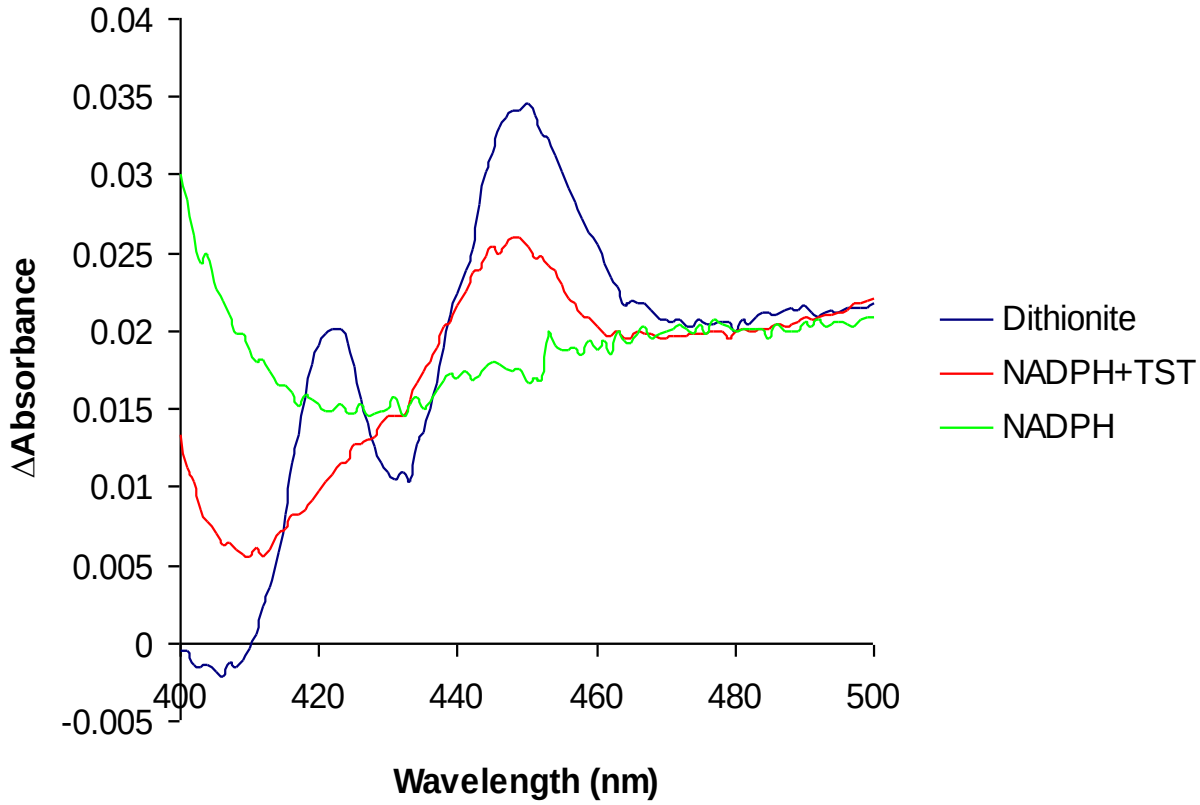

Proteoliposomes contained 0.1 μM CPR and 0.1 μM P450 3A4, reduced with 0.2 mM NADPH and a few milligrams of sodium dithionite.

These results are consistent with the work of Reed et al (Reed, Kelley, et al. 2006), who published their findings after we had done our work on the development of our reconstituted system. Their work demonstrated that incorporation of CPR with P450 2B4 or 1A2 into liposomes by cholate dialysis or cholate-gel-filtration method results in 12-fold stimulation in P450 monooxygenase activity compared with SRS prepared using a standard method. They used three different methods to prepare the reconstituted system, cholate dialysis, gel-filtration and a standard procedure. The standard method involved solubilising CPR, P450, liposomes (either using dilauroylphosphatidylcholine (DLPC) or bovine liver phosphatidylcholine (BPC) with sodium cholate and

preincubating the SRS for 1.5-2 hours prior to assays). Gel-filtration method involved removal of sodium cholate by Superdex G25 column, whereas in CD method, detergent is reduced from SRS by dialyzing with several changes of large volume of buffer. Reconstituted systems prepared by all three methods where subjected to characterisation on Superose 6 column. Whereas, our procedure involved incorporation of CHAPS solubilised CPR and P450 3A4 into preformed liposomes with final dilution into KPB (pH 7.40) containing 0.1% w/v CHAPS followed by pre-incubatiion of the SRS at room temperature for 10 minutes prior to subjecting on the Superose 6 chromatography. The protein incorporation efficiency reported by Reed et al were, 40% of the CPR and 27% of the P450 2B4 incorporated into DLPC and 13% of the CPR and 37% of the P450 2B4 incorporated into BPC by gel filteration. With CD method, 40% of the CPR and 96% of the P450 2B4 were found to be incorporating into liposomes. Whereas, 98% of the P450 1A2 embedded in BPC and P450 1A2 also better facilitated the incorporation of CPR (64%) than did P450 2B4. Although, the CD and gel-filtration methods were effective in incorporating higher amount of CPR and P450 into liposomes, both methods were found to have caused a significant loss in spectrally detectable carbonmonoxy haem in P450 enzyme, which was attributed to incubation of P450 with sodium cholate, consisted with our findings with sodium cholate. In a more recent study, Reed et al (Reed, Brignac-Huber, et al. 2008) have reported further improvements to the reconstitution method by using Biobeads SM-2 to remove the detergent instead of employing lengthy dialysis procedure or size exclusion chromatography. This optimised method resulted in higher incorporation efficiencies and decreased protein degradation.

These findings all suggest that physically anchoring enzymes into liposomes stimulates P450 reduction and catalytic activity, which is a likely cause of bringing two

enzymes together productively when incorporated in the liposomes and thus providing a more favorable environment for catalysis.

3.6.2 Electron microscopy of proteoliposomes

Liposomes and proteoliposomes were also characterised by negative staining electron microscopy. As shown in Figure 3.22, liposomes are observed as relatively spherical particles with average diameter of 107 ±6 nm, which is consistent in size, as the liposomes were prepared by extrusion technique that involved lipid suspension being forced through two stacked polycarbonate filters of 100 nm pore size. By contrast, proteoliposomes are seen as discrete particles that are predominantly ellipsoidal in shape and have a mean diameter of approximately 201 ±15 nm. Some structures appear to be shrunken and collapsed, which is likely due to the dehydration steps used during sample preparation for this technique.

Figure 3.22 Electron micrographs of negatively stained (A) liposomes and (B) proteoliposomes.

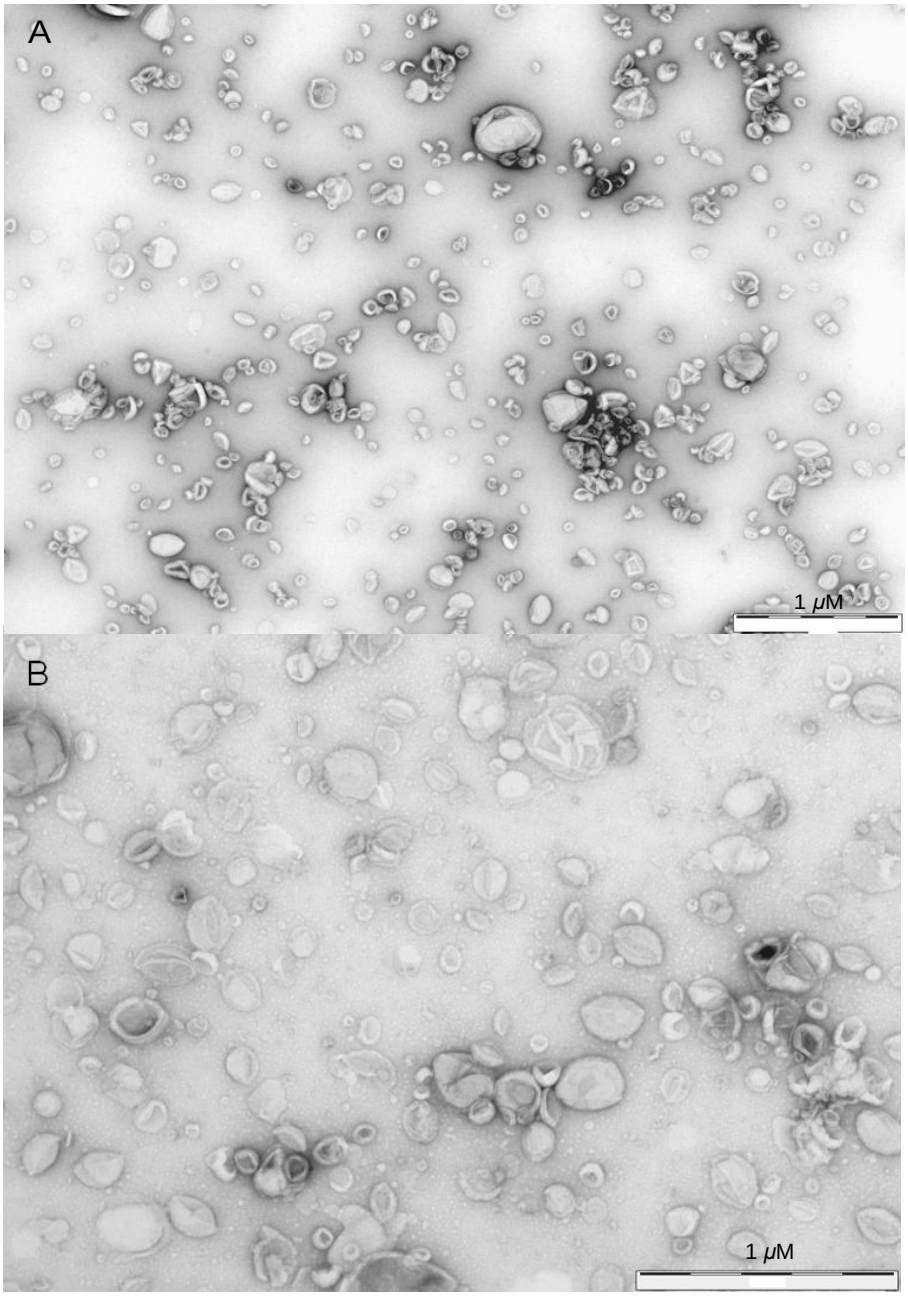

The liposomes and proteoliposomes samples were taken from the void volume of Superose 6 column and were handed to the Electron Microscopy lab at University of Leicester. See section 2.9.1 for complete method.

3.6.3 Calculation of the number of proteins in each liposome

Figure 3.22 reveals an average diameter of proteoliposomes of 201 ± 15 nm and the total surface area of a sphere of this size is (4π x 1000 $Å^2$); this must be doubled to take account of the two surfaces of the bilayer, giving a total surface area of 12 500 000 $Å^2$. Assuming that the surface area of each phospholipid molecule is 70 $Å^2$, this would give ~357 000 lipids per liposome. If the proteins are on average equally distributed between the liposomes, an L:P ratio of 1000:1 would predict 350 protein molecules per liposome.

3.7 Substrate binding: haem spin state equilibrium measurements

Electron paramagnetic resonance and optical spectroscopy studies have shown that bacterial and mammalian P450s exist in a thermal equilibrium between the low and high spin states of the haem iron (Sligar 1976). The spin state equilibrium of substrate free P450 101, has been shown to be affected by temperature, pH and ionic strength, but the major effect is seen on substrate binding (Lange, Bonfils, et al. 1977, Lange, Hui Bon Hoa, et al. 1979, Lange, Pierre, et al. 1980, Sligar 1976).

Upon binding of various ligands to P450, small but characteristic changes in the UV/visible spectrum of the haem chromophore are observed. The substrate induced spectral changes were first classified into three distinct types by Schenkman et al. (Schenkman, Remmer, et al. 1967). A Type I binding spectrum is characterised by the appearance of a Soret peak around 390 nm and trough at around 420 nm. This is indicative of the shift in the spin state equilibrium of the haem iron from low to high spin, which is brought about by the displacement of water molecule bound to the haem iron in the ferric enzyme, converting the iron from six coordinated to five-coordinate (Schenkman, Sligar, et al. 1981). The large majority of compounds metabolised by P450 produce a Type I change upon complex formation. However, a number (e.g. ketones,

alcohols and in particular drugs like phenacetin) produce a 'reverse Type I' spectrum, with maximum at around 420 nm and minimum at around 390 nm. This is correlated with an increase in the low spin state of the ferric haem iron; addition of these substrates is believed to stabilise the water to iron coordination bond in a mixed spin state system. Lastly, a third group of compounds shift the Soret band to longer wavelengths, exhibiting absorption maxima between 425 nm and 445 nm and minima between 390 nm and 420 nm. This change is termed Type II and is caused as a result of direct coordination of the compound, typically by a nitrogen atom, to the haem iron. These compounds usually act as inhibitors, since they prevent oxygen coordination to the haem, which is the prerequisite for metabolism to occur.

Optical difference spectroscopy was used to monitor changes in the spin state of P450 in the proteoliposomes upon binding of testosterone and erythromycin. In this study, testosterone was the main substrate for investigation, as it has been successfully employed in the past with detergent solubilised P450 3A4 in our laboratory (Ward 2003). It is commonly used in studies of P450 3A4 and demonstrates both homotropic and heterotropic cooperativity (Baas, Denisov, et al. 2004, Roberts and Atkins 2007, Roberts, Campbell, et al. 2005).

Although the quality of the difference spectra was limited by the turbidity of proteoliposome samples, Figure 3.23 shows binding of testosterone to P450 3A4 in proteoliposomes produces a classical Type I optical difference spectrum with maximum at ~390 nm and a minimum at ~418 nm, indicative of the displacement of water as the sixth ligand resulting a change in haem iron from low to high spin (Schenkman, Sligar, et al. 1981). The optical binding data were analysed by applying Hill and hyperbolic equations. A fitting of the data by the hyperbolic equation (which assumes a single binding site and non-cooperative behaviour) resulted in an estimated K_d of 55 ± 12.3 μM

while Hill fit gave a K_d of 36 ± 6 μM and a Hill coefficient of 1.62 ±0.2. This suggested that there is more than one binding site with positive homotropic cooperativity between them. Both equations describe the data well as demonstrated by r^2 values (Table 3.4), and the scatter of the data did not allow them to be distinguished. Testosterone binding yielded a final high spin content of 90%.

The effect of CPR on the binding affinity of testosterone to P450 in proteoliposomes was also investigated by increasing CPR concentration relative to P450. The K_d and A_{max} values determined using both equations are shown in Table 3.4. The findings show that K_d and A_{max} nearly double as CPR:P450 >1:1 ratio, while, *n* values appear to decrease. These results indicate that CPR binding may be decreasing the affinity of P450 for testosterone, but are also causing a shift of P450 spin equilibrium towards high spin state.

Sligar and co-authors (Baas, Denisov, et al. 2004) have reported K_d of 58 μM, and *n* of 2.24 for testosterone binding to P450 3A4 in Nanodiscs (~10 nm diameter phospholipid bilayer surrounded by apolipoprotein), while in the presence of CPR, K_d of 28 μM, and *n* of 1.6 was observed (Denisov, Baas, et al. 2007). The testosterone binding data for P450 3A4 in proteoliposomes with equimolar CPR are very comparable to those reported for homogeneous Nanodiscs, where the ratio will also be 1:1. Kim et al (Kim, Ahn, et al. 2003) have reported K_d of 21 μM for P450 3A4 inserted in the same liposomes used herein and Hosea et al (Hosea, Miller, et al. 2000) have reported K_d of 41 μM, and *n* of 1.3 for testosterone binding to P450 3A4 in SRS containing CPR.

Figure 3.23 Optical data for testosterone binding.

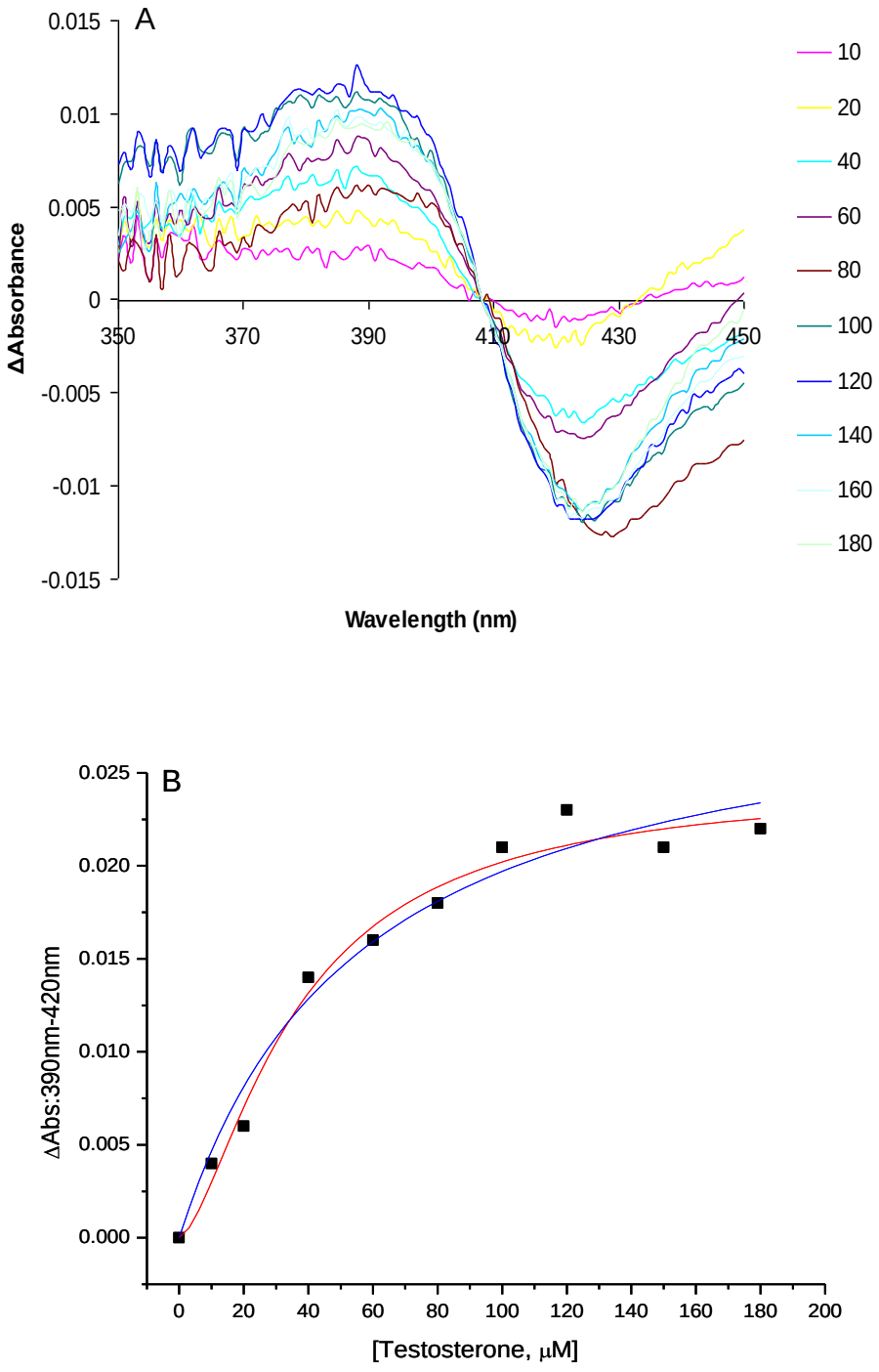

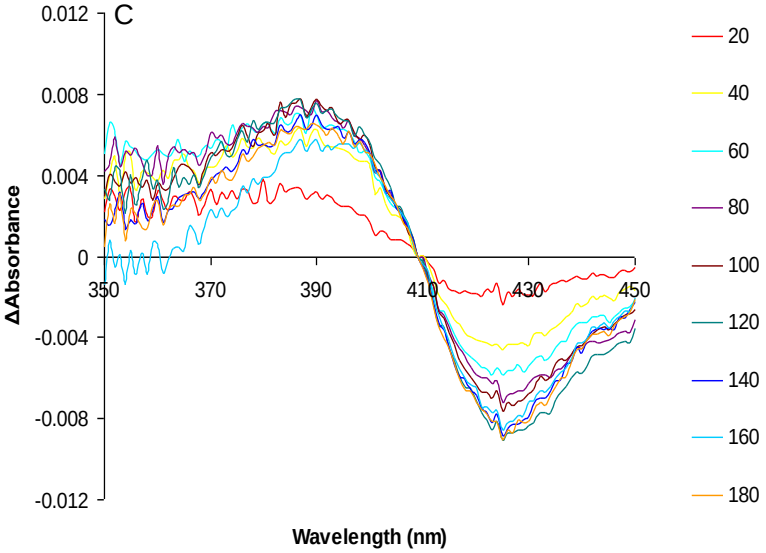

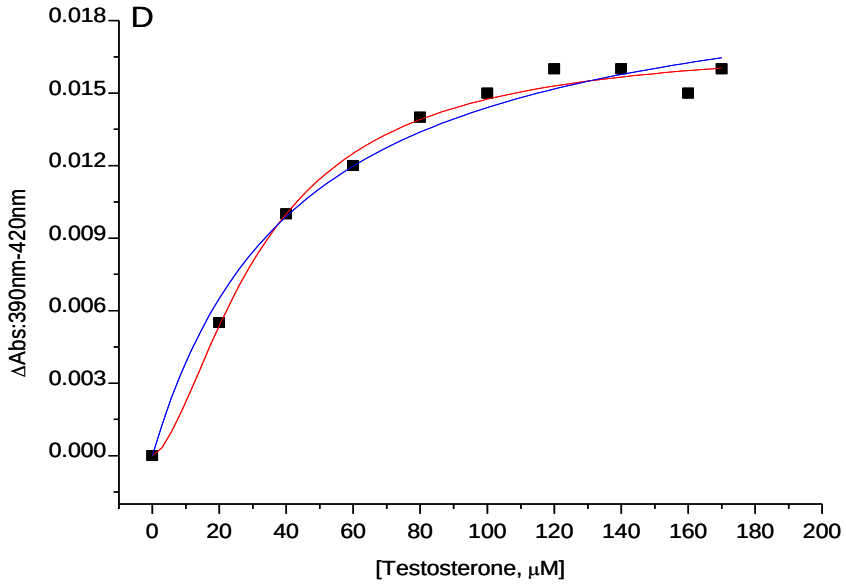

(A) Difference spectra upon binding of testosterone (numbers to the right of spectra are concentrations in μM) to 0.2 μM of P450 3A4 and 0.2 μM CPR in proteoliposomes and (B) Hill (red line) and hyperbolic fits (blue line) to binding data. (C) Difference spectra upon binding of testosterone (numbers to the right of spectra are concentration in μM) to 0.2 μM of P450 3A4 in proteoliposomes and (D) Hill (red line) and hyperbolic (blue line) fit to binding data.

Table 3.4 Apparent dissociation constants (K_d values), maximum absorbance changes (Amax) and Hill coefficients (n values) determined for testosterone binding by hyperbolic and Hill fits.

Molar ratio of CPR:P450	**^1K_d (μM) Hill fits**	**Amax**	***n***	**r^2**	**K_d (μM) hyperbolic fits**	**Amax**	**r^2**
No CPR	32.4 ±2.6	0.017	1.62 ±0.2	0.95	44.5 ± 8.0	0.022	0.96
1:1	36 ±6.0	0.024	1.54 ±0.3	0.93	55 ± 12.3	0.033	0.94
2:1	73.3 ±10	0.042	1.22 ±0.4	0.96	96.4 ± 2.3	0.050	0.98
4:1	69.5 ±14	0.040	1.07 ±0.2	0.94	98 ± 8.5	0.053	0.97

Goodness of fit is indicated by correlation coefficient (r^2) values. ^1K_d is the apparent dissiociation constant is the substrate concentration giving absorbance change of 50% $A_{max.}$ The results are means ±SD of at least three experiments.

Figure 3.24 shows spectral changes upon binding of erythromycin to P450 3A4 in proteoliposomes; fitting by the hyperbolic equation gave K_d of 125 ±20 μM. There is a lot of scattering in the spectra and it was diffcult to pick a particular wavelength of maximum or minimum absorbance change. The maximum absorbance change was small, suggesting that binding resulted in only 10% high spin content. This is comparable with the study of Das et al, who reported an increase in high spin content from 11% for substrate free P450 3A4 in Nanodiscs to 22% high spin upon binding of erythromycin (Das, Grinkova, et al. 2007). The study demonstrated that haem spin equilibrium modulates the redox potential of the P450, a mechanism that has been well known for many years for bacterial P450s (Sligar 1976, Sligar and Gunsalus 1976).

Figure 3.24 Optical data for erythromycin binding.

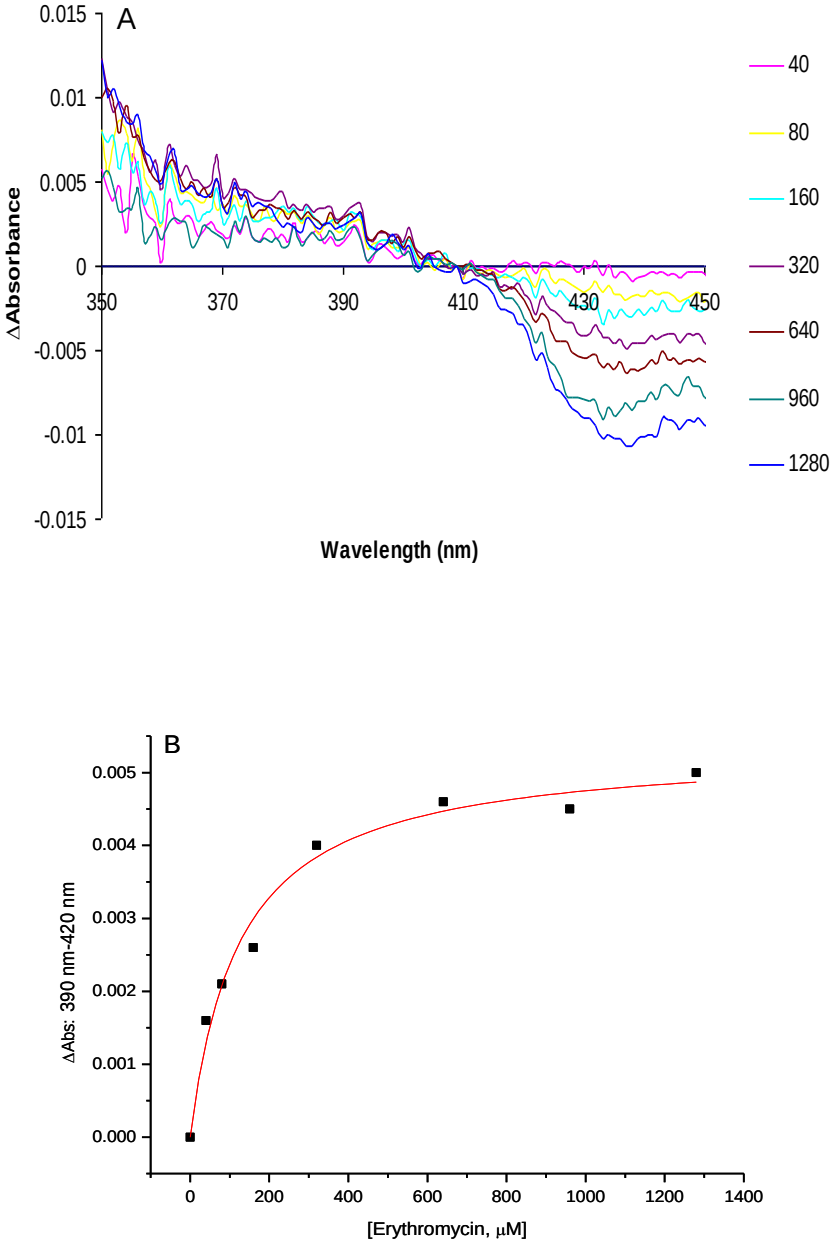

(A) Spectral changes associated with the binding of erythromycin (numbers to the right of spectra are concentrations in μM) to 0.2 μM P450 3A4 in proteoliposomes. (B) A hyperbolic fit to binding data.

3.8 Conclusions

Both CPR and P450 3A4 were prepared in a highly pure state as judged by SDS-PAGE; however ~70% of the CPR flavoprotein was found truncated to the soluble form. Optimisation of the purification method A to give method B resulted in significantly improved stability of the full-length protein. Site directed mutagenesis studies were attempted to engineer CPR, which was stable to bacterial proteases, but for all three mutants, analysis by SDS-PAGE showed proteolysis of N-terminal membrane binding sequence still occurred.

Purified enzymes were reconstituted into liposomes with final dilution in 0.1 M KPB (pH 7.40) containing 0.1% CHAPS. The P450 monooxygenase system in this SRS was catalytically active, with biphasic reduction kinetics observed. The SRS was then subjected to purification by gel-filtration, which obtained homogenous highely functional proteoliposomes, with good activity and almost completely reducible P450 3A4 in a very simple controllable system. Negative staining electron microscopy revealed proteoliposomes of having an average diameter of 201 ±15 nm in size and incorporating 350 proteins per liposome. Binding of testosterone to P450 in proteoliposomes produced a Type I spectra indicating overall 90%. Whereas binding of erythromycin resulted overall 10% spin state change to high spin state.

Chapter 4
Studies of electron transfer from cytochrome P450 reductase to cytochrome P450 3A4

4.0 Introduction

This Chapter describes investigations of the transfer of the first electron from CPR to P450 3A4 in the purified proteoliposomes characterized in Chapter 3 by stopped-flow absorbance measurements. The rate of the second electron transfer in the same system is also studied, estimated from the rate of testosterone 6β-hydroxylation.

4.1 Reduction of ferric P450 3A4 in proteoliposomes

Initially, control experiments with purified liposomes and proteoliposomes without P450 were carried out to establish the reduction of CPR, Figure 4.1. The rapid decrease in absorbance change arises from the reduction of flavins of CPR and also, to a lesser extent, from a mixing artifact due to light scattering changes caused by the dilution of the liposomes upon mixing with NADPH solution. The transient was best fitted by a biexponential function yielding rate constants of k_1 = 20.5 s^{-1} and k_2 = 4.0 s^{-1} and the values are in excellent agreement with those reported for soluble human CPR of k_1 = 20 s^{-1} and k_2 = 3.5 s^{-1} (Gutierrez, Lian, et al. 2001).

Figure 4.1 Kinetics of reduction of CPR in proteoliposomes and mixing of liposomes in the stopped flow spectrophotometer.

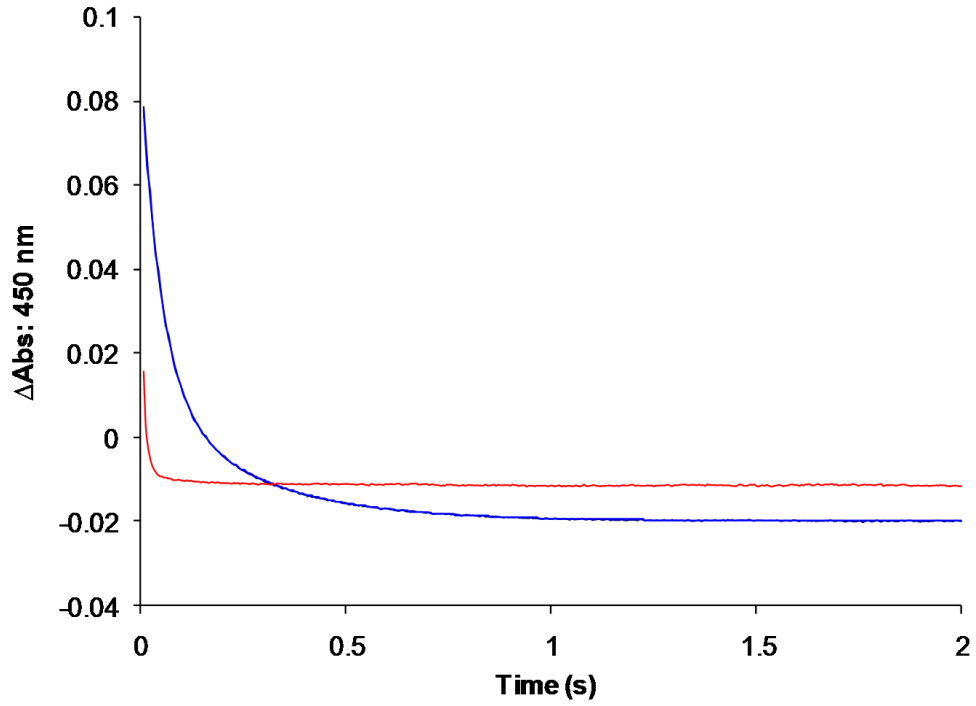

0.1 M KPB containing 0.4 μM CPR proteoliposomes (blue trace) were mixed with an equal volume of the same buffer containing 0.4 mM NADPH in the stopped-flow spectrophotometer. Reduction was monitored at 450 nm and the trace was fitted by a biexponential function yielding values of k_1 *= 20.5* s^{-1} *and* k_2 *= 4.0* s^{-1}*. Purified liposomes (red trace) in 0.1 M KPB were mixed with an equal volume of the same buffer containing 0.4 mM NADPH and monitored at 450 nm.*

The reduction of ferric P450 3A4 by CPR in proteoliposomes (containing equimolar CPR and P450) was measured by mixing the proteoliposome suspension with an equal volume of NADPH solution in the presence of CO in the stopped-flow spectrophotometer, so as to trap the enzyme after first electron transfer in the form of the ferrous CO-complex. Figure 4.2 shows the time course of P450 reduction in the presence and absence of testosterone and residuals are shown in the bottom plot of the figure. The increase in absorbance change at 448 nm, which follows the initial decrease

corresponds to the reduction of P450 and is biphasic, with 89% of the P450 reduced at a rate of 12.4 s^{-1} and 11% at 0.67 s^{-1}. In the absence of substrate, P450 reduction is very slow and the gradual increase in absorbance was fitted by a single exponential corresponding to a rate of 0.03 s^{-1}, Figure 4.2 trace b. These results demonstrate that the rate of P450 reduction is strongly dependent on the presence of substrate, which is consistent with the general view from the literature on P450s (Jansson and Schenkman 1987, Perret and Pompon 1998).

Figure 4.2 Reduction of ferric P450 3A4 in the proteoliposomes (1 CPR: 1 P450 ratio).

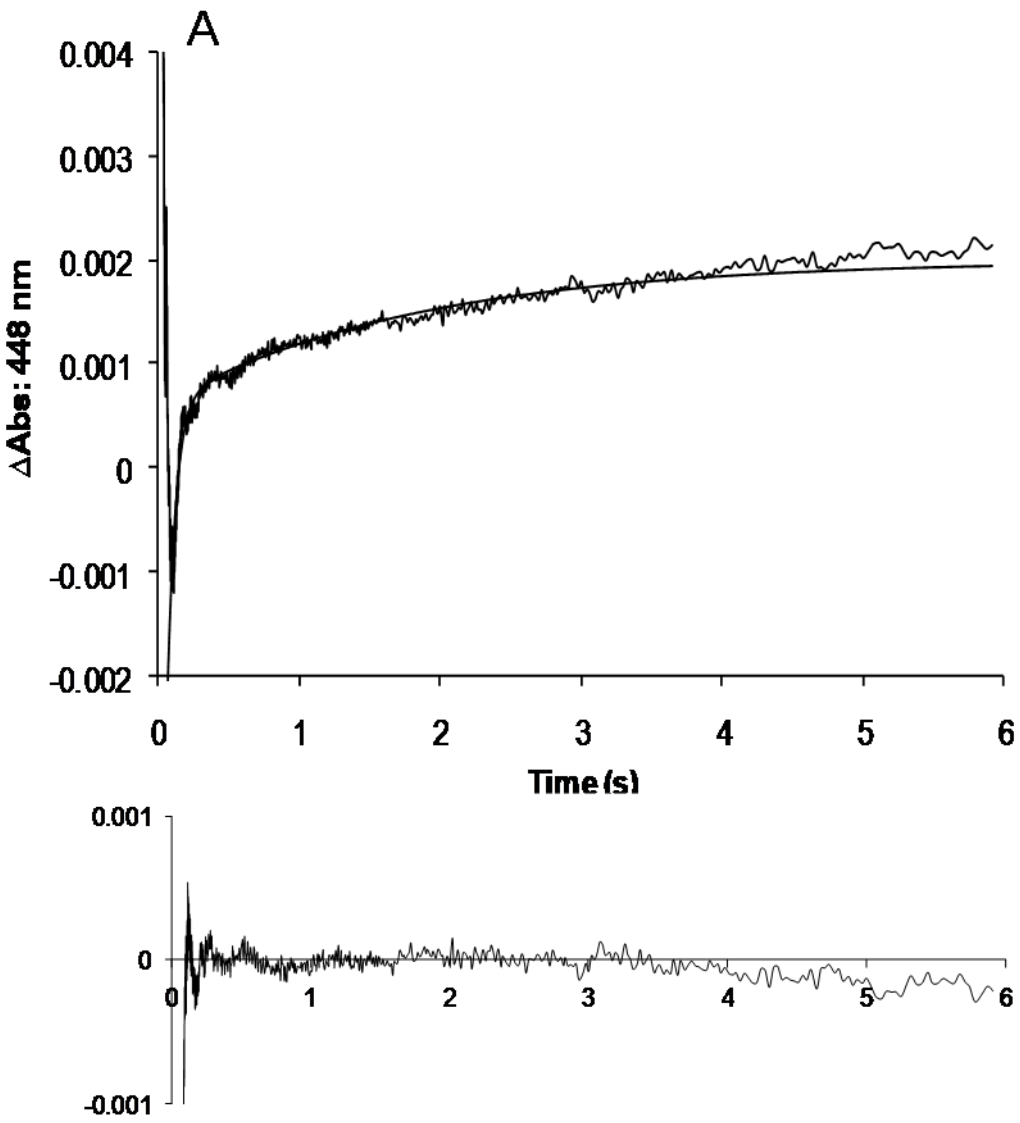

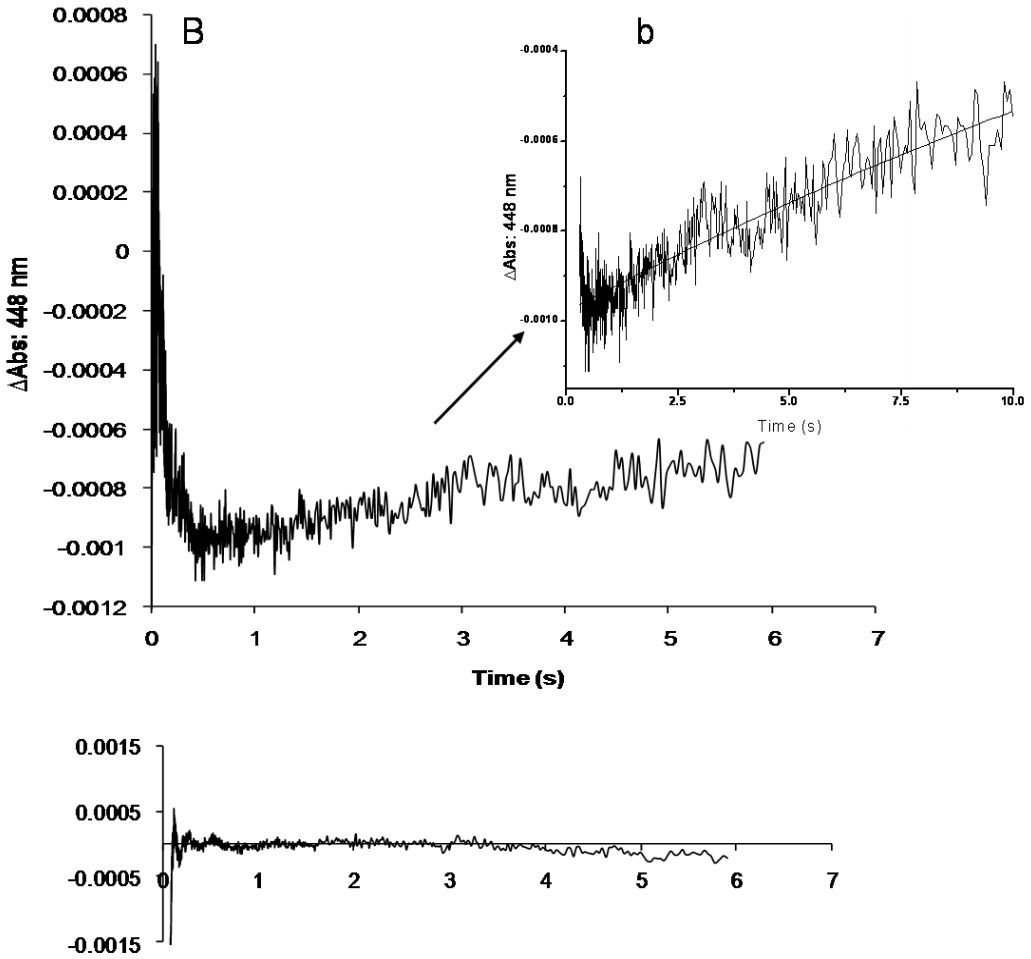

(A) 0.1 M KPB (pH 7.40) containing 0.1 μM CPR and 0.1 μM P450 in proteoliposomes and 0.5 mM testosterone was mixed with an equal volume of the same buffer containing 0.4 mM NADPH and 0.5 mM testosterone. Reduction was monitored at 448 nm by the formation of the Fe^{II}-CO complex. The trace is fit by a biexponential function with rates of k_1 = 12.4 s^{-1} and k_2 = 0.67 s^{-1} (B) Same conditions as A, but without 0.5 mM testosterone, this trace is also shown in the inset (b) with a longer timebase and fit by a single exponential with rate of 0.033 s^{-1}.

Strikingly, the rate of P450 reduction by CPR in the purified proteoliposomes with testosterone is considerably faster (40-fold for the fast phase and 20-fold for the slow phase) than that observed in our SRS (see section 3.3.3 in Chapter 3). Guengerich

et al. (Guengerich and Johnson 1997) have reported rate of ~20 s^{-1} for P450 3A4 with testosterone in SRS, which differed from ours in that it contains b_5, glutathione, Mg^{2+}, sodium cholate and is not purified using gel-filtration chromatography. It is not clear which of the above differences in proteoliposomes in the absence of b_5 produced rapid and reproducible reduction of P450. However, the results do indicate that our method for incorporating protein into liposomes and purifying the proteoliposomes has led to significant improvements in both rate and the amount of P450 reduced. Measurements of the rates of first electron transfer have been reported for other human P450s in SRSs and are summarised in Table 4.1. The rate values indicate that substrate is not obligatory for rapid reduction in all P450s and in general, P450s display biphasic reduction kinetics and require b_5.

Table 4.1 Rates of reduction of microsomal P450s.

P450	**Substrate**	***b_5***	**P450 reduction s^{-1}**	**% reduced in faster phase**
[a]1A2	-	-	13.3	-
[a] 1A2	-	+	11.5	-
[a] 1A2	Phenacetin	-	12.2	-
[a] 1A2	Phenacetin	+	8.5	-
[a] 2C9	-	-	0.07	-
[a] 2C9	-	+	0.07	-
[a] 2C9	(S)-warfarin	-	3.33/0.18	37
[a] 2C9	(S)-warfarin	+	2.7/0.18	45
[b]2A6	Coumarin	-	7.5/0.13	-
[c]2B4	-	-	11.5/2.0	55
[c] 2B4	Benzphetamine	-	18.2/1.6	91

Data taken from, [a](Guengerich and Johnson 1997), [b] (Yun, Kim, et al. 2005) [c](Backes and Reker-Backes 1988).

4.1.1 Effect of P450 spin state on reduction kinetics

Testosterone binding produces 90% shift of the haem iron to high spin form whereas erythromycin binding produced only 10% high spin shift (see section 3.7 in

Chapter 3). In order to assess the effect of the spin state shift, the reduction of P450 was measured in the presence of erythromycin. As shown by Figure 4.3, reduction was monophasic with rate ~3 fold faster than observed without substrate, but with no change in the amount of P450 reduced. The rate and amplitude change were substantially lower than in the presence of testosterone, ~125-fold lower than the fast phase rate seen with testosterone and 6-fold lower than the slow phase rate.

It has been proposed that biphasic reduction kinetics are a result of haem spin state equilibrium of the P450 iron, i.e. the high spin form is reduced in the fast phase reduction and the low spin form in the slow phase. However, the comparison of the results reported here with testosterone and erythromycin demonstrate that in our system biphasic reduction kinetics cannot be simply explained in terms of a high spin rate and low spin rate. This is in agreement with the findings of Guengerich et al (Guengerich and Johnson 1997) who have shown that in baculovirus microsomes low spin P450 3A4 is reduced rapidly even in the absence of a substrate.

Figure 4.3 Reduction of ferric P450 3A4 in the presence of erythromycin.

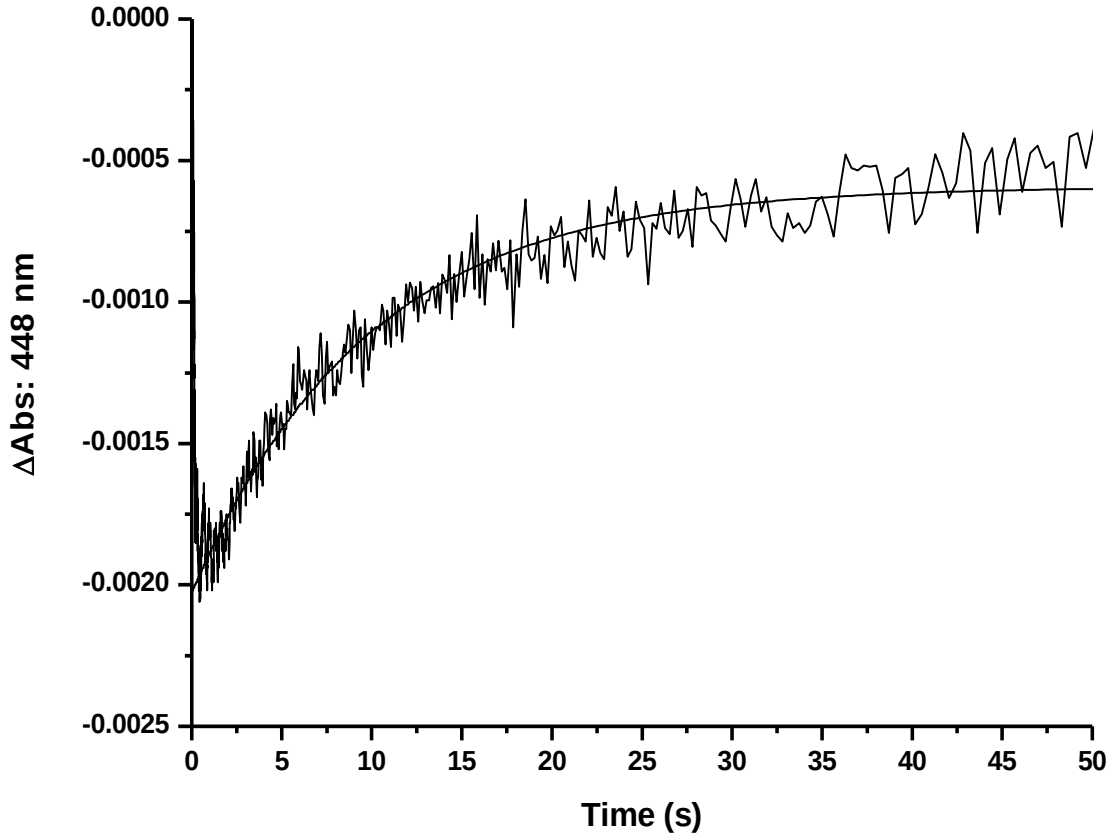

0.1 M KPB (pH 7.40) containing 0.08 μM CPR, 0.08 μM P450 proteoliposomes and 1 mM erythromycin were mixed with an equal volume of the same buffer containing 0.4 mM NADPH and 1 mM erythromycin. Reduction was monitored at 448 nm by the formation of Fe^{II}-CO complex and is fit by a single exponential yielding rate of 0.1 s^{-1}.

4.2 The effect of the CPR:P450 molar ratio on the kinetics of the first electron transfer

To obtain information on the mechanism of first electron transfer between CPR and P450 3A4 in proteoliposomes, we varied the CPR:P450 molar ratio over a 36 fold range; this was achieved by changing the concentration of each protein in the initial reconstitution mixture and the incubation time prior to loading on the Superose 6 column. SDS-PAGE gel analysis was done after each Superose 6 run to estimate the

ratio of individual proteins incorporated into liposomes, Figure 4.4. Figures 4.5-8 show the kinetic traces obtained at different CPR:P450 molar ratios in the presence of testosterone, and Table 4.2 summarises the kinetic data. All traces were best fitted by a biphasic exponential function, with average rates, k_1 = 14 ± 2 s^{-1} and k_2 = 0.6 ± 0.06 s^{-1}; the data demonstrated that the rate of reduction is unaffected by changes in CPR:P450 molar ratio. The amplitude of reduction in the fast phase averages 90 ± 3%, but the absolute amplitudes do show a dependence on the CPR:P450 molar ratio.

Figure 4.4 SDS-PAGE analysis of estimation of molar ratio of CPR:P450 incorporated into liposomes by Superose 6 column.

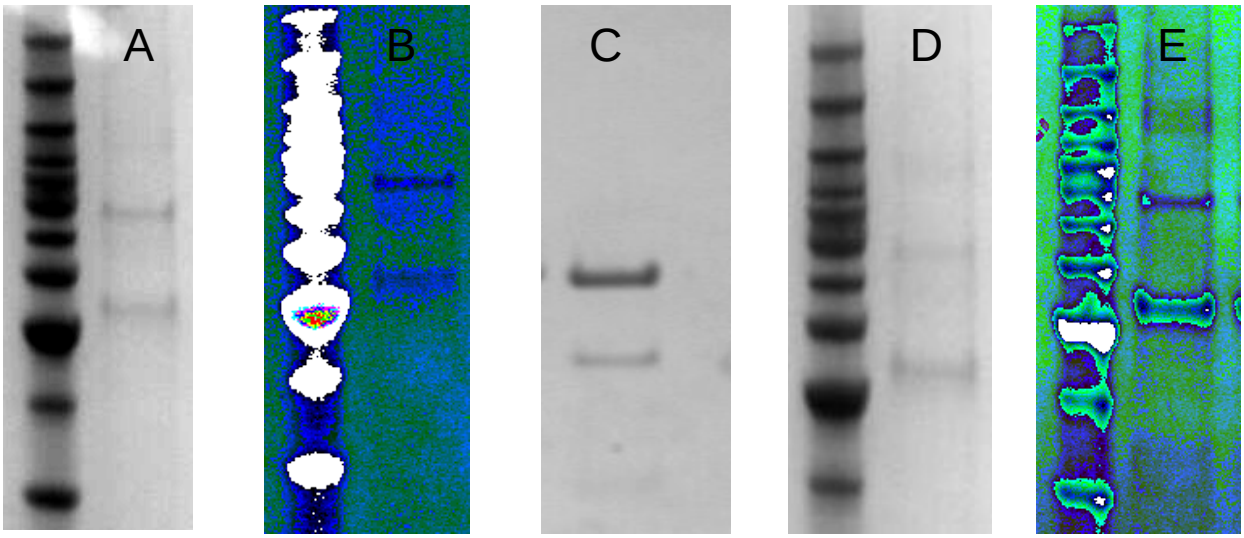

Lane 1: Molecular weight markers, lane 2: Upper band full-length CPR (78 kDa) and lower band P450 3A4 (55 kDa). Gels: (A) 1 CPR: 1 P450 ratio, (B) 3 CPR: 1 P450 ratio, (C) 6 CPR: 1 P450 ratio, (D) 1 CPR: 3 P450 ratio, and (E) 1 CPR: 6 P450.

Figure 4.5 Reduction of ferric P450 3A4 in the proteoliposomes (3 CPR: 1 P450).

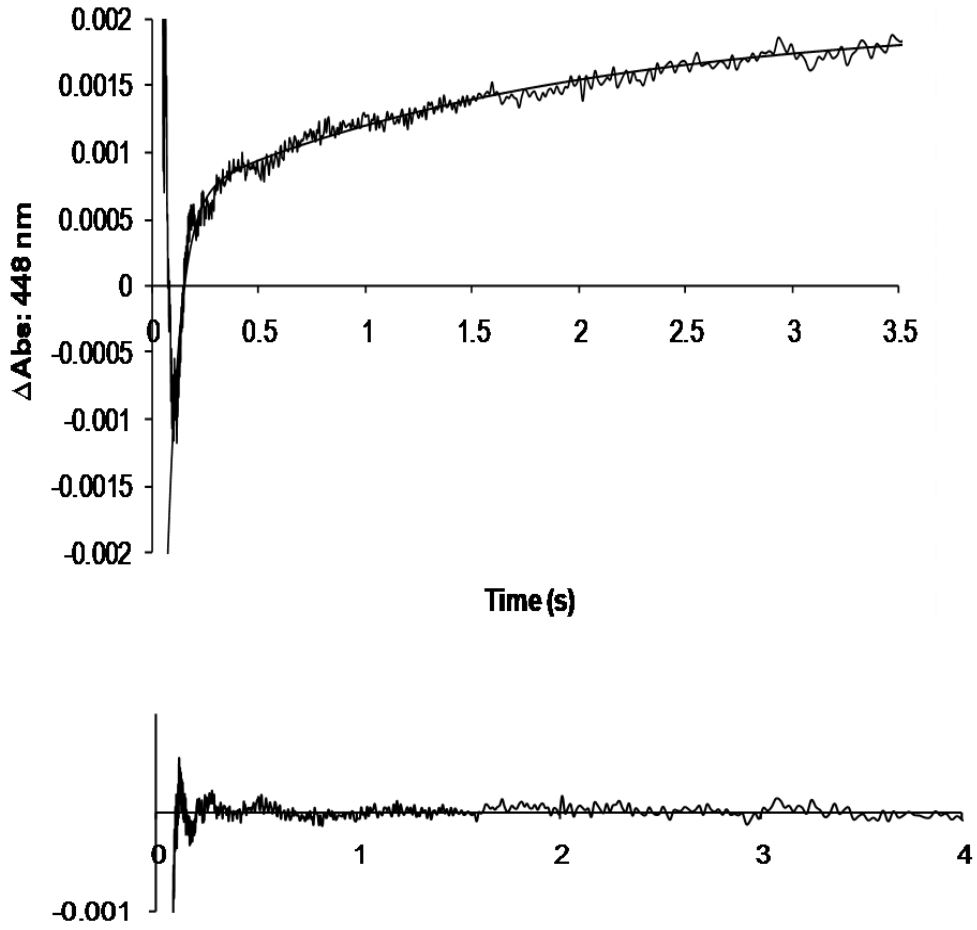

0.1 M KPB (pH 7.40) containing 0.31 μM CPR, 0.1 μM P450 proteoliposomes and 0.5 mM testosterone were mixed with an equal volume of the same buffer 0.4 mM NADPH and 0.5 mM testosterone. Reduction was monitored at 448 nm by the formation of Fe^{II} - CO complex. The trace is fit by a biexponential function with rates of k_1 =16.7 s^{-1} and k_2 = 0.57 s^{-1}.

Figure 4.6 Reduction of ferric P450 3A4 in the proteoliposomes (6 CPR: 1 P450).

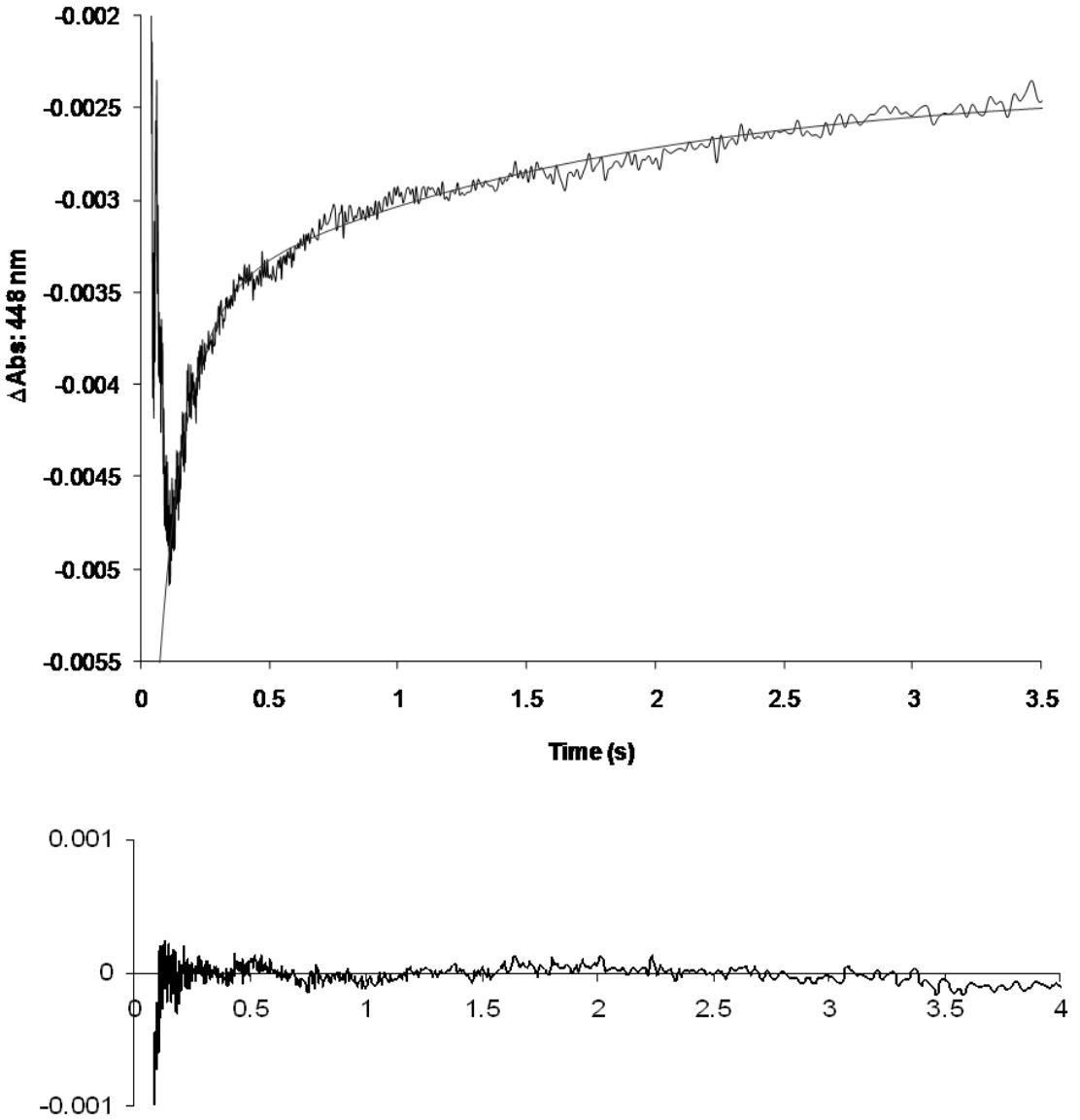

0.1 M KPB (pH 7.40) containing 0.48 μM CPR, 0.08 μM P450 proteoliposomes and 0.5 mM testosterone were mixed with an equal volume of the same buffer containing 0.4 mM NADPH and 0.5 mM testosterone. Reduction was monitored at 448 nm by the formation of Fe^{II}-CO complex. The trace is fit by a biexponential function with rate of k_1 = 11.5 s^{-1} and k_2 = 0.63 s^{-1}.

Figure 4.7 Reduction of ferric P450 3A4 in proteoliposomes (1 CPR: 3 P450).

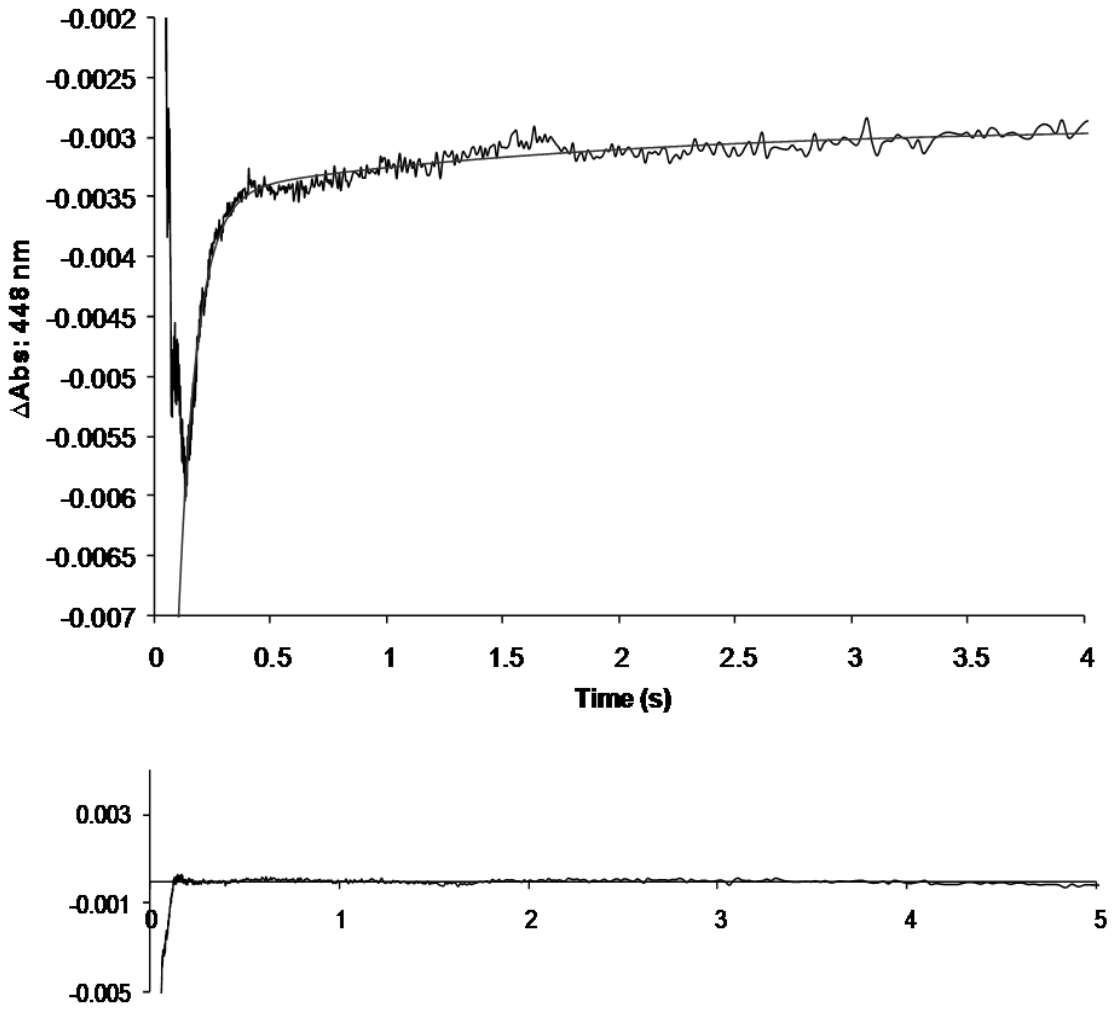

0.1M KPB (pH 7.40) containing 0.08 μM CPR, 0.24 μM P450 and 0.5 mM testosterone were mixed with an equal volume of the same buffer containing 0.4 mM NADPH and 0.5 mM testosterone and reduction was monitored at 448 nm by the formation of Fe^{II} CO complex. The trace is fit by a biexponential function with rate of $k = 12.5\ s^{-1}$ and $k_2 = 0.57\ s^{-1}$.

Figure 4.8 Reduction of ferric P450 3A4 in the proteoliposomes (1 CPR: 6 P450).

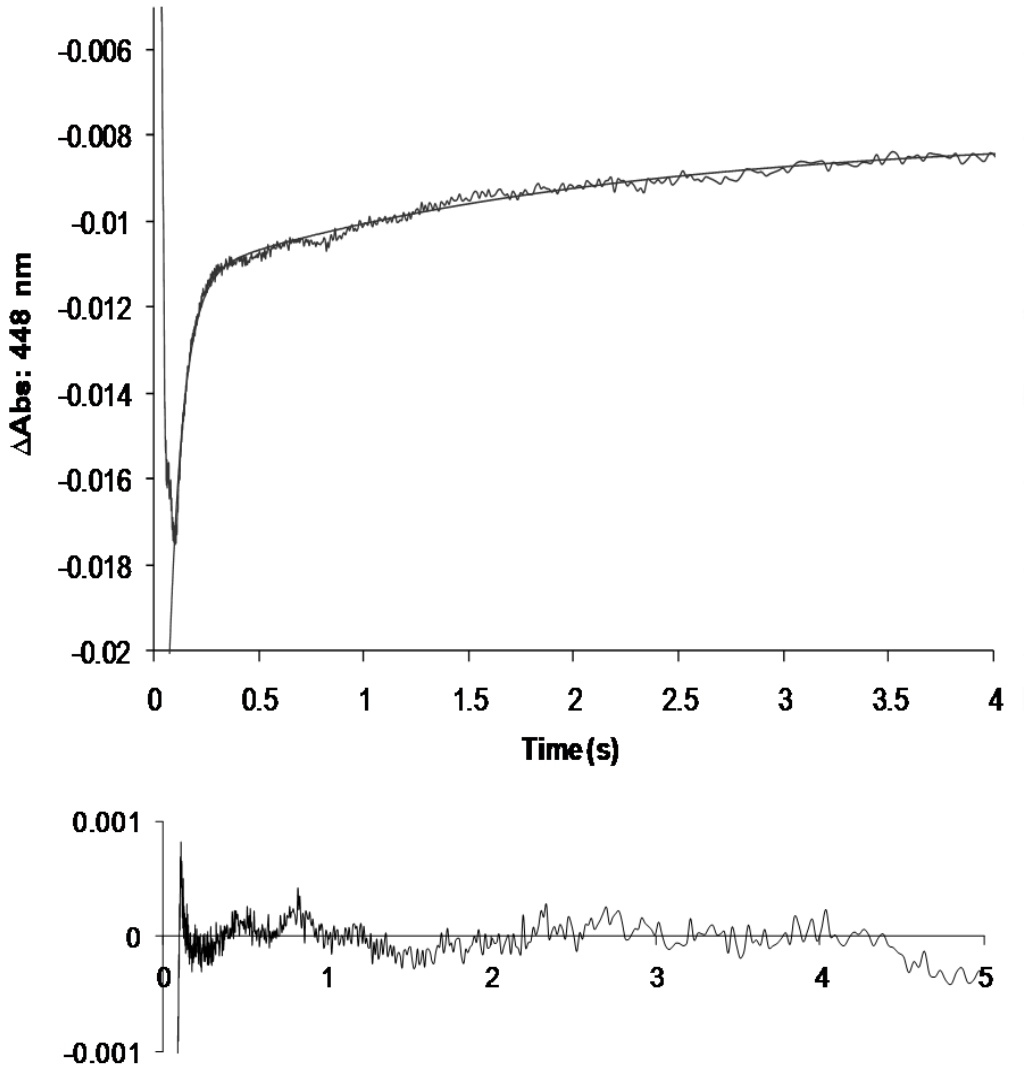

0.1 KPB (pH 7.40) containing 0.08 μM CPR, 0.55 μM P450 proteoliposomes and 0.5 mM testosterone were mixed with an equal volume of the same buffer containing 0.4 mM NADPH and 0.5 mM testosterone and reduction was monitored at 448 nm by the formation of Fe^{II} CO complex. The trace is fit by a biexponential function with rate of k_1 = 14.9 s^{-1} and k_2 = 0.50 s^{-1}.

Table 4.2 Effect of the CPR:P450 3A4 ratio in the proteoliposomes on the rate of reduction of P450 3A4

[CPR] μM	**[P450 3A4] μM**	**CPR:P450 Molar ratio**	**k_1, s^{-1}**	**Fast phase amplitude, ΔA/[P450] μM**	**k_2, s^{-1}**	**Slow phase amplitude, ΔA/[P450] μM**	**% of P450 reduced in the fast phase**	**Refs. to relevant Figure**
0.48	0.08	6.0	11.5 ± 0.6	0.14 ± 0.01	0.63 ± 0.1	0.0175 ± 0.0006	88	4.6
0.31	0.1	3.1	16.7 ± 0.4	0.10 ± 0.005	0.57 ± 0.08	0.015 ± 0.0004	87	4.5
0.1	0.1	1.0	12.4 ± 0.3	0.10 ± 0.01	0.67 ± 0.03	0.013 ± 0.0005	89	4.2
0.08	0.24	0.33	12.5 ± 0.3	0.05 ± 0.003	0.57 ± 0.15	0.0025 ± 0.0002	95	4.7
0.09	0.55	0.16	14.9 ± 0.4	0.03 ± 0.008	0.50 ± 0.1	0.003 ± 0.0005	88	4.8
Without testosterone								
0.1	0.1	1.0	0.03 ± 0.008	0.015 ± 0.0002	-	-	100	4.2b
Erythromycin in place of testosterone								
0.08	0.08	1.0	0.10 ± 0.003	0.016 ± 0.0002	-	-	100	4.3

CPR concentration was determined by cytochrome c reductase assay. The P450 concentration was determined by dithionite reduced CO-difference spectroscopy. All rates are the average of 3-8 experiments.

As shown by Figure 4.9, the amplitude of both phases (corrected for differences in P450 3A4 concentration in different samples) increase as the CPR:P450 ratio increase and reach approximate plateau when CPR is in excess over P450. This would be expected for CPR:P450 complexes that are stable on time scale of the first electron transfer (lifetimes of the order of hundreds of milliseconds) and have a 1:1 stochiometric ratio. The stoichiometry of the CPR:P450 monooxygenase system is as high as 25:1 in favour of P450 in liver microsomes (Estabrook, Franklin, et al. 1971). Therefore, for an efficient monooxygenase reaction the CPR must transfer electrons to each of the crowd of P450 molecules; CPR thus represents the 'enzyme' for the 'substrate' P450. A Michaelis-Menten type mechanism, in which the formation of a CPR:P450 complex is followed by rate limiting electron transfer (k) and then complex dissociation, is shown in equation 4-1.

$$CPR_{red} + P450_{ox} \underset{k_{-1}}{\overset{k_1}{\rightleftharpoons}} CPR_{red}\,P450_{ox} \xrightarrow{k} CPR_{ox}\,P450_{red} \underset{k_{-2}}{\overset{k_2}{\rightleftharpoons}} CPR_{ox} + P450_{red}$$

Equation 4.1

The rate of electron transfer to P450 is thus determined by following equation 4-2.

$$\text{Rate} = k\,[CPR_{red}\,P450_{ox}]$$

Equation 4.2

By dissociating the P450 monooxygenase system using detergents and varying the CPR to P450 ratio, a monophasic first order process has been observed in microsomes and in the SRS (Blanck, Rohde, et al. 1979, Rohde, Blanck, et al. 1983). There is no published report

on the effects of changing CPR:P450 ratio in reconstituted systems for P450 3A4. However for P450 2B4 it has been reported that on increasing the CPR:P450 ratio in SRS, the rate as well as the amplitude of reduction increases tending to approach saturation at CPR:P450 >1, consistent with formation of 1:1 complexes (Blanck, Smettan, et al. 1984). Taniguchi et al (Taniguchi, Imai, et al. 1979) have found that rate of reduction increases with increasing CPR:P450 ratio and decreases as the L:P ratio is increased. This observation has led Taniguchi et al to propose that the first electron transfer occurs through a diffusional collision process. In contrast, we observed in our purified proteoliposomes that the rate constants for both the fast and slow phases of reduction are independent of the CPR:P450 ratio. Our data can be interpreted in terms of a model in which electron transfer between CPR and P450 takes places within a preformed CPR:P450 complex.

Figure 4.9 Effect CPR:P450 molar ratio on the reduction of P450 3A4.

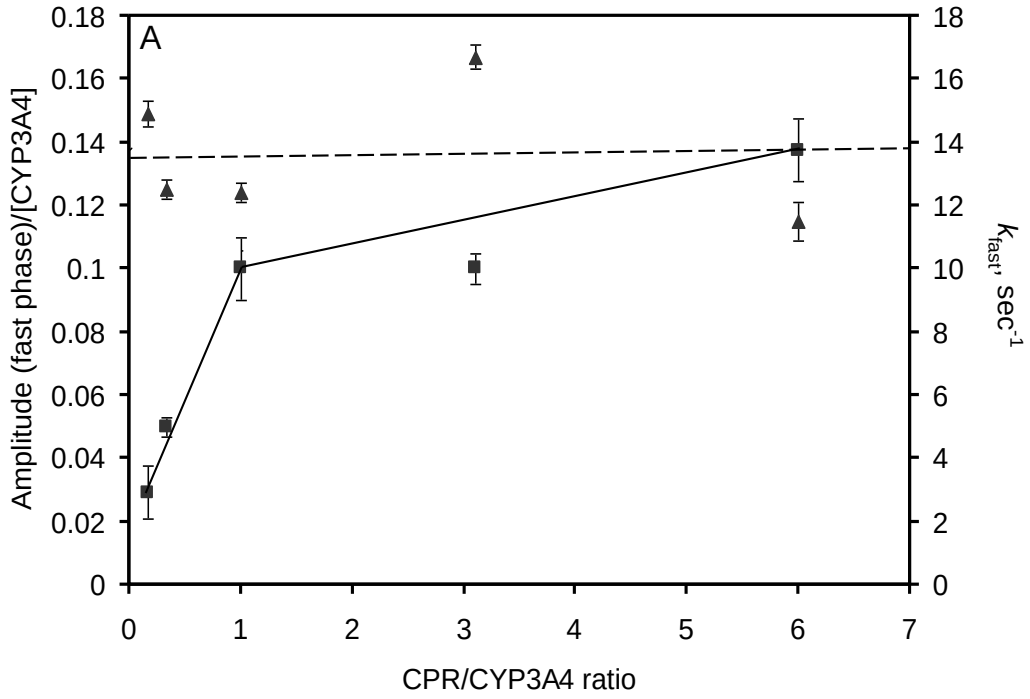

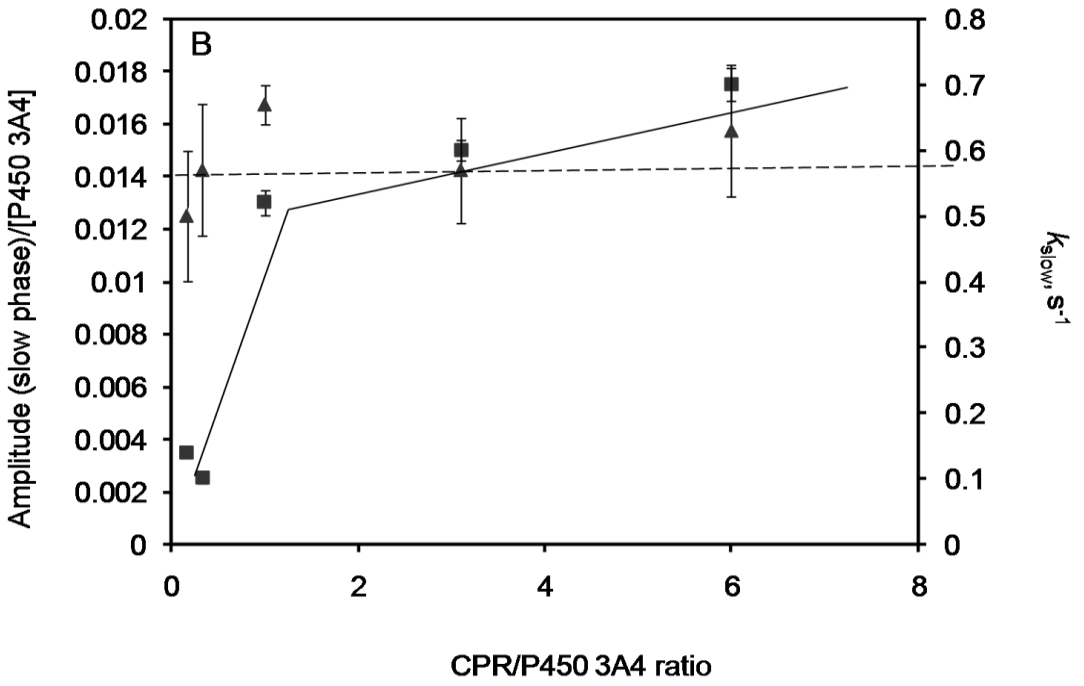

The rates ▲ and amplitudes ■ of fast (A) and slow (B) kinetic phases are shown as function of CPR:P450 ratio in the proteoliposomes. Amplitudes are corrected for the difference in absolute P450 3A4 concentration in each sample. Solid line for rates and dashed line for amplitudes are intended as guides to the eye and have no theoretical significance.

The small amount of P450 reduction in the slow phase does not appear to represent reduction of the low spin form of P450, as the rate of interconversion of spin states is orders of magnitude faster than the rate of reduction (Backes and Eyer 1989, Ziegler, Blanck, et al. 1983). Nor is it the reduction of P450 molecules outside the CPR:P450 complex, as the amplitude of the slow phase increases as function of CPR:P450 ratio.

Rather, the biphasicity of the reduction kinetics of P450 3A4 in proteoliposomes may be attributed to conformational heterogeneity of P450 3A4. It is possible that P450 3A4 in proteoliposomes exists as two or more enzyme pools with each having different positions of the spin equilibrium (and hence redox potential) and/or affinity for CPR. Evidence for

conformational heterogeneity of P450 3A4 has been reported by Davydov et al (Davydov, Fernando, et al. 2005). The authors studied the kinetics of dithionite reduction of P450 3A4 in solution (oligomers), in Nanodiscs and in proteoliposomes. The results showed that P450 3A4 oligomers in solution were reduced with tri-exponential kinetics with or without the substrate bromocriptine. Binding of bromocriptine decreased the overall rate of reduction and caused an increase in the amplitude of the third phase of the reduction at the expense of the first phase, while the fraction of P450 reduced in the middle phase changed very little. Addition of 0.15% Emulgen-913 caused monomerisation of the haem protein and monophasic reduction kinetics was observed and the presence of bromocriptine then had no effect on the reduction kinetics.

Likewise, incorporation of P450 3A4 into Nanodiscs or into large proteoliposomes of high lipid to P450 ratio (726:1 mol/mol) resulted in virtually monophasic reduction kinetics. In Nanodiscs, reduction was rapid and 84% of the low spin haem protein was reduced in the fast first phase in the absence of substrate, while with bromocriptine, nearly the entire amplitude of the fast phase of reduction was shifted towards the second slower phase, the amplitude of which was proportional to the degree of saturation of the enzyme with substrate. The fraction of reduction in the fast and slow phases was found to differ with the spin state. In high lipid to P450 ratio proteoliposomes, P450 reduction decreased in the presence of bromocriptine and shifted the reduction towards slower second phase (high spin form), which indicated that low spin haem is reduced more rapidly. In the case of protein-rich liposomes (L/P = 112:1 mol/mol, resembling the endoplasmic reticulum membrane), rate constants for reduction were similar to those seen in P450 oligomers with data fitted by a tri-exponential equation, which suggested heterogeneity of the enzyme. The authors concluded that P450 3A4 in the microsomal membrane is distributed between two persistent conformers that differ in spin equilibrium and accessibility to the reducing agent, and do not interconvert in the time

frame of the experiment. One population of enzyme exists in substrate dependent transition between two states with different rate constants, while other has no response upon substrate binding. This type of behaviour may also account in our proteoliposomes for the small fraction of slow phase of reduction, which may be attributed to a conformer that does not respond to testsoterone binding during the time frame of the experiment and thus its rate of reduction is unaltered. In another study, Davydov and colleagues (Davydov, Halpert, et al. 2003) carried out high pressure spectroscopic studies with P450 3A4 in solution and in the microsomes, which revealed the presence of two conformers with different spin equilibrium and different barotropic properties.

Reed and Hollenberg (Reed and Hollenberg 2003, Reed and Hollenberg 2003) have carried out pre-steady reduction studies of P450 2B4 in the presence of various substrates, at different concentrations of CPR to see if the binding of reduced CPR to P450 in SRS was rate limiting and if this was responsible for multiphasic reduction of P450 2B4. In the presence of some substrates, P450 2B4 reduction was slower at saturating concentrations of CPR than at equimolar CPR and P450. They postulated that there is an equilibrium between three different conformations of P450 2B4 that regulates P450 reduction and that binding of reduced CPR to P450 inhibits P450 conformational changes after reduction. If the rate of dissociation of the CPR:P450 complex is different for each of the three P450 conformers than the reduction of P450 would be multiphasic.

4.3 What determines the rate of electron transfer in the CPR:P450 complex?

The average rate of 14 s^{-1} measured for the first electron transfer in proteoliposomes is orders of magnitude slower than the expected intrinsic electron transfer in complexes that

have donor and acceptor redox proteins in close proximity. For efficient intra- and interprotein electron transfer to take place, the shortest distance between the edges of the redox centers is predicted to be 14 Å or less (by the surveys of physiological electron transfers in many redox proteins) although unproductive reactions can extend this limit and electron transfer may instead take place involving the side chains of amino acids that have upper limit of 25-30 Å (Page, Moser, et al. 1999). There are a number of structural and kinetic studies suggesting that protein dynamics control rate of electron transfer and that protein electron transfer is kinetically gated by diffusional motion needed to bring two redox centers within the electron transfer distances. For example, Leys et al (Leys, Basran, et al. 2003) have reported the crystal structure of a ternary complex of the iron sulfur–protein trimethylamine dehydrogenase (TMADH) and electron transfer flavoprotein (ETF). In the TMADH-2ETF complex structure, the electron density for the FAD domain of ETF was absent indicating high mobility. The crystal structure shows that ETF makes a dual interaction with TMADH, one part acts as a static anchor, allowing the other (FAD domain) to sample large range of conformations, some compatible with fast electron transfer. Mutagenesis experiments in CPR have identified 3 clusters of acidic residues on the surface of FMN binding domain that are important for binding and electron transfer to cytochrome *c* and P450 (Figure 4.10) (Shen and Kasper 1995, Zhao, Modi, et al. 1999).

Figure 4.10 Schematic of the rat liver CPR showing negatively charged clusters involved in binding cytochrome c and P450.

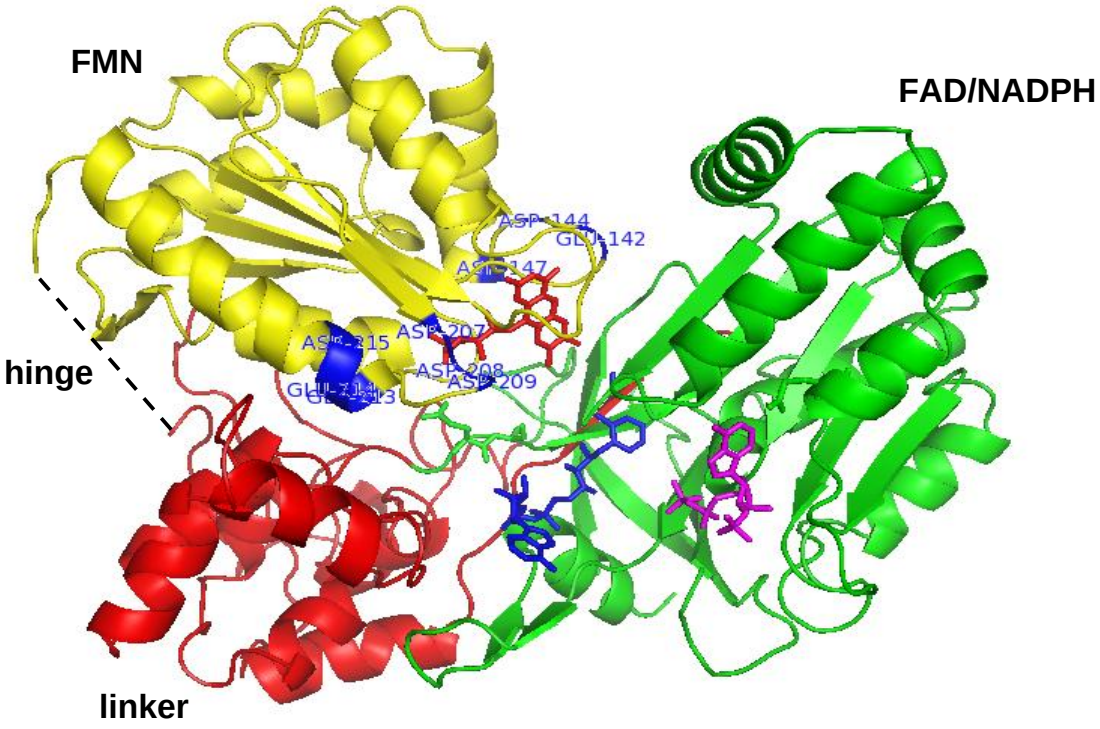

The residues shown in blue are of clusters 1, 2 and 3, respectively. The FMN-binding domain is shown in yellow, linker domain in red, and the FAD/NADPH binding domain is represented in green.cThe linker 'hinge' is shown in dashed line and ball-and-stick cofactors are FMN in red, FAD in blue, and the $NADP^+$, in magenta (PDB file code: 1AMO).

The findings of the experiments have revealed that modification of cluster 1; ^{207}ASP-ASP-ASP^{209}, (specifically ASP208) decreased P450 activity by 70%, but had no effect on the cytochrome *c* reductase activity. While, mutations in cluster 2; Glu^{213}, Glu^{214}, ASP^{215} decreased cytochrome *c* reductase activity without affecting P450 monooxygenase activity. Cluster 3, Glu^{142}, ASP^{144}, Asp^{147} resulted in modest decrease in P450 activity without affecting cytochrome *c* reductase activity. The fact that clusters 1 and 3 affected only the

activity of P450 suggested that P450 binds at the tip of FMN domain in a way to cover the co-factor. However, this is difficult to reconcile with the crystal structure of rat CPR, as the two flavins are only 4 Å apart and in this compact conformation, for FMN binding domain to transfer electrons from FAD to the haem of P450, it would need to move in and out in relative to the rest of CPR molecule (Wang, Roberts, et al. 1997).

In our lab, extensive kinetic studies with soluble human CPR have shown that binding of 2',5'-ADP moiety of the NADPH triggers conformational changes involving movement of domains which affect the rate of interdomain electron transfer and the interaction with cytochrome *c* (Grunau, Paine, et al. 2006, Gutierrez, Paine, et al. 2002). A variety of methods including mutagenesis and SAXS experiments were then used to investigate the mechanism of propagation of the effects of 2',5'-ADP binding through the structure of human CPR (Grunau, Geraki, et al. 2007). Mutations were produced in the 14 amino acid long interdomain loop or hinge (shown as dashed lines in crystal structure because of the missing electron density, Figure 4.10) that connects the FMN binding domain to the linker and FAD/NADPH binding domains. The interdomain loop is located ~60 Å away from where the binding of 2',5'-ADP takes place and is thought to function by orientating the FAD and FMN binding domains for optimal electron transfer within CPR and to P450. A 5 amino acid segment of the interdomain loop was either removed or replaced by 5 or 10 residues of poly-proline repeats. The measured rate of interdomain electron transfer in the deletion mutant was 50 fold slower than the wild-type CPR and reduction of cytochrome *c* was also decreased by 5 fold. Furthermore, the SAXS data has revealed that binding of this ligand results in more compact domain organization with overall maximum molecular diameter reducing from 110 Å (in the ligand free enzyme) to 100 Å. The study showed that binding of 2',5'-ADP triggers global structural changes of CPR that brings the two domains into an orientation more favorable for interflavin

electron transfer. Hamdane et al (Hamdane, Xia, et al. 2009) have provided evidence that CPR in an open conformation is capable of reducing P450. Mutants of the flexible hinge were created, with either increasing its length or shortening it, and mutating key residues. All three mutants were crystallised and interflavin electron transfer as well as electron transfer to P450 2B4 were measured. The deletion mutant (^{236}TGEE^{239}) had dramatic decrease in the interdomain electron transfer, and in turn affected its ability to reduce P450. The crystal structure of this mutant showed a change in the relative orientation and position of the FMN and FAD binding domains such that FMN was further from FAD and was more solvent accessible. Further evidence of the domain mobility in this enzyme needed for its function has been provided by our group using NMR and SAXS experiments (Ellis, Gutierrez, et al. 2009). NMR experiments were carried out of the soluble CPR and were compared with the previously assigned spectrum of isolated FMN binding domain (Barsukov, Modi, et al. 1997), in order to compare its environment in different situations. The results showed that there were clear chemical shift differences in the residues of the FMN domain of CPR which were solvent accessible in the crystal structure, suggesting that CPR has a second conformation to that of crystal structure in which the FMN domain is involved in different interdomain interface. SAXS experiments were done with oxidized and reduced enzyme and data showed that upon binding of NADPH, CPR adopts a compact structure whereas the oxidized enzyme exists as mixture of equal amount of two conformations, one consistent with the crystal structure and the other an open conformation consistent with the NMR data.

The rate of first electron transfer measured in the proteoliposomes is the same as reported for reduction of cytochrome *c* by soluble CPR and both rates are ~4 fold slower than the reduction of FAD domain by NADPH (Grunau, Paine, et al. 2006). The concentration independence of first electron transfer rate clearly suggests that complex formation between

CPR:P450 does not contribute to the rate limiting step, but the data strongly suggests that domain movements in CPR, arising from the fact that the domain position needed for interdomain electron transfer differs from that needed for electron transfer from FMN domain to the haem centre of P450, contribute to the rate limiting step of electron transfer in CPR:P450 complex.

However, if the closed as well as the open conformation binds to P450 in the microsomal membrane, this would also suggest that there is a binding site other than on the FMN domain for P450. The linker domain appears to play an important role in modulating the two catalytic domains into proper orientation for binding and electron transfer to redox partner proteins. If the closed conformation binds to P450, then the linker domain is likely to interact with P450 and modulate its catalytic activity, which is yet to be investigated.

4.4 Effect of the CPR:P450 molar ratio on the rate of NADPH oxidation and of 6β-hydroxy-testosterone formation

The effect of variation of the CPR:P450 molar ratio on the steady-state kinetics of NADPH oxidation and 6β-hydroxy-testosterone (6β-OH) formation were measured and data are presented in Table 4.3. The steady-state kinetics were performed in the spectrophotometer at 25 ^{o}C and a cuvette containing 0.48 mL of proteoliposome sample with or without 0.5 mM testosterone was preincubated for 3 minutes in the spectrophotometer and reaction was initiated by 20 μL of 2.5 mM NADPH solution and monitered for decrease in absorption change at 340 nm for 5, 10 or 30 minutes (reaction progress was linear over the time points). In the absence of testosterone, we are measuring uncoupled reaction, where all the reducing equivilants from NADPH are lost through formation of reactive oxygen species (ROS), primarily superoxide anion and hydrogen peroxide (steps a and b in Figure 1.3, Chapter 1).

Uncoupled reactions thus lead to cellular damage as well as enzyme inactivation, with the haem group in particular prone to oxidative damage.

At an equimolar ratio, the rate of NADPH oxidation is 0.12 ± 0.017 s^{-1}, which increases by 4 fold to 0.46 ± 0.03 s^{-1} in the presence of testosterone. This confirms that substrate binding is a physiological gate for electron flow from CPR to P450, which markedly enhances the rate of NADPH oxidation. The effect of testosterone on the rate of NADPH consumption is clearly modest in comparison to its effect on the first electron transfer. NADPH oxidation rates in the presence of testosterone in various systems are between 0.3-4.5 s^{-1} (Denisov, Baas, et al. 2007, Kim, Ahn, et al. 2003, Perret and Pompon 1998, Shet, Faulkner, et al. 1995). Figure 4.11, illustrates the reaction scheme of testosterone hydroxylation to 6β-OH testosterone and a typical HPLC chromatogram of this reaction.

Table 4.3 Effect of the CPR:P450 3A4 ratio in the proteoliposomes on the rate of consumption of NADPH and the rate of formation of 6β-hydroxy-testosterone.

[CPR] µM	**[P450 3A4] µM**	**CPR:P450 Molar ratio**	**NADPH oxidation (– testosterone), s^{-1}**	**NADPH oxidation (+ testosterone), s^{-1}**	**6β-hydroxy-testosterone formation, s^{-1}**	**Coupling[1] (%)**
0.6	0.1	6.0	0.31 ± 0.04	1.12 ± 0.05	0.01 ± 0.0004	0.87
0.3	0.1	3.0	0.123 ± 0.004	0.85 ± 0.05	0.008 ± 0.0002	0.92
0.17	0.08	2.13	0.127 ± 0.004	0.63 ± 0.04	0.008 ± 0.00005	1.23
0.1	0.1	1.0	0.117 ± 0.017	0.46 ± 0.03	0.002 ± 0.00005	0.43
0.08	0.24	0.33	0.047 ± 0.002	0.31 ± 0.04	0.0018 ± 0.00005	0.63
0.08	0.5	0.16	0.027 ± 0.003	0.19 ± 0.007	0.0018 ± 0.0001	0.92

CPR concentration was deterimined by cytochrome c reductase assay. The P450 concentration was deterimined by dithionite reduced CO-difference spectroscopy. All rates are expressed relative to the concentration of P450 3A4 in the individual sample and are the average of at least three experiments .[1] 100 x (rate of product formation)/(rate of NADPH consumption)

Figure 4.11 Testosterone hydroxylation by P450 3A4 in proteoliposomes.

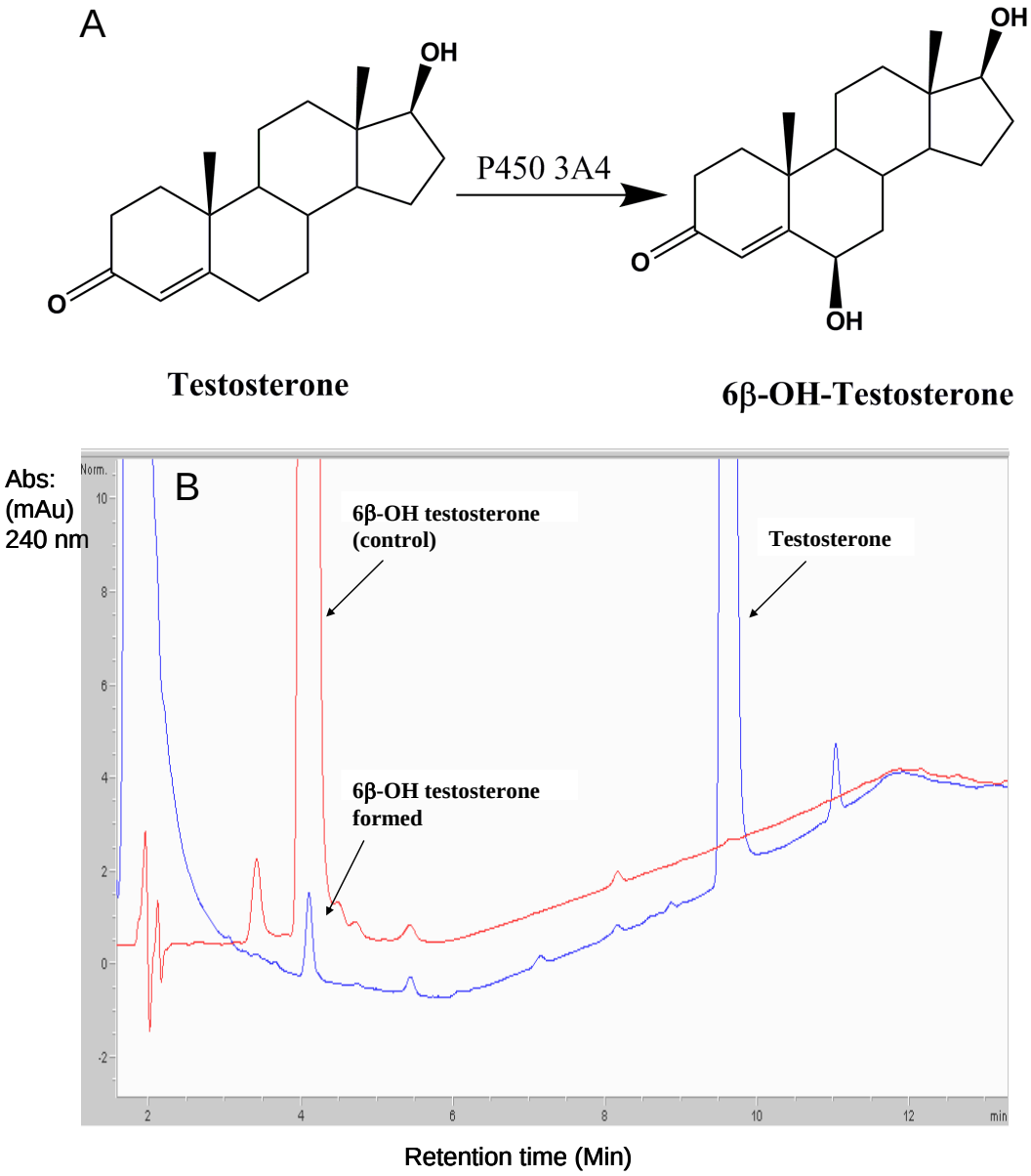

(A) Reaction scheme of 6β-OH testosterone formation by P450 3A4. (B) A HPLC chromatogram of P450 3A4 catalysed 6β-OH testosterone by proteoliposomes containing 0.1 μM each of CPR and P450 3A4 (blue line) and of 6β-OH testosterone standard metabolite (red line).

We observed 90% high spin form of P450 in proteoliposomes on saturation with testosterone, but the maximum rate of NADPH oxidation is 1.12 s^{-1} and 6β-OH testosterone formation is 0.01 s^{-1} (~200 fold less at 2:1 CPR:P450 ratio), with optimal coupling efficiency of 1.23%, which reflects a electron leaky or uncoupled system. The product formation is inefficient process with most of the NADPH used in 'futile' or 'uncoupled' reactions, which produces hydrogen peroxide or water rather than 6β-OH testosterone (steps b and c in Figure 1.4, Chapter 1). This high uncoupling of the enzyme is a characteristic of most microsomal P450s and 6β-OH testosterone formation rate is comparable to the reported rates in the literature for P450 3A4 in various systems, see Table 4.4.

Table 4.4 Rates of testoterone 6β-hydroxylation in systems containing P450 3A4

System	6β-hydroxy-testosterone formation, s^{-1}	Reference
SRS (containing phospholipids, sodium cholate, Mg^{2+}, $b_{5)}$	0.2	(Yamazaki, Nakano, et al. 1996)
SRS (-b_5)	0.02	Yamazaki, Nakano, et al. 1996)
SRS (containing $b_{5,}$ POPC and POPA, 50:50 mol %)	0.13	(Kim, Ahn, et al. 2003)
Liver microsomes	0.1	Yamazaki, Nakano, et al. 1996
Baculovirus microsomes (- b_5)	0.6	(Yamazaki, Nakajima, et al. 1999) (Guengerich and Johnson 1997)
Baculovirus microsomes (+ b_5)	1.1	(Yamazaki, Nakajima, et al. 1999)
E. coli membranes containing CPR, P450 and b_5	1.05	(Yamazaki, Nakajima, et al. 1999)
E. coli membranes containing CPR and P450	0.7	(Yamazaki, Nakajima, et al. 1999)
Yeast membranes containing CPR, P450 and b_5	0.3	(Perret and Pompon 1998)
Nanodisc system containing 1:1 CPR:P450 3A4	0.36	(Denisov, Baas, et al. 2007)

In soluble bacterial P450 systems, such as the well characterized P450 101, the substrate turnover rates are between 10-40 s^{-1}, and the consumption of pyridine

nucleotide is tightly coupled with product formation. The oxy-ferrous complex has been suggested to be the major route of uncoupling in P450 3A4 (Denisov, Grinkova, et al. 2006). In the absence of substrate, the oxyferrous complex decomposes very quickly to ROS and saturation with substrates causes significant stabilization of this intermediate.

Denisov et al. (Denisov, Baas, et al. 2007) have carried out measurements of NADPH oxidation and testosterone hydroxylation as function of substrate concentration. They reported that up to 3 molecules of testosterone can bind into P450 3A4 active site; the first binding event results in no product formation with NADPH consumption completely uncoupled in P450 3A4. It is the second molecule of testosterone that leads to maximum value of product formation (0.4 s^{-1}) and is the switch to productive state of CPR:P450 complex. Whereas, third testosterone molecule leads to significant decrease of reducing equivalents with no change in product forming rate (0.36 s^{-1}) and thus results in improved coupling efficiency (5% to 14%). The reported spin shift on testosterone binding is 24% for the first molecule, 98% and 96% for second and third.

As shown in Table 4.3, rates of NADPH oxidation and 6β-OH testosterone formation increase as CPR:P450 ratio in the proteoliposome increases. At the maximum molar ratio tested of 6:1 CPR:P450, the rate of NADPH oxidation is increased by ~2.5 fold with and without testosterone and a 5 fold stimulation in 6β-OH testosterone formation occurs. Addition of 4 fold excess of purified CPR in SRS containing recombinant P450 3A4:CPR fusion protein have been shown to stimulate the rate of 6β-OH testosterone formation and NADPH consumption by ~10 fold (Shet, Faulkner, et al. 1995), but at a higher molar ratio than 4 CPR to 1 P450, the reaction was inhibited. In bacterial membranes increasing to an 8 fold excess of CPR to P450 ratio, the activities

of 6β-OH testosterone formation were found to increase by 2 fold (Yamazaki, Nakajima, et al. 1999). The testosterone hydroxylation reaction requires both electrons from CPR to P450 3A4 and indeed NADPH consumption is also a reflection of both electron transfers. The very different dependencies on the CPR to P450 ratio of rate of first electron transfer and rate of 6β-OH testosterone formation observed in the present work suggest that it is likely the second electron transfer that is limiting substrate turnover. The rate of second electron transfer increases with increasing CPR:P450 ratio in the proteoliposomes, which in turn suggests that the mechanism of second electron transfer is collisional, involving lateral diffusion of CPR and P450 in the plane of membrane. It is very difficult to measure the rate of second electron transfer directly because the intermediates beyond the ferrous dioxygen intermediate are extremely unstable (Denisov, Makris, et al. 2005). However, the different observations for the first and second electron transfer can be reconciled by considering the very different timescale of the two processes. If the lifetime of CPR:P450 complexes is about 200 ms, with the measured rate herein of 14 s^{-1}, the first electron transfer would take place within the stable complex, but on the slow second electron transfer (0.005 s^{-1}, approximating from testosterone hydroxylation), the complex will dissociate laterally in the membrane and show characteristic of collision mechanism. Denisov et al (Denisov, Baas, et al. 2007) have measured a high rate of testosterone hydroxylation of 0.36 s^{-1} in Nanodiscs of 1:1 CPR:P450 3A4 ratio. Nanodiscs are very small phospholipid bilayer particles which contain only one molecule of CPR and one of P450 and where the two proteins are in very close proximity; in such system the possibility of the CPR-P450 complex to diffuse apart is very limited, so the reported rate may approximate the rate of testosterone hydroxylation within the complex.

As shown in Figure 4.12, rates of NADPH oxidation and 6β-OH testosterone formation were plotted as function of CPR concentration. Each data set was fitted by a rectangular hyperbola function to estimate the values of apparent equilibrium dissociation constant (*Ks*) for the CPR:P450 complex. While the data did not extend to sufficiently high CPR concentrations to allow precise estimates, a value of 0.37 ± 0.1 µM was obtained from the NADPH consumption measurements and an essentially identical value of 0.41 ± 0.1 µM from testosterone hydroxylation. Davydov et al (Davydov, Knyushko, et al. 1996) have measured *Ks* of 0.035 µM for the CPR:P450 2B4 complex in solution by fluorescence resonance energy transfer, while an early study by French et al (French, Guengerich, et al. 1980) estimated *Ks* of 0.12 µM without substrate and 0.035 µM in the presence of benzphetamine for the CPR:P450 2B4 complex in SRS. These estimates were obtained in systems which do not correspond to our proteoliposomes but all the values, in the range 40-400 nM, are clearly consistent with lifetimes for the CPR:P450 complexes which are long relative to the rate of the first electron transfer but short compared to the rate of the second electron transfer.

Figure 4.12 Effect of CPR:P450 concentration on the rates of NADPH consumption and 6β-OH testosterone formation.

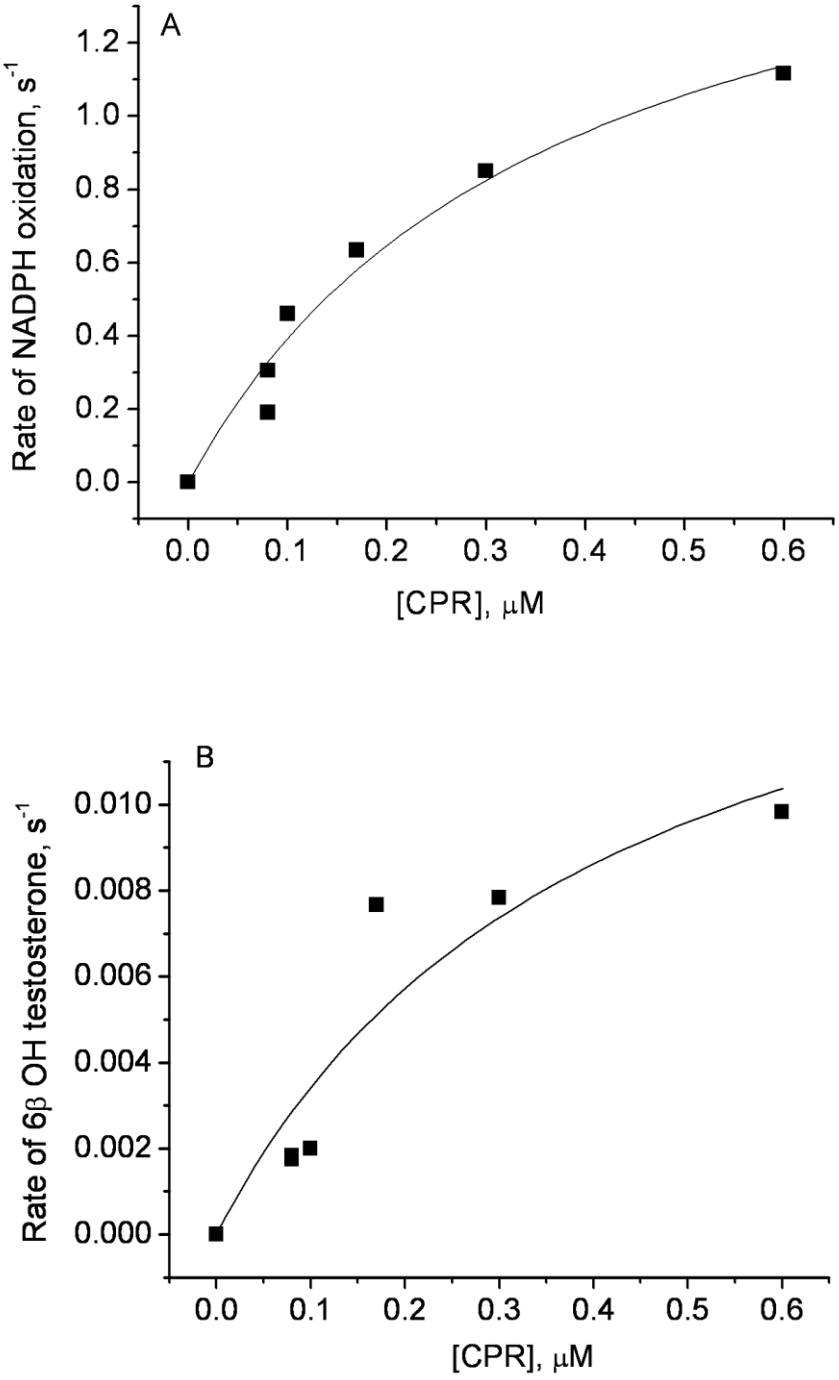

(A) NADPH oxidation and (B) 6β-OH testosterone formation rates as function of CPR: P450 concentration in proteoliposomes. The data was fitted by a rectangular hyperbola, resulting in apparent dissociation constant (Ks) values of (A) 0.37 ± 0.1 μM and (B) 0.41 ± 0.1 μM.

4.5 Conclusions

The study has determined that the first electron transfer between CPR and P450 3A4 in proteoliposomes was very slow without substrate, whereas in the presence of testosterone it was rapid and biphasic process. On average 90% of the P450 was reduced in the faster phase and in the presence of erythromycin P450 reduction was monophasic with a rate ~125 fold slower than the fast phase observed with testosterone. On variation of the CPR:P450 ratio in proteoliposomes, the rate of first electron transfer was independent of the molar ratio of the two enzymes. Thus, we interpreted the data in terms of a model where the first electron transfer takes place within preformed CPR:P450 complexes. The amplitudes of both phases of reduction increases as the CPR:P450 ratio is increased, reaching a plateau when CPR is in excess over P450. These results indicate that CPR and P450 exist in complexes that have 1:1 stoichiometry and have lifetime of the order of hundreds of milliseconds.

The slow phase of P450 reduction does not represent the low spin form of P450 being reduced or the reduction of P450 molecules outside the CPR:P450 complexes because the amplitude of reduction increases as function of CPR:P450 ratio. The slow phase of P450 reduction may be attributed to heterogeneity of P450 3A4 in proteoliposomes, which are possibly distributed among several populations with each having different rate of reduction. The measured rate of the first electron transfer from CPR to P450 3A4 is orders of magnitude slower than the rate predicted by electron transfer theory between two redox centres. We suggest that the first electron transfer is conformationally gated by domain motions of CPR that contribute to the rate limiting step of first electron transfer in the CPR:P450 complex. The rate of NADPH consumption and 6β-OH testosterone formation was measured as function of CPR and P450 3A4 ratio in proteoliposomes. Both rates were much slower than the rate of first

electron transfer reflecting the poor coupling efficiency of P450 3A4. The rate of NADPH consumption and 6β-OH testosterone formation were dependent on the CPR:P450 ratio and the findings indicated that it is likely second electron transfer that is dependent on CPR:P450 ratio. The *Ks* for binding of the two enzymes in proteoliposomes was ~0.4 μM, consistent with a complex that has a short lifetime that would dissociate and reform between first and second electron transfer, and indicating that electron transfer takes place by collisional mechanism.

Chapter 5
General conclusions and future directions

5.0 Introduction

Cytochrome P450s are a large family of proteins that are found throughout the phylogentic spectrum. Mammalian P450s are of particular interest because they play an important role in the metabolism of drugs, fatty acids, steroids and xenobiotic compounds. Unlike bacterial P450s, their structure, function and catalytic features are less defined to date. This is mainly due to microsomal P450s being highly hydrophobic which makes them prone to misfolding and aggregation. P450 3A4 is the most abundant P450 in human liver, which metabolises ~50% of the administered drugs and it is known that multiple drugs can bind in the active site of P450 3A4 often leading to adverse side effects. In recent years, P450 3A4 has been subject of numerous structural and mechanistic investigations. Its inherent propensity to aggregate makes the enzyme difficult to isolate and study *in vitro*. Historically, P450 3A4 catalytic activities *in vitro* required reconstitution with CPR, phospholipids and other stimulatory components. However, kinetic results have varied from one lab to another and thus detailed characterisation of individual steps of the reaction cycle remains unclear. Functional characterisation of individual steps of the P450 catalytic cycle is fundamental for drug development and understanding the metabolism of both endogenous and xenobiotic substrates.

5.1 General conclusions

The main objective of this thesis was to examine the kinetics of first electron transfer between CPR and P450 3A4 in a reconstituted system *in vitro.* For CPR to interact with P450 productively, it's essential for 60 residue hydrophobic domain of CPR to remain intact, as it spans the lipid membrane and anchors the flavoprotein to its surface. However, during expression and purification of the flavoprotein by method A,

the membrane anchor was cleaved leaving ~30% of the full-length CPR. In an attempt to recover the maximum amount of the full-length flavoprotein and eliminate proteolysis, several changes were made to method A; *E. coli* JM109 strain was changed to BL21 (DE3) pLysS in order to improve the stability of the protein in the host cell strain; cell culture temperature and harvesting times were reduced and PMSF was changed to complete protease inhibitors to minimise the effect of proteolysis during purification. These several changes resulted in at least 80% of the full-length CPR content retained after purification, with good catalytic activity as measured by cytochrome *c* reductase assay. Site-directed mutageneses were carried out at the cleavage site, thereonine 58 (T58) of the membrane anchor and in total three mutants were generated (T58A, K55Q, and K55QT58A). All three mutants were found to make a slight improvement to the overall yield of the full-length CPR, but membrane anchor was still found to be proteolysed. P450 3A4 was prepared using the established method in our lab with slight modification in that 5 mM CHAPS instead of 2 mM was used in purification buffers. One step purifcation by Nickel Hi-Trap™ chelating column resulted in pure protein with a single band on the SDS-PAGE gel.

The haem protein was reducible by dithionite CO-difference spectroscopy with very little amount of P420 formed. SRS was then prepared by reconstitution of CPR purified by method A or B, P450 3A4 and preformed liposomes in KPB (pH 7.40). 7-BQ assay was carried out to measure the catalytic activity of P450 3A4 in the SRS and in solution. P450 3A4 was catalytically active in turning over 7-BQ, but turnover rates were slower in the presence of Triton X-100 purified CPR, indicating that detergent inhibits P450 activity. In order to establish the amount of P450 interacting with CPR in the SRS and also in *E. coli* membranes co-expressing equivalent amounts of CPR and P450 3A4, CO-difference spectral studies were carried out. The studies established that

in the SRS, P450 reduction in the presence of Triton CPR was higher than with CHAPS CPR, but all spectra displayed a large amount of P420. In the absence of liposomes, reduction was negligible indicating that proteins have not been incorporated into liposomes, which could be attributed to high amount of protein aggregation. Reduction was distinctly stimulated in the presence of either testosterone or 7-BQ in the SRS and in *E. coli* membranes. Higher amount of P450 was reduced with Triton CPR in the SRS suggesting that proteins are incorporating into detergent:lipid micelles, and indicated that Triton had not been removed from CPR by the use dialysis because of its high CMC and thus CPR was routinely purified by CHAPS. SRS was then subjected to stopped-flow kinetic studies to measure first electron transfer between CPR and P450. P450 3A4 displayed biphasic reduction kinetics in the presence of testosterone with 70% of reduction occurring at k_1= 0.32 s^{-1}, and 30% at k_2= 0.03 s^{-1}. The rate of reduction was 10 fold higher than previously observed for P450 3A4 in the SRSs (Yamazaki, Johnson, et al. 1996).

SRS was then purified by glycerol density centrifugation to isolate unbound proteins from bound proteins (proteoliposomes). The proteoliposomes were reducible by NADPH CO-difference spectra, suggesting that isolation from unbound protein aggregates results in a homogenous and catalytically active proteoliposomes. To make a better assessment of the oligomeric state of the individual components of the SRS and remove the bound detergent, SRS was subjected to purification by gel filteration chromatography. The main advantage of using gel filteration method was to obtain enough volume of proteoliposomes which could be used for kinetic experiments. Superose 6 chromatography column was employed to isolate proteoliposomes from large aggregates and the truncated CPR as it had the largest exclusion limit for separation. In order to find optimal reconstitution conditions, L:P ratio was optimised

(40:1 to 1000:1) and SRS was incubated for 10 minutes prior to loading on the Superose 6 column. Three distinct peaks were observed, first peak eluting in the void volume containing proteoliposomes, which was considered to contain only physically anchored CPR and P450. Second peak was aggregated proteins and third containing the truncated CPR. P450 and CPR concentration in proeoliposomes was deterimined by dithionite reduced CO-difference spectroscopy and cytochrome *c* reductase assay. Between 20-30% protein was recovered from the total amount of protein initially added in the mixture used to prepare the SRS and at least 75% of the P450 was reduced by NADPH in comparison to reduction in SRS, an increase of at least 10 fold was observed in the presence of testosterone. Reed et al (Reed, Kelley, et al. 2006) observed 12 fold stimulation in the P450 2B4 and 1A2 monooxygenase activity when SRS was purified by Superose 6 chromatography, in agreement with our findings. Negative staining electron microscopy was carried out on the liposomes and proteoliposomes; liposomes revealed an average size of 107 ±6 nm and 201 ±15 nm that incorporated 350 protein molecules per liposome. Type 1 spectral changes were observed on binding of testosterone and erythromycin. Testosterone binding was sigmoidal with K_d of 36 μM ±6 and *n* of 1.62 ±0.2 suggesting positive coopertivity with more than one molecule of testosterone binding to P450 3A4. Testosterone yielded final 90% haem iron spin shift to high form. Whereas, erythromycin binding resulted in K_d of 128 μM ±6 with final high spin content of 10%.

First electron transfer from CPR to P450 in the proteoliposomes was highly dependent on the presence of substrate. In the presence of testosterone (at equimolar ratio) P450 reduction was rapid and biphasic process, with 89% of the P450 reduced at k_1= 12.4 s^{-1}, and 11% at k_2= 0.67 s^{-1}, without testosterone, single exponential kinetics were observed with rate of 0.03 s^{-1}; suggesting substrate binding is prerequisite for P450

3A4 reduction. The rate of P450 reduction in purified proteoliposomes in the presence of testosterone is substantially faster and higher amount of P450 was reduced than in the SRS, which strongly indicated that purification of SRS has led to productive interaction between CPR and P450 in the proteoliposomes and the purification method better stimulated the phospholipids. Whereas, reduction in the presence of erythromycin was monosphasic with rate ~3 fold faster than without substrate and ~125 fast phase rate and ~6 fold for slower phase rate with testosterone. The data suggested that the biphasic reduction kinetics observed with testosterone cannot be simply explained by the haem iron spin equilibrium model (i.e high spin rate and low spin rate of reduction), which is one of the earliest model put forward to explain the nature of P450 reduction (Backes and Eyer 1989).

As the total P450 concentration in microsomal membrane exceeds the CPR concentration by at least 10:1 ratio (Estabrook, Franklin, et al. 1971), we adjusted CPR:P450 ratios over 36 fold range in the proteoliposomes and measured the rate of P450 3A4 reduction in order to obtain information on the mechanism of electron transfer between the two enzymes in the proteoliposomes. The rate of first electron transfer was independent of the molar ratio of the two enzymes, but the absolute amplitude of both phases of P450 reduction increased with CPR to P450 ratio (see Table 4.1), reaching a plateau when CPR is in excess over P450. The results strongly suggested that electron transfer between CPR and P450 occurs through preformed CPR:P450 complexes that have 1:1 stoichiometry and a lifetime of the order of hundreds of milliseconds. The slow phase of P450 reduction is not conclusive from our experiments and does not appear to represent the low spin form of P450 reduction or the reduction of P450 molecules outside the preformed CPR:P450 complexes by diffusion mechanism as the absolute amplitude of reduction increases as a function of CPR:P450

ratio. We assume that the slow phase of P450 reduction may be attributed to P450 heterogeneity in the proteoliposomes that probably are distributed among several populations with having different rate constants of reduction or which do not respond to testosterone binding.

The measured rate of the first electron transfer from CPR to P450 is orders of magnitude slower than the rate predicted by electron transfer theory between the two redox centres. We suggest that first electron transfer is conformationally gated by domain motions of CPR that contributes to the rate limiting step of the first electron transfer in the CPR:P450 complex. The rate of NADPH consumption and 6β-OH testosterone formation was measured as function of CPR:P450 3A4 ratio in proteoliposomes. Both rates were much slower than the rate of first electron transfer, reflecting the poor coupling efficiency of P450 3A4 and indicating that tesosterone hydroxylation is not limited by the first electron transfer. The rate of NADPH consumption and 6β-OH testosterone formation were dependent on the CPR:P450 ratio and indicated that it is likely the second electron transfer that is dependent on CPR:P450 ratio, which occurs by the collisional process in the proteoliposomal membrane. The apparent *Ks* for binding of the two enzymes in proteoliposomes is ~0.4 μM, consistent with a complex that has a short lifetime that would dissociate and reform between first and second electron.

5.2 Suggestion for future work

5.2.1 The influence of cytochrome b_5 in P450 catalyzed reactions

Although CPR and P450 are the major components of the P450 monooxygenase system, other components such as b_5 was early found to influence microsomal P450 activity, in a way highly dependent on the P450 isoenzyme, nature of substrate and

experimental conditions (Schenkman 2003). In microsomes, its catalytic function is not fully understood, although antibodies to b_5 are found to inhibit the microsomal activity of P450 3A4 suggesting that it is important *in vivo* (Guengerich, Martin, et al. 1986). In SRSs, its effect is variable, from stimulating (Yamazaki, Nakamura, et al. 2002), inhibiting (Gruenke, Konopka, et al. 1995), or having no effect on the catalysis by P450. One of the many roles involves electron input to P450 monooxygenase cycle and it's thought to be the second electron rather than first due to having less favorable redox potential than CPR. It is suggested to provide faster input of second electron than the rate of superoxide anion release (i.e. preventing uncoupling) and thereby allowing more products to form (Vergeres and Waskell 1995). Perret and Pompon has likewise proposed that b_5 can stabilize the oxyferrous P450 complex and thus inhibit the decay of this intermediate to form superoxide, while regenerating the ferric P450 (Perret and Pompon 1998). A number of studies have suggested that b_5 functions as an effector in the P450 monooxgenase reaction rather than have a redox role. For example, apo-b_5 (devoid of haem) has been shown to stimulate the catalytic activities of P450 3A4 in SRS (Yamazaki, Gillam, et al. 1997) and in *E. coli* membranes containing CPR and P450 3A4 (Yamazaki, Nakajima, et al. 1999). It is believed that b_5 interaction with P450 3A4 causes redistribution of the P450 3A4 pool between two distinct population that differ in accessibility to reducing agents (Kumar, Davydov, et al. 2005). Recent findings have shown that under single turnover conditions, b_5 catalyses product formation faster than CPR, leaving less time for side product formation and competes with CPR for binding site on the proximal side of the P450 2B4 (Zhang, Im, et al. 2007). In the SRS, b_5 is reported to increase the rate of first electron transfer and testosterone hydroxylation in P450 3A4 reactions (Guengerich and Johnson 1997, Yamazaki, Shimada, et al. 2001). It is possible that b_5 binding increases stability of CPR:P450 complex and

thereby it protects the complex from the effects of detergent. The rapid first electron transfer observed in our proteoliposomes without b_5 than with the SRS used by Guengerich may be from the heterogeneity in the samples prepared by reconstitution procedure and as a result of the difference in the stability of the complex in two systems. The maximum rates of 6β-OH testosterone formation reported in the SRS containing b_5 are between 0.35-0.5 s^{-1} (Yamazaki, Nakano, et al. 1996, Yamazaki, Shimada, et al. 2001) and is similar to what is measured in the Nanodiscs, which indicates that it is the activity of the fully formed CPR:P450 complex that has a lifetime longer than order of several hundred milliseconds.

In order to investigate the effects of b_5 on the catalytic activity of P450 3A4 in our proteoliposomes, future studies can be initiated by expressing, purifying and reconstituting b_5 into proteoliposomes. Stopped-flow measurements of the first electron transfer from CPR to P450 and steady state kinetics of NADPH oxidation and 6β-OH testosterone formation can be carried out. K_d values and the amount of haem iron spin state change upon testosterone and erythromycin binding to P450 can be measured by optical difference spectroscopy. The molar ratio of the individual proteins can be varied to determine the effect on the rate of first electron transfer and on the NADPH consumption and testosterone hydroxylation. In order to determine if b_5 has a conformational role rather than direct electron input, apo-b_5 (devoid of haem) can be incorporated in the proteoliposomes and rate of first electron transfer and NADPH consumption and 6β-OH testosterone formation can be measured. Apparent *Ks* for CPR:P450:b_5 complex can also be deduced from the data.

5.2.2 Mutagenesis studies of interaction between CPR and P450

Detailed modelling and mutagenesis studies can be carried out to identify key residues involved in interaction and electron transfer between CPR and P450 complex. Early mutation experiments of the FMN binding domain have shown that P450 binds over acidic cluster 1 and 3 (see Figure 4.10) at the tip of FMN domain in a way to cover the cofactor, indicating that CPR may adopt a different conformation to that observed in the crystal structure where the FAD and FMN are in close contact for rapid interflavin electron transfer, but not electron transfer to P450 (Shen and Kasper 1995, Zhao, Modi, et al. 1999). Making mutants of cluster 1 and 3 of the FMN binding domain of CPR and measuring rate of first electron transfer and carrying out steady state kinetic analysis of NADPH oxidation and testosterone hydroxylation would provide interesting findings. Further experiments can be carried out to examine if the closed conformation of CPR binds to P450 by mutating the residues in the linker domain, as this domain is suggested to be involved in modulating the positioning of the FMN and FAD/NADPH binding domains for rapid electron transfer. The flexible hinge region, which is absent in the crystal structure is also thought to play a role in orienting the functional domains for interaction and electron transfer with its redox partners. Mutants can be designed of the flexible hinge and can be used to measure rate of first electron transfer and carry out steady state kinetic analysis of NADPH consumption and testosterone hydroxylation. A *Ks* value of CPR:P450 complex can also be deduced from the data.

A number of studies have reported that CPR as well as other redox partners bind on the proximal side of P450 where the haem is closest to the surface and electrostatic interactions mediate complex formation (Davydov, Kariakin, et al. 2000). Designing mutants of the proximal surface of the P450 3A4 would allow us to pinpoint the residues that affect the P450 3A4 monooxygenase activity. In particular residues of

helices F and G, the F/G and B/C-loops, which could form part of the membrane binding surface and the substrate access channel (Poulos and Johnson 2005, Williams, Cosme, et al. 2000). Residues in this flexible region can be mutated to determine their effect on the catalytic activity of P450 3A4 and interaction with substrate.

In the crystal structure of P450 3A4, a cluster of highly ordered hydrophobic core of phenylalanine residues sits above the haem plane of the active site, which has been shown to change the substrate specificity and the residues in this region may be involved in binding redox partners (Kumar, Davydov, et al. 2005, Williams, Cosme, et al. 2004, Yano, Wester, et al. 2004). Mutating residues of the phenylalanine cluster region would allow us to pinpoint residues that are important for interaction and electron transfer between CPR, P450 and b_5.

In conclusion, we have developed an improved reconstitution system for CPR and P450 3A4 by employing gel filteration chromatography. We obtained a homogenous and highely functional proteoliposomes, with good activity and almost completely reducible P450 3A4 in a simple controllable system. The present study demonstrates that the mechanism of electron transfer between CPR and P450 3A4 in proteoliposomes takes place by preformed CPR:P450 complexes that have stoichiometry of 1:1 and a lifetime of order of several hundreds of milliseconds. Steady-state kinetic assays of NADPH consumption and 6β-OH testosterone have shown that CPR:P450 complex can dissociate and reform between first and second electron transfer, indicating that second electron takes place by diffusion mechanism.

Appendix

Some definitions:

Liposomes are bilayer of phospholipids.

SRS (simple reconstituted system) is composed of proteins incorporated in the phospholipids without gel filteration purification.

Proteoliposomes are proteins anchored in the liposomes, which are purified by gel filteration (Superose 6 chromatography).

Buffer Solutions:

Buffers used in purification of CPR by method A:

Buffer A: 50 mM Tris-HCl, 10% v/v glycerol, 0.5 mM EDTA, 0.5 mM DTT, pH 7.80.

Buffer B: 30 mM Tris-HCl, 0.1% v/v Triton X-100, 10% v/v glycerol, 1 M NaCl, 0.1 mM DTT, 0.1 mM EDTA , pH 7.6.

Buffer C: 30 mM Tris-HCl, 0.1% v/v Triton X-100, 10% v/v glycerol, 0.15 M NaCl, 0.1 mM DTT, 0.1 mM EDTA , pH 7.6.

Buffer D: 100 mM KPB, 0.1% v/v Triton X-100, 10% v/v glycerol, pH 7.4.

For method B buffers were same as method A except without 0.1% Triton X-100.

Buffers for P450 3A4 purfication were:

Buffer A1: 50 mM KPB, 0.5 M KCl, 20% v/v glycerol, pH 7.40.

Buffer A2: 50 mM KPB, 5 mM CHAPS, 1 M imidazole and 10% v/v glycerol, pH 7.40.

Buffer A3: 100 mM KPB, 0.1 mM DTT, 0.1 mM EDTA, 5 mM CHAPS, and 20% v/v glycerol, pH 7.40.

Buffers used to prepare *E. coli* membranes:

TSE Buffers; 50 mM Tris-acetate, 250 mM sucrose, and 0.25mM EDTA.

Resuspension buffer; 100mM KPB, pH7.60, 6 mM magnesium acetate, 20% glycerol and 0.1mM DTT.

Buffer used to prepare phospholipids:

25 mM Tris-HCL solution, pH 7.40, containing 0.1M NaCL and 0.5 mM EDTA.

Gel filteration buffer:

0.1M potassium phosphate (KPB) , pH 7.40.

Human cytochrome P450 reductase (CPR)

CPR amino acid sequence, % composition, calculated theoretical PI value, extinction coefficient at A_{280} nm and molecular weight. The information was obtained by importing amino acid sequence into ProtParam program on the 'ExPASy' website (http://www.expasy.ch/cgi-bin/protparam).

Amino acid sequence (680):

MINMGDSHVD TSSTVSEAVA EEVSLFSMTD MILFSLIVGL LTYWFLFRKK KEEVPEFTKI QTLTSSVRESSF VEKMKKTGR NIIVFYGSQT GTAEEFANR LSKDAHRYGM RGMSADPEEYDLADLSSLPE IDNALVVFCM ATYGEGDPTD NAQDFYDWLQ ETDVDLSGVK FAVFGLGNKTYEHFNAMGKY VDKRLEQLGA QRIFELGLGD DDGNLEEDFI TWREQFWPAV CEHFGVEATGEESSIRQYEL VVHTDIDAAK VYMGEMGRLK SYENQKPPFD AKNPFLAAVT TNRKLNQGTE RHLMHLELDI SDSKIRYESG DHVAVYPAND SALVNQLGKI LGADLDVVMS LNNLDEESNKKHPFPCPTSY RTALTYYLDI TNPPRTNVLY ELAQYASEPS EQELLRKMAS SSGEGKELYLSWVVEARRHI LAILQDCPSL RPPIDHLCEL LPRLQARYYS IASSSKVHPN SVHICAVVVEYETKAGRINK GVATNWLRAK EPAGENGGRA LVPMFVRKSQ FRLPFKATTP VIMVGPGTGVAPFIGFIQER AWLRQQGKEV GETLLYYGCR RSDEDYLYRE ELAQFHRDGA LTQLNVAFSR EQSHKVYVQH LLKQDREHLW KLIEGGAHIY VCGDARNMAR DVQNTFYDIV AELGAMEHAQAVDYIKKLMT KGRYSLDVWS

Molecular weight: 77048.1

Theoretical pI: 5.38

Amino acid composition

Ala (A)	51	7.5%
Arg (R)	38	5.6%
Asn (N)	26	3.8%
Asp (D)	41	6.0%
Cys (C)	8	1.2%
Gln (Q)	26	3.8%
Glu (E)	56	8.2%
Gly (G)	45	6.6%
His (H)	19	2.8%
Ile (I)	28	4.1%
Leu (L)	65	9.6%
Lys (K)	36	5.3%
Met (M)	19	2.8%
Phe (F)	28	4.1%
Pro (P)	26	3.8%
Ser (S)	45	6.6%
Thr (T)	34	5.0%
Trp (W)	9	1.3%
Tyr (Y)	31	4.6%
Val (V)	49	7.2%
Pyl (O)	0	0.0%
Sec (U)	0	0.0%

Total number of negatively charged residues (Asp + Glu): 97
Total number of positively charged residues (Arg + Lys): 74

Extinction coefficients:

Extinction coefficients are in units of M^{-1} cm^{-1}, at 280 nm measured in water.

Ext. coefficient 96190
Abs 0.1% (=1 g/l) 1.248, assuming ALL Cys residues appear as half cystines

Ext. coefficient 95690
Abs 0.1% (=1 g/l) 1.242, assuming NO Cys residues appear as half cystines

Human cytochrome P450 3A4 (P450 3A4)

P450 3A4 amino acid sequence, % composition, calculated theoretical PI value, extinction coefficient at A_{280} nm and molecular weight. The information was obtained by importing amino acid sequence into ProtParam program on the 'ExPASy' website (http://www.expasy.ch/cgi-bin/protparam).

Amino acid sequence (503):

MALIPDLAME TWLLLAVSLV LLYLYGTHSH GLFKKLGIPG PTPLPFLGNI
LSYHKGFCMFDMECHKKYGK VWGFYDGQQP VLAITDPDMI KTVLVKECYS
VFTNRRPFGP VGFMKSAISIAEDEEWKRLR SLLSPTFTSG KLKEMVPIIA
QYGDVLVRNL RREAETGKPV TLKDVFGAYSMDVITSTSFG VNIDSLNNPQ
DPFVENTKKL LRFDFLDPFF LSITVFPFLI PILEVLNICV FPREVTNFLR
KSVKRMKESR LEDTQKHRVD FLQLMIDSQN SKETESHKAL SDLELVAQSI
IFIFAGYETT SSVLSFIMYE LATHPDVQQK LQEEIDAVLP NKAPPTYDTV
LQMEYLDMVVNETLRLFPIA MRLERVCKKD VEINGMFIPK GVVVMIPSYA
LHRDPKYWTE PEKFLPERFSKKNKDNIDPY IYTPFGSGPR NCIGMRFALM
NMKLALIRVL QNFSFKPCKE TQIPLKLSLGGLLQPEKPVV LKVESRDGTV SGA

Molecular weight: 57343.1

Theoretical pI: 8.27

Amino acid composition

Ala (A)	20	4.0%
Arg (R)	22	4.4%
Asn (N)	18	3.6%
Asp (D)	26	5.2%
Cys (C)	7	1.4%
Gln (Q)	15	3.0%
Glu (E)	31	6.2%
Gly (G)	26	5.2%
His (H)	8	1.6%
Ile (I)	30	6.0%

Leu (L)	59	11.7%
Lys (K)	38	7.6%
Met (M)	19	3.8%
Phe (F)	32	6.4%
Pro (P)	35	7.0%
Ser (S)	31	6.2%
Thr (T)	27	5.4%
Trp (W)	4	0.8%
Tyr (Y)	16	3.2%
Val (V)	39	7.8%
Pyl (O)	0	0.0%
Sec (U)	0	0.0%

Total number of negatively charged residues (Asp + Glu): 57
Total number of positively charged residues (Arg + Lys): 60

Extinction coefficients:

Extinction coefficients are in units of M^{-1} cm^{-1}, at 280 nm measured in water.

Ext. coefficient 46215
Abs 0.1% (=1 g/l) 0.806, assuming ALL Cys residues appear as half cystines

Ext. coefficient 45840
Abs 0.1% (=1 g/l) 0.799, assuming NO Cys residues appear as half cystines

References

Alston, K., Robinson, R.C., Park, S.S., Gelboin, H.V. and Friedman, F.K. (1991) Interactions among cytochromes P-450 in the endoplasmic reticulum. Detection of chemically cross-linked complexes with monoclonal antibodies. J Biol Chem, 266, 735-739.

Anzenbacher, P. and Anzenbacherova, E. (2001) Cytochromes P450 and metabolism of xenobiotics. Cell Mol Life Sci, 58, 737-747.

Atkins, W.M. (2005) Non-Michaelis-Menten kinetics in cytochrome P450-catalyzed reactions. Annu Rev Pharmacol Toxicol, 45, 291-310.

Baas, B.J., Denisov, I.G. and Sligar, S.G. (2004) Homotropic cooperativity of monomeric cytochrome P450 3A4 in a nanoscale native bilayer environment. Arch Biochem Biophys, 430, 218-228.

Backes, W.L., Batie, C.J. and Cawley, G.F. (1998) Interactions among P450 enzymes when combined in reconstituted systems: formation of a 2B4-1A2 complex with a high affinity for NADPH-cytochrome P450 reductase. Biochemistry, 37, 12852-12859.

Backes, W.L. and Eyer, C.S. (1989) Cytochrome P-450 LM2 reduction. Substrate effects on the rate of reductase-LM2 association. J Biol Chem, 264, 6252-6259.

Backes, W.L. and Kelley, R.W. (2003) Organization of multiple cytochrome P450s with NADPH-cytochrome P450 reductase in membranes. Pharmacol Ther, 98, 221-233.

Backes, W.L. and Reker-Backes, C.E. (1988) The effect of NADPH concentration on the reduction of cytochrome P-450 LM2. J Biol Chem, 263, 247-253.

Backes, W.L., Sligar, S.G. and Schenkman, J.B. (1982) Kinetics of hepatic cytochrome P-450 reduction: correlation with spin state of the ferric heme. Biochemistry, 21, 1324-1330.

Barr, D.P., Martin, M.V., Guengerich, F.P. and Mason, R.P. (1996) Reaction of cytochrome P450 with cumene hydroperoxide: ESR spin-trapping evidence for the homolytic scission of the peroxide O-O bond by ferric cytochrome P450 1A2. Chem Res Toxicol, 9, 318-325.

Barsukov, I., Modi, S., Lian, L.Y., Sze, K.H., Paine, M.J., Wolf, C.R. and Roberts, G.C. (1997) 1H, 15N and 13C NMR resonance assignment, secondary structure and global fold of the FMN-binding domain of human cytochrome P450 reductase. J Biomol NMR, 10, 63-75.

Bartoszek, A. and Wolf, C.R. (1992) Enhancement of doxorubicin toxicity following activation by NADPH cytochrome P450 reductase. Biochem Pharmacol, 43, 1449-1457.

Bernhardt, R. (2006) Cytochromes P450 as versatile biocatalysts. J Biotechnol, 124, 128-145.

Bernhardt, R., Kraft, R., Otto, A. and Ruckpaul, K. (1988) Electrostatic interactions between cytochrome P-450 LM2 and NADPH-cytochrome P-450 reductase. Biomed Biochim Acta, 47, 581-592.

Bhattacharyya, A.K., Hurley, J.K., Tollin, G. and Waskell, L. (1994) Investigation of the Rate-Limiting Step for Electron-Transfer from Nadph -Cytochrome-P450 Reductase to Cytochrome-B(5) - a Laser Flash-Photolysis Study. Archives of Biochemistry and Biophysics, 310, 318-324.

Blanck, J., Rohde, K., Behlke, J., Janig, G.R., Pfeil, D. and Ruckpaul, K. (1979) NADPH reduction of cytochrome P-450 at different integrational levels of the enzyme system. Acta Biol Med Ger, 38, 399-408.

Blanck, J., Smettan, G., Ristau, O., Ingelman-Sundberg, M. and Ruckpaul, K. (1984) Mechanism of rate control of the NADPH-dependent reduction of cytochrome P-450 by lipids in reconstituted phospholipid vesicles. Eur J Biochem, 144, 509-513.

Bligh, H.F., Bartoszek, A., Robson, C.N., Hickson, I.D., Kasper, C.B., Beggs, J.D. and Wolf, C.R. (1990) Activation of mitomycin C by NADPH:cytochrome P-450 reductase. Cancer Res, 50, 7789-7792.

Bonina, T.A., Gilep, A.A., Estabrook, R.W. and Usanov, S.A. (2005) Engineering of Proteolytically Stable NADPH-Cytochrome P450 Reductase. Biochemistry (Mosc), 70, 357-365.

Bridges, A., Gruenke, L., Chang, Y.T., Vakser, I.A., Loew, G. and Waskell, L. (1998) Identification of the binding site on cytochrome P450 2B4 for cytochrome b5 and cytochrome P450 reductase. J Biol Chem, 273, 17036-17049.

Cawley, G.F., Batie, C.J. and Backes, W.L. (1995) Substrate-dependent competition of different P450 isozymes for limiting NADPH-cytochrome P450 reductase. Biochemistry, 34, 1244-1247.

Correia, M.A. and Ortiz de Montellano, P.R. (2004) Inhibition of cytochrome P450 enzymes. In Ortiz de Montellano, P.R.e.s.e.s. (ed), Cytochrome P450: Structure, Mechanism and Biochemistry. New York: Plenum Press.

Cvrk, T. and Strobel, H.W. (2001) Role of LYS271 and LYS279 residues in the interaction of cytochrome P4501A1 with NADPH-cytochrome P450 reductase. Arch Biochem Biophys, 385, 290-300.

Das, A., Grinkova, Y.V. and Sligar, S.G. (2007) Redox Potential Control by Drug Binding to Cytochrome P450 3A4. J Am Chem Soc.

Davydov, D.R., Fernando, H., Baas, B.J., Sligar, S.G. and Halpert, J.R. (2005) Kinetics of Dithionite-Dependent Reduction of Cytochrome P450 3A4: Heterogeneity of the Enzyme Caused by Its Oligomerization. Biochemistry, 44, 13902-13913.

Davydov, D.R., Halpert, J.R., Renaud, J.P. and Hui Bon Hoa, G. (2003) Conformational heterogeneity of cytochrome P450 3A4 revealed by high pressure spectroscopy. Biochem Biophys Res Commun, 312, 121-130.

Davydov, D.R., Kariakin, A.A., Petushkova, N.A. and Peterson, J.A. (2000) Association of cytochromes P450 with their reductases: opposite sign of the electrostatic interactions in P450BM-3 as compared with the microsomal 2B4 system. Biochemistry, 39, 6489-6497.

Davydov, D.R., Knyushko, T.V., Kanaeva, I.P., Koen, Y.M., Samenkova, N.F., Archakov, A.I. and Hui Bon Hoa, G. (1996) Interactions of cytochrome P450 2B4 with NADPH-cytochrome P450 reductase studied by fluorescent probe. Biochimie, 78, 734-743.

Dean, W.L. and Gray, R.D. (1982) Hydrodynamic properties of monomeric cytochromes P-450LM2 and P-450LM4 in n-octylglucoside solution. Biochem Biophys Res Commun, 107, 265-271.

Degtyarenko, K.N. and Archakov, A.I. (1993) Molecular evolution of P450 superfamily and P450-containing monooxygenase systems. FEBS Lett, 332, 1-8.

Denisov, I.G., Baas, B.J., Grinkova, Y.V. and Sligar, S.G. (2007) Cooperativity in cytochrome P450 3A4 - Linkages in substrate binding, spin state, uncoupling, and product formation. Journal of Biological Chemistry, 282, 7066-7076.

Denisov, I.G., Baas, B.J., Grinkova, Y.V. and Sligar, S.G. (2007) Cooperativity in P450 CYP3A4: Linkages in substrate binding, spin state, uncoupling and product formation. J Biol Chem.

Denisov, I.G., Grinkova, Y.V., Baas, B.J. and Sligar, S.G. (2006) The ferrous-dioxygen intermediate in human cytochrome P450 3A4. Substrate dependence of formation and decay kinetics. J Biol Chem, 281, 23313-23318.

Denisov, I.G., Makris, T.M., Sligar, S.G. and Schlichting, I. (2005) Structure and chemistry of cytochrome P450. Chem Rev, 105, 2253-2277.

Denk, H., Schenkman, J.B., Bacchin, P.G., Hutterer, F., Schaffner, F. and Popper, H. (1971) Mechanism of cholestasis. 3. Interaction of synthetic detergents with the microsomal cytochrome P-450 dependentbiotransformation system in vitro. A comparison between the effects of detergents, the effects of bile acids, and the findings in bile duct ligated rats. Exp Mol Pathol, 14, 263-276.

Duppel, W. and Ullrich, V. (1976) Membrane effects on drug monooxygenation activity in hepatic microsomes. Biochim Biophys Acta, 426, 399-407.

Ekroos, M. and Sjogren, T. (2006) Structural basis for ligand promiscuity in cytochrome P450 3A4. Proc Natl Acad Sci U S A, 103, 13682-13687.

Ellis, J., Gutierrez, A., Barsukov, I.L., Huang, W.C., Grossmann, J.G. and Roberts, G.C. (2009) Domain motion in cytochrome P450 reductase: conformational equilibria revealed by NMR and small-angle X-ray scattering. J Biol Chem.

Enoch, H.G. and Strittmatter, P. (1979) Cytochrome b5 reduction by NADPH-cytochrome P-450 reductase. J Biol Chem, 254, 8976-8981.

Estabrook, R.W., Franklin, M.R., Cohen, B., Shigamatzu, A. and Hildebrandt, A.G. (1971) Biochemical and genetic factors influencing drug metabolism. Influence of hepatic microsomal mixed function oxidation reactions on cellular metabolic control. Metabolism, 20, 187-199.

Eyer, C.S. and Backes, W.L. (1992) Relationship between the rate of reductase-cytochrome P450 complex formation and the rate of first electron transfer. Arch Biochem Biophys, 293, 231-240.

Franklin, M.R. and Estabrook, R.W. (1971) On the inhibitory action of mersalyl on microsomal drug oxidation: a rigid organization of the electron transport chain. Arch Biochem Biophys, 143, 318-329.

French, J.S. and Coon, M.J. (1979) Properties of NADPH-cytochrome P-450 reductase purified from rabbit liver microsomes. Arch Biochem Biophys, 195, 565-577.

French, J.S., Guengerich, F.P. and Coon, M.J. (1980) Interactions of cytochrome P-450, NADPH-cytochrome P-450 reductase, phospholipid, and substrate in the reconstituted liver microsomal enzyme system. J Biol Chem, 255, 4112-4119.

Galetin, A., Clarke, S.E. and Houston, J.B. (2003) Multisite kinetic analysis of interactions between prototypical CYP3A4 subgroup substrates: midazolam, testosterone, and nifedipine. Drug Metab Dispos, 31, 1108-1116.

Gibson, G.G., Cinti, D.L., Sligar, S.G. and Schenkman, J.B. (1980) The effect of microsomal fatty acids and other lipids on the spin state of partially purified cytochrome P-450. J Biol Chem, 255, 1867-1873.

Gillam, E.M., Baba, T., Kim, B.R., Ohmori, S. and Guengerich, F.P. (1993) Expression of modified human cytochrome P450 3A4 in Escherichia coli and purification and reconstitution of the enzyme. Arch Biochem Biophys, 305, 123-131.

Gonzalez, F.J. (1990) Molecular genetics of the P-450 superfamily. Pharmacol Ther, 45, 1-38.

Gonzalez, F.J. and Korzekwa, K.R. (1995) Cytochromes P450 expression systems. Annu Rev Pharmacol Toxicol, 35, 369-390.

Griffith, O.W. and Stuehr, D.J. (1995) Nitric oxide synthases: properties and catalytic mechanism. Annu Rev Physiol, 57, 707-736.

Gruenke, L.D., Konopka, K., Cadieu, M. and Waskell, L. (1995) The stoichiometry of the cytochrome P-450-catalyzed metabolism of methoxyflurane and benzphetamine in the presence and absence of cytochrome b5. J Biol Chem, 270, 24707-24718.

Grunau, A., Geraki, K., Grossmann, J.G. and Gutierrez, A. (2007) Conformational dynamics and the energetics of protein--ligand interactions: role of interdomain loop in human cytochrome P450 reductase. Biochemistry, 46, 8244-8255.

Grunau, A., Paine, M.J., Ladbury, J.E. and Gutierrez, A. (2006) Global effects of the energetics of coenzyme binding: NADPH controls the protein interaction properties of human cytochrome P450 reductase. Biochemistry, 45, 1421-1434.

Guengerich, F.P. (1983) Oxidation-reduction properties of rat liver cytochromes P-450 and NADPH-cytochrome p-450 reductase related to catalysis in reconstituted systems. Biochemistry, 22, 2811-2820.

Guengerich, F.P. (1999) Cytochrome P-450 3A4: regulation and role in drug metabolism. Annu Rev Pharmacol Toxicol, 39, 1-17.

Guengerich, F.P. (2002) Rate-limiting steps in cytochrome P450 catalysis. Biol Chem, 383, 1553-1564.

Guengerich, F.P. (2004) Human cytochrome P450 enzymes. In:. In Ortiz de Montellano, P.R.e. (ed), Cytochrome P450: structure, Mechanism, and Biochemistry. New York: Plenum Press.

Guengerich, F.P. and Johnson, W.W. (1997) Kinetics of ferric cytochrome P450 reduction by NADPH-cytochrome P450 reductase: rapid reduction in the absence of substrate and variations among cytochrome P450 systems. Biochemistry, 36, 14741-14750.

Guengerich, F.P., Martin, M.V., Beaune, P.H., Kremers, P., Wolff, T. and Waxman, D.J. (1986) Characterization of rat and human liver microsomal cytochrome P-450 forms involved in nifedipine oxidation, a prototype for genetic polymorphism in oxidative drug metabolism. J. Biol. Chem., 261, 5051-5060.

Guo, L.Q., Taniguchi, M., Xiao, Y.Q., Baba, K., Ohta, T. and Yamazoe, Y. (2000) Inhibitory effect of natural furanocoumarins on human microsomal cytochrome P450 3A activity. Jpn J Pharmacol, 82, 122-129.

Gut, J., Richter, C., Cherry, R.J., Winterhalter, K.H. and Kawato, S. (1982) Rotation of cytochrome P-450. II. Specific interactions of cytochrome P-450 with NADPH-cytochrome P-450 reductase in phospholipid vesicles. J Biol Chem, 257, 7030-7036.

Gutierrez, A., Lian, L.Y., Wolf, C.R., Scrutton, N.S. and Roberts, G.C. (2001) Stopped-flow kinetic studies of flavin reduction in human cytochrome P450 reductase and its component domains. Biochemistry, 40, 1964-1975.

Gutierrez, A., Munro, A.W., Grunau, A., Wolf, C.R., Scrutton, N.S. and Roberts, G.C.K. (2003) Interflavin electron transfer in human cytochrome P450 reductase is enhanced by coenzyme binding - Relaxation kinetic studies with coenzyme analogues. European Journal of Biochemistry, 270, 2612-2621.

Gutierrez, A., Paine, M., Wolf, C.R., Scrutton, N.S. and Roberts, G.C. (2002) Relaxation kinetics of cytochrome P450 reductase: internal electron transfer is limited by conformational change and regulated by coenzyme binding. Biochemistry, 41, 4626-4637.

Hamdane, D., Xia, C., Im, S.C., Zhang, H., Kim, J.J. and Waskell, L. (2009) Structure and function of an NADPH-cytochrome P450 oxidoreductase in an open conformation capable of reducing cytochrome P450. J Biol Chem, 284, 11374-11384.

Harlow, G.R. and Halpert, J.R. (1997) Alanine-scanning mutagenesis of a putative substrate recognition site in human cytochrome P450 3A4. Role of residues 210 and 211 in flavonoid activation and substrate specificity. J Biol Chem, 272, 5396-5402.

Harlow, G.R. and Halpert, J.R. (1998) Analysis of human cytochrome P450 3A4 cooperativity: construction and characterization of a site-directed mutant that displays hyperbolic steroid hydroxylation kinetics. Proc Natl Acad Sci U S A, 95, 6636-6641.

He, X. and de Montellano, P.R. (2004) Radical rebound mechanism in cytochrome P-450-catalyzed hydroxylation of the multifaceted radical clocks alpha- and beta-thujone. J Biol Chem, 279, 39479-39484.

He, Y.A., Roussel, F. and Halpert, J.R. (2003) Analysis of homotropic and heterotropic cooperativity of diazepam oxidation by CYP3A4 using site-directed mutagenesis and kinetic modeling. Arch Biochem Biophys, 409, 92-101.

Henderson, C.J., Otto, D.M.E., Carrie, D., Magnuson, M.A., McLaren, A.W., Rosewell, I. and Wolf, C.R. (2003) Inactivation of the hepatic cytochrome P450 system by conditional deletion of hepatic cytochrome P450 reductase. Journal of Biological Chemistry, 278, 13480-13486.

Heuman, D.M., Gallagher, E.J., Barwick, J.L., Elshourbagy, N.A. and Guzelian, P.S. (1982) Immunochemical evidence for induction of a common form of hepatic cytochrome P-450 in rats treated with pregnenolone-16 alpha-carbonitrile or other steroidal or non-steroidal agents. Mol Pharmacol, 21, 753-760.

Hosea, N.A. and Guengerich, F.P. (1998) Oxidation of nonionic detergents by cytochrome P450 enzymes. Arch Biochem Biophys, 353, 365-373.

Hosea, N.A., Miller, G.P. and Guengerich, F.P. (2000) Elucidation of distinct ligand binding sites for cytochrome P450 3A4. Biochemistry, 39, 5929-5939.

Hosten, C.M., Sullivan, A.M., Palaniappan, V., Fitzgerald, M.M. and Terner, J. (1994) Resonance Raman spectroscopy of the catalytic intermediates and derivatives of chloroperoxidase from Caldariomyces fumago. J Biol Chem, 269, 13966-13978.

Imaoka, S., Imai, Y., Shimada, T. and Funae, Y. (1992) Role of phospholipids in reconstituted cytochrome P450 3A form and mechanism of their activation of catalytic activity. Biochemistry, 31, 6063-6069.

Ingelman-Sundberg, M. (2002) Polymorphism of cytochrome P450 and xenobiotic toxicity. Toxicology, 181-182, 447-452.

Ingelman-Sundberg, M. (2004) Human drug metabolising cytochrome P450 enzymes: properties and polymorphisms. Naunyn Schmiedebergs Arch Pharmacol, 369, 89-104.

Ingelman-Sundberg, M., Hagbjork, A.L., Ueng, Y.F., Yamazaki, H. and Guengerich, F.P. (1996) High rates of substrate hydroxylation by human cytochrome P450 3A4 in reconstituted membranous vesicles: influence of membrane charge. Biochem Biophys Res Commun, 221, 318-322.

Ingelman-Sundberg, M. and Johansson, I. (1980) Catalytic properties of purified forms of rabbit liver microsomal cytochrome P-450 in reconstituted phospholipid vesicles. Biochemistry, 19, 4004-4011.

Iyanagi, T. and Mason, H.S. (1973) Some properties of hepatic reduced nicotinamide adenine dinucleotide phosphate-cytochrome c reductase. Biochemistry, 12, 2297-2308.

Jansson, I. and Schenkman, J.B. (1987) Influence of cytochrome b5 on the stoichiometry of the different oxidative reactions catalyzed by liver microsomal cytochrome P-450. Drug Metab Dispos, 15, 344-348.

Kapelyukh, Y., Paine, M.J., Marechal, J.D., Sutcliffe, M.J., Wolf, C.R. and Roberts, G. (2008) Multiple substrate binding by cytochrome P450 3A4: estimation of the number of bound substrate molecules. Drug Metab Dispos.

Karplus, P.A., Daniels, M.J. and Herriott, J.R. (1991) Atomic structure of ferredoxin-NADP+ reductase: prototype for a structurally novel flavoenzyme family. Science, 251, 60-66.

Kawato, S., Gut, J., Cherry, R.J., Winterhalter, K.H. and Richter, C. (1982) Rotation of cytochrome P-450. I. Investigations of protein-protein interactions of cytochrome P-450 in phospholipid vesicles and liver microsomes. J Biol Chem, 257, 7023-7029.

Kim, K.H., Ahn, T. and Yun, C.H. (2003) Membrane properties induced by anionic phospholipids and phosphatidylethanolamine are critical for the membrane binding and catalytic activity of human cytochrome P450 3A4. Biochemistry, 42, 15377-15387.

Klingenberg, M. (1958) Pigments of rat liver microsomes. Arch Biochem Biophys, 75, 376-386.

Kocarek, T.A., Schuetz, E.G., Strom, S.C., Fisher, R.A. and Guzelian, P.S. (1995) Comparative analysis of cytochrome P4503A induction in primary cultures of rat, rabbit, and human hepatocytes. Drug Metab Dispos, 23, 415-421.

Koley, A.P., Buters, J.T., Robinson, R.C., Markowitz, A. and Friedman, F.K. (1995) CO binding kinetics of human cytochrome P450 3A4. Specific interaction of substrates with kinetically distinguishable conformers. J Biol Chem, 270, 5014-5018.

Koley, A.P., Robinson, R.C. and Friedman, F.K. (1996) Cytochrome P450 conformation and substrate interactions as probed by CO binding kinetics. Biochimie, 78, 706-713.

Kominami, S. and Takemori, S. (1982) Effect of spin state on reduction of cytochrome P-450 (P-450C21) from bovine adrenocortical microsomes. Biochim Biophys Acta, 709, 147-153.

Kumar, S., Davydov, D.R. and Halpert, J.R. (2005) Role of cytochrome B5 in modulating peroxide-supported cyp3a4 activity: evidence for a conformational transition and cytochrome P450 heterogeneity. Drug Metab Dispos, 33, 1131-1136.

Lamb, D.C., Warrilow, A.G., Venkateswarlu, K., Kelly, D.E. and Kelly, S.L. (2001) Activities and kinetic mechanisms of native and soluble NADPH-cytochrome P450 reductase. Biochem Biophys Res Commun, 286, 48-54.

Lange, R., Bonfils, C. and Debey, P. (1977) The low-spin/high-spin transition equilibrium of camphor-bound cytochrome P-450. Effects of medium and temperature on equilibrium data. Eur J Biochem, 79, 623-628.

Lange, R., Hui Bon Hoa, G., Debey, P. and Gunsalus, I.C. (1979) Spin transition of camphor-bound cytochrome P-450. 2. Kinetics following rapid changes of the local paH at sub-zero temperatures. Eur J Biochem, 94, 491-496.

Lange, R., Pierre, J. and Debey, P. (1980) Visible and ultraviolet spectral transitions of camphor-bound cytochrome P-450. A comprehensive study. Eur J Biochem, 107, 441-445.

Lasic, D.D. (1997) Liposomes in gene delivery. CRC Press LLC, Boca Raton, FL.

Leclerc, D., Wilson, A., Dumas, R., Gafuik, C., Song, D., Watkins, D., Heng, H.H., Rommens, J.M., Scherer, S.W., Rosenblatt, D.S. and Gravel, R.A. (1998) Cloning and

mapping of a cDNA for methionine synthase reductase, a flavoprotein defective in patients with homocystinuria. Proc Natl Acad Sci U S A, 95, 3059-3064.

Lee, Y.T., Wilson, R.F., Rupniewski, I. and Goodin, D.B. (2010) P450cam visits an open conformation in the absence of substrate. Biochemistry, 49, 3412-3419.

Lewis, D.F. (1996) Cytochromes P450: Structure, Function and Mechanism. Taylor & Francis, London

Leys, D., Basran, J., Talfournier, F., Sutcliffe, M.J. and Scrutton, N.S. (2003) Extensive conformational sampling in a ternary electron transfer complex. Nat Struct Biol, 10, 219-225.

Lu, A.Y., Junk, K.W. and Coon, M.J. (1969) Resolution of the cytochrome P-450-containing omega-hydroxylation system of liver microsomes into three components. J Biol Chem, 244, 3714-3721.

Lu, A.Y., Levin, W. and Kuntzman, R. (1974) Reconstituted liver microsomal enzyme system that hydroxylates drugs, other foreign compounds and endogenous substrates. VII. Stimulation of benzphetamine N-demethylation by lipid and detergent. Biochem Biophys Res Commun, 60, 266-272.

Makris, T.M., Denisov, I., Schlichting, I., and Sligar, S.G. (2005) Activation of molecular oxygen by cytochrome P450. In Ortiz de Montellano, P.R. (ed), Cytochrome P450: Structure Mechanism and Biochemistry. Kluwer Academic / Plenum, New York.

McGinnity, D.F. and Riley, R.J. (2001) Predicting drug pharmacokinetics in humans from in vitro metabolism studies. Biochem Soc Trans, 29, 135-139.

McLean, K.J., Sabri, M., Marshall, K.R., Lawson, R.J., Lewis, D.G., Clift, D., Balding, P.R., Dunford, A.J., Warman, A.J., McVey, J.P., Quinn, A.M., Sutcliffe, M.J., Scrutton, N.S. and Munro, A.W. (2005) Biodiversity of cytochrome P450 redox systems. Biochem Soc Trans, 33, 796-801.

Miwa, G.T. and Lu, A.Y. (1984) The association of cytochrome P-450 and NADPH-cytochrome P-450 reductase in phospholipid membranes. Arch Biochem Biophys, 234, 161-166.

Miwa, G.T., West, S.B., Huang, M.T. and Lu, A.Y. (1979) Studies on the association of cytochrome P-450 and NADPH-cytochrome c reductase during catalysis in a reconstituted hydroxylating system. J Biol Chem, 254, 5695-5700.

Munro, A.W., Girvan, H.M. and McLean, K.J. (2007) Cytochrome P450--redox partner fusion enzymes. Biochim Biophys Acta, 1770, 345-359.

Munro, A.W., Noble, M.A., Robledo, L., Daff, S.N. and Chapman, S.K. (2001) Determination of the redox properties of human NADPH-cytochrome P450 reductase. Biochemistry, 40, 1956-1963.

Murataliev, M.B., Feyereisen, R. and Walker, F.A. (2004) Electron transfer by diflavin reductases. Biochim Biophys Acta, 1698, 1-26.

Myasoedova, K.N. and Berndt, P. (1990) Immobilized cytochrome P-450LM2. Dissociation and reassociation of oligomers. FEBS Lett, 270, 177-180.

Nadler, S.G. and Strobel, H.W. (1991) Identification and characterization of an NADPH-cytochrome P450 reductase derived peptide involved in binding to cytochrome P450. Arch Biochem Biophys, 290, 277-284.

Nagano, S., Shimada, H., Tarumi, A., Hishiki, T., Kimata-Ariga, Y., Egawa, T., Suematsu, M., Park, S.Y., Adachi, S., Shiro, Y. and Ishimura, Y. (2003) Infrared spectroscopic and mutational studies on putidaredoxin-induced conformational changes in ferrous CO-P450cam. Biochemistry, 42, 14507-14514.

Nagano, S., Tosha, T., Ishimori, K., Morishima, I. and Poulos, T.L. (2004) Crystal structure of the cytochrome p450cam mutant that exhibits the same spectral perturbations induced by putidaredoxin binding. J Biol Chem, 279, 42844-42849.

Narhi, L.O. and Fulco, A.J. (1986) Characterization of a catalytically self-sufficient 119,000-dalton cytochrome P-450 monooxygenase induced by barbiturates in Bacillus megaterium. J Biol Chem, 261, 7160-7169.

Nelson, D.R., Koymans, L., Kamataki, T., Stegeman, J.J., Feyereisen, R., Waxman, D.J., Waterman, M.R., Gotoh, O., Coon, M.J., Estabrook, R.W., Gunsalus, I.C. and Nebert, D.W. (1996) P450 superfamily: update on new sequences, gene mapping, accession numbers and nomenclature. Pharmacogenetics, 6, 1-42.

Nelson, D.R., Zeldin, D.C., Hoffman, S.M., Maltais, L.J., Wain, H.M. and Nebert, D.W. (2004) Comparison of cytochrome P450 (CYP) genes from the mouse and human genomes, including nomenclature recommendations for genes, pseudogenes and alternative-splice variants. Pharmacogenetics, 14, 1-18.

Ngui, J.S., Chen, Q., Shou, M., Wang, R.W., Stearns, R.A., Baillie, T.A. and Tang, W. (2001) In vitro stimulation of warfarin metabolism by quinidine: increases in the formation of 4'- and 10-hydroxywarfarin. Drug Metab Dispos, 29, 877-886.

Ngui, J.S., Tang, W., Stearns, R.A., Shou, M., Miller, R.R., Zhang, Y., Lin, J.H. and Baillie, T.A. (2000) Cytochrome P450 3A4-mediated interaction of diclofenac and quinidine. Drug Metab Dispos, 28, 1043-1050.

Nielson, K.A.a.B.L.M. (2004) Cytochrome P450s in Plant, In:. In Ortiz de Montellano, P.e. (ed), Cytochrome P450: structure, Mechanism, and Biochemistry. New York: Plenum Press.

Nilsson, J., Persson, B. and von Heijne, G. (2005) Comparative analysis of amino acid distributions in integral membrane proteins from 107 genomes. Proteins, 60, 606-616.

Noshiro, M., Ullrich, V. and Omura, T. (1981) Cytochrome b5 as electron donor for oxy-cytochrome P-450. Eur J Biochem, 116, 521-526.

Omura, T. (2006) Mitochondrial P450s. Chem Biol Interact, 163, 86-93.

Omura, T. and Sato, R. (1964) The Carbon Monoxide-Binding Pigment of Liver Microsomes. I. Evidence for Its Hemoprotein Nature. J Biol Chem, 239, 2370-2378.

Oprian, D.D., Vatsis, K.P. and Coon, M.J. (1979) Kinetics of reduction of cytochrome P-450LM4 in a reconstituted liver microsomal enzyme system. J Biol Chem, 254, 8895-8902.

Ortiz de Montellano, P.R. (2005) Cytochrome P450: Structure, Mechanism and Biochemistry.

Ortiz de Montellano, P.R. (2005) Cytochrome P450: Structure, Mechanism, and Biochemistry. Kluwer Academic/Plenum,.

Ortiz de Montellano, P.R. (2010) Hydrocarbon hydroxylation by cytochrome P450 enzymes. Chem Rev, 110, 932-948.

Otyepka, M., Skopalik, J., Anzenbacherova, E. and Anzenbacher, P. (2007) What common structural features and variations of mammalian P450s are known to date? Biochim Biophys Acta, 1770, 376-389.

Page, C.C., Moser, C.C., Chen, X. and Dutton, P.L. (1999) Natural engineering principles of electron tunnelling in biological oxidation-reduction. Nature, 402, 47-52.

Paine, M.J., Garner, A.P., Powell, D., Sibbald, J., Sales, M., Pratt, N., Smith, T., Tew, D.G. and Wolf, C.R. (2000) Cloning and characterization of a novel human dual flavin reductase. J Biol Chem, 275, 1471-1478.

Paine, M.J.I., Scrutton, N.S., Munro, A.W., Gutierrez, A., Roberts, G.C.K. and and Wolf, C.R. (2005) Electron Transfer Partners of Cytochrome P450. In Ortiz de Montellano, P.R. (ed), Cytochrome P450: Structure, Mechanism and Biochemistry. Kluwer Academic / Plenum, New York, pp. 115-148.

Perret, A. and Pompon, D. (1998) Electron shuttle between membrane-bound cytochrome P450 3A4 and b5 rules uncoupling mechanisms. Biochemistry, 37, 11412-11424.

Peterson, J.A., Ebel, R.E., O'Keeffe, D.H., Matsubara, T. and Estabrook, R.W. (1976) Temperature dependence of cytochrome P-450 reduction. A model for NADPH-cytochrome P-450 reductase:cytochrome P-450 interaction. J Biol Chem, 251, 4010-4016.

Peterson, J.A. and Griffin, B.W. (1972) Carbon monoxide binding by Pseudomonas putida cytochrome P-450. Arch Biochem Biophys, 151, 427-433.

Pompon, D. and Coon, M.J. (1984) On the mechanism of action of cytochrome P-450. Oxidation and reduction of the ferrous dioxygen complex of liver microsomal cytochrome P-450 by cytochrome b5. J Biol Chem, 259, 15377-15385.

Poulos, T.L., Finzel, B.C., Gunsalus, I.C., Wagner, G.C. and Kraut, J. (1985) The 2.6-A crystal structure of Pseudomonas putida cytochrome P-450. J Biol Chem, 260, 16122-16130.

Poulos, T.L. and Johnson, E.F. (2005) Structures of cytochrome P450 enzymes. In Ortiz de Montellano, P.R. (ed), Cytochrome P450: Structure, Mechanism and Biochemistry. Kluwer Academic / Plenum
New York
pp. 87-114.

Pritchard, M.P., Ossetian, R., Li, D.N., Henderson, C.J., Burchell, B., Wolf, C.R. and Friedberg, T. (1997) A general strategy for the expression of recombinant human cytochrome P450s in Escherichia coli using bacterial signal peptides: expression of CYP3A4, CYP2A6, and CYP2E1. Arch Biochem Biophys, 345, 342-354.

Ravichandran, K.G., Boddupalli, S.S., Hasermann, C.A., Peterson, J.A. and Deisenhofer, J. (1993) Crystal structure of hemoprotein domain of P450BM-3, a prototype for microsomal P450's. Science, 261, 731-736.

Reed, J.R., Brignac-Huber, L.M. and Backes, W.L. (2008) Physical incorporation of NADPH-cytochrome P450 reductase and cytochrome P450 into phospholipid vesicles using glycocholate and Bio-Beads. Drug Metab Dispos, 36, 582-588.

Reed, J.R. and Hollenberg, P.F. (2003) Examining the mechanism of stimulation of cytochrome P450 by cytochrome b5: the effect of cytochrome b5 on the interaction between cytochrome P450 2B4 and P450 reductase. J Inorg Biochem, 97, 265-275.

Reed, J.R. and Hollenberg, P.F. (2003) New perspectives on the conformational equilibrium regulating multi-phasic reduction of cytochrome P450 2B4 by cytochrome P450 reductase. J Inorg Biochem, 97, 276-286.

Reed, J.R., Kelley, R.W. and Backes, W.L. (2006) An evaluation of methods for the reconstitution of cytochromes P450 and NADPH P450 reductase into lipid vesicles. Drug Metab Dispos, 34, 660-666.

Rendic, S. (2002) Summary of information on human CYP enzymes: human P450 metabolism data. Drug Metab Rev, 34, 83-448.

Rigaud, J.L. and Levy, D. (2003) Reconstitution of membrane proteins into liposomes. Methods Enzymol, 372, 65-86.

Roberts, A.G. and Atkins, W.M. (2007) Energetics of heterotropic cooperativity between alpha-naphthoflavone and testosterone binding to CYP3A4. Arch Biochem Biophys, 463, 89-101.

Roberts, A.G., Campbell, A.P. and Atkins, W.M. (2005) The thermodynamic landscape of testosterone binding to cytochrome P450 3A4: ligand binding and spin state equilibria. Biochemistry, 44, 1353-1366.

Rohde, K., Blanck, J. and Ruckpaul, K. (1983) Kinetics of elementary steps in the cytochrome P-450 reaction sequence. VI. Model treatment of the NADPH-dependent first electron transfer reaction between cytochrome P-450 reductase and cytochrome P-450 LM2 in solution. Biomed Biochim Acta, 42, 651-662.

Rota, C., Barr, D.P., Martin, M.V., Guengerich, F.P., Tomasi, A. and Mason, R.P. (1997) Detection of free radicals produced from the reaction of cytochrome P-450 with linoleic acid hydroperoxide. Biochem J, 328 (Pt 2), 565-571.

Ruckpaul, K., Rein, H. and Blank, J. (1989) Regulation mechanisms of the activity of the hepatic endoplasmic cytochrome p450
In Ruckpaul, K. and Rein, H. (eds), *Basis and mechanisms of regulation of cytochrome P450*. Tayler and Francis, pp. 1-65.

Schacter, B.A., Nelson, E.B., Marver, H.S. and Masters, B.S. (1972) Immunochemical evidence for an association of heme oxygenase with the microsomal electron transport system. J Biol Chem, 247, 3601-3607.

Schenkman, J.B., and Jansson, I. (2003) The many roles of cytochrome b5. Pharmacology & Therapeutics, 97, 139-152.

Schenkman, J.B., Remmer, H. and Estabrook, R.W. (1967) Spectral studies of drug interaction with hepatic microsomal cytochrome. Mol Pharmacol, 3, 113-123.

Schenkman, J.B., Sligar, S.G. and Cinti, D.L. (1981) Substrate interaction with cytochrome P-450. Pharmacol Ther, 12, 43-71.

Schlichting, I., Berendzen, J., Chu, K., Stock, A.M., Maves, S.A., Benson, D.E., Sweet, R.M., Ringe, D., Petsko, G.A. and Sligar, S.G. (2000) The catalytic pathway of cytochrome p450cam at atomic resolution. Science, 287, 1615-1622.

Schmider, J., Greenblatt, D.J., von Moltke, L.L., Harmatz, J.S. and Shader, R.I. (1995) N-demethylation of amitriptyline in vitro: role of cytochrome P-450 3A (CYP3A) isoforms and effect of metabolic inhibitors. J Pharmacol Exp Ther, 275, 592-597.

Schuetz, E.G. (2001) Induction of cytochromes P450. Curr Drug Metab, 2, 139-147.

Schuler, M.A. (1996) The role of cytochrome P450 monooxygenases in plant-insect interactions. Plant Physiol, 112, 1411-1419.

Schwab, G.E., Raucy, J.L. and Johnson, E.F. (1988) Modulation of rabbit and human hepatic cytochrome P-450-catalyzed steroid hydroxylations by alpha-naphthoflavone. Mol Pharmacol, 33, 493-499.

Scott, E.E. and Halpert, J.R. (2005) Structures of cytochrome P450 3A4. Trends Biochem Sci, 30, 5-7.

Sem, D.S. and Kasper, C.B. (1994) Kinetic mechanism for the model reaction of NADPH-cytochrome P450 oxidoreductase with cytochrome c. Biochemistry, 33, 12012-12021.

Sevrioukova, I.F., Garcia, C., Li, H., Bhaskar, B. and Poulos, T.L. (2003) Crystal structure of putidaredoxin, the [2Fe-2S] component of the P450cam monooxygenase system from Pseudomonas putida. J Mol Biol, 333, 377-392.

Sevrioukova, I.F., Li, H. and Poulos, T.L. (2004) Crystal structure of putidaredoxin reductase from Pseudomonas putida, the final structural component of the cytochrome P450cam monooxygenase. J Mol Biol, 336, 889-902.

Shen, A.L. and Kasper, C.B. (1995) Role of acidic residues in the interaction of NADPH-cytochrome P450 oxidoreductase with cytochrome P450 and cytochrome c. J Biol Chem, 270, 27475-27480.

Shen, A.L., O'Leary, K.A. and Kasper, C.B. (2002) Association of multiple developmental defects and embryonic lethality with loss of microsomal NADPH-cytochrome P450 oxidoreductase. J Biol Chem, 277, 6536-6541.

Shen, A.L., Porter, T.D., Wilson, T.E. and Kasper, C.B. (1989) Structural analysis of the FMN binding domain of NADPH-cytochrome P-450 oxidoreductase by site-directed mutagenesis. J Biol Chem, 264, 7584-7589.

Shet, M.S., Faulkner, K.M., Holmans, P.L., Fisher, C.W. and Estabrook, R.W. (1995) The effects of cytochrome b5, NADPH-P450 reductase, and lipid on the rate of 6 beta-

hydroxylation of testosterone as catalyzed by a human P450 3A4 fusion protein. Arch Biochem Biophys, 318, 314-321.

Shou, M., Grogan, J., Mancewicz, J.A., Krausz, K.W., Gonzalez, F.J., Gelboin, H.V. and Korzekwa, K.R. (1994) Activation of CYP3A4: evidence for the simultaneous binding of two substrates in a cytochrome P450 active site. Biochemistry, 33, 6450-6455.

Shriver, D.F. and Atkins, P.W. (2006) Shriver and Atkins' inorganic chemistry

Sligar, S.G. (1976) Coupling of spin, substrate, and redox equilibria in cytochrome P450. Biochemistry, 15, 5399-5406.

Sligar, S.G., Cinti, D.L., Gibson, G.G. and Schenkman, J.B. (1979) Spin state control of the hepatic cytochrome P450 redox potential. Biochem Biophys Res Commun, 90, 925-932.

Sligar, S.G. and Gunsalus, I.C. (1976) A thermodynamic model of regulation: modulation of redox equilibria in camphor monoxygenase. Proc Natl Acad Sci U S A, 73, 1078-1082.

Smith, D.A. and Jones, B.C. (1992) Speculations on the substrate structure-activity relationship (SSAR) of cytochrome P450 enzymes. Biochem Pharmacol, 44, 2089-2098.

Smith, G.C., Tew, D.G. and Wolf, C.R. (1994) Dissection of NADPH-cytochrome P450 oxidoreductase into distinct functional domains. Proc Natl Acad Sci U S A, 91, 8710-8714.

Sono, M., Roach, M.P., Coulter, E.D. and Dawson, J.H. (1996) Heme-Containing Oxygenases. Chem Rev, 96, 2841-2888.

Stewart, J.C. (1980) Colorimetric determination of phospholipids with ammonium ferrothiocyanate. Anal Biochem, 104, 10-14.

Stier, A. and Sackmann, E. (1973) Spin labels as enzyme substrates. Heterogeneous lipid distribution in liver microsomal membranes. Biochim Biophys Acta, 311, 400-408.

Strobel, H.W., Nadler, S.G. and Nelson, D.R. (1989) Cytochrome P-450: cytochrome P-450 reductase interactions. Drug Metab Rev, 20, 519-533.

Taniguchi, H., Imai, Y., Iyanagi, T. and Sato, R. (1979) Interaction between NADPH-cytochrome P-450 reductase and cytochrome P-450 in the membrane of phosphatidylcholine vesicles. Biochim Biophys Acta, 550, 341-356.

Taniguchi, H., Imai, Y. and Sato, R. (1984) Role of the electron transfer system in microsomal drug monooxygenase reaction catalyzed by cytochrome P-450. Arch Biochem Biophys, 232, 585-596.

Taniguchi, H., Imai, Y. and Sato, R. (1987) Protein-protein and lipid-protein interactions in a reconstituted cytochrome P-450 dependent microsomal monooxygenase. Biochemistry, 26, 7084-7090.

Thompson, J.A. and Wand, M.D. (1985) Interaction of cytochrome P-450 with a hydroperoxide derived from butylated hydroxytoluene. Mechanism of isomerization. J Biol Chem, 260, 10637-10644.

Thummel, K.E. and Wilkinson, G.R. (1998) In vitro and in vivo drug interactions involving human CYP3A. Annu Rev Pharmacol Toxicol, 38, 389-430.

Ueng, Y.F., Kuwabara, T., Chun, Y.J. and Guengerich, F.P. (1997) Cooperativity in oxidations catalyzed by cytochrome P450 3A4. Biochemistry, 36, 370-381.

Uvarov, V., Sotnichenko, A.I., Vodovozova, E.L., Molotkovsky, J.G., Kolesanova, E.F., Lyulkin, Y.A., Stier, A., Krueger, V. and Archakov, A.I. (1994) Determination of membrane-bound fragments of cytochrome P-450 2B4. Eur J Biochem, 222, 483-489.

Vergeres, G. and Waskell, L. (1995) Cytochrome b5, its functions, structure and membrane topology. Biochimie, 77, 604-620.

Vermilion, J.L., Ballou, D.P., Massey, V. and Coon, M.J. (1981) Separate roles for FMN and FAD in catalysis by liver microsomal NADPH-cytochrome P-450 reductase. J Biol Chem, 256, 266-277.

Vermilion, J.L. and Coon, M.J. (1978) Purified liver microsomal NADPH-cytochrome P-450 reductase. Spectral characterization of oxidation-reduction states. J Biol Chem, 253, 2694-2704.

Voznesensky, A.I. and Schenkman, J.B. (1992) The cytochrome P450 2B4-NADPH cytochrome P450 reductase electron transfer complex is not formed by charge-pairing. J Biol Chem, 267, 14669-14676.

Wagner, S.L., Dean, W.L. and Gray, R.D. (1984) Effect of a zwitterionic detergent on the state of aggregation and catalytic activity of cytochrome P-450LM2 and NADPH-cytochrome P-450 reductase. J Biol Chem, 259, 2390-2395.

Wagner, S.L., Dean, W.L. and Gray, R.D. (1987) Zwitterionic detergent mediated interaction of purified cytochrome P-450LM4 from 5,6-benzoflavone-treated rabbits with MADPH-cytochrome P-450 reductase. Biochemistry, 26, 2343-2348.

Wallin, E. and von Heijne, G. (1998) Genome-wide analysis of integral membrane proteins from eubacterial, archaean, and eukaryotic organisms. Protein Sci, 7, 1029-1038.

Walton, M.I., Wolf, C.R. and Workman, P. (1992) The role of cytochrome P450 and cytochrome P450 reductase in the reductive bioactivation of the novel benzotriazine di-N-oxide hypoxic cytotoxin 3-amino-1,2,4-benzotriazine-1,4-dioxide (SR 4233, WIN 59075) by mouse liver. Biochem Pharmacol, 44, 251-259.

Wang, M., Roberts, D.L., Paschke, R., Shea, T.M., Masters, B.S. and Kim, J.J. (1997) Three-dimensional structure of NADPH-cytochrome P450 reductase: prototype for FMN- and FAD-containing enzymes. Proc Natl Acad Sci U S A, 94, 8411-8416.

Ward, R.J. (2003) Preparation and characterisation of P450 3A4, Ph.D. thesis. Biochemistry.

Watenpaugh, K.D., Sieker, L.C. and Jensen, L.H. (1973) The binding of riboflavin-5'-phosphate in a flavoprotein: flavodoxin at 2.0-Angstrom resolution. Proc Natl Acad Sci U S A, 70, 3857-3860.

Williams, J.A., Ring, B.J., Cantrell, V.E., Jones, D.R., Eckstein, J., Ruterbories, K., Hamman, M.A., Hall, S.D. and Wrighton, S.A. (2002) Comparative metabolic capabilities of CYP3A4, CYP3A5, and CYP3A7. Drug Metab Dispos, 30, 883-891.

Williams, P.A., Cosme, J., Sridhar, V., Johnson, E.F. and McRee, D.E. (2000) Mammalian microsomal cytochrome P450 monooxygenase: structural adaptations for membrane binding and functional diversity. Mol Cell, 5, 121-131.

Williams, P.A., Cosme, J., Vinkovic, D.M., Ward, A., Angove, H.C., Day, P.J., Vonrhein, C., Tickle, I.J. and Jhoti, H. (2004) Crystal structures of human cytochrome P450 3A4 bound to metyrapone and progesterone. Science, 305, 683-686.

Yamazaki, H., Gillam, E.M., Dong, M.S., Johnson, W.W., Guengerich, F.P. and Shimada, T. (1997) Reconstitution of recombinant cytochrome P450 2C10(2C9) and comparison with cytochrome P450 3A4 and other forms: effects of cytochrome P450-P450 and cytochrome P450-b5 interactions. Arch Biochem Biophys, 342, 329-337.

Yamazaki, H., Johnson, W.W., Ueng, Y.F., Shimada, T. and Guengerich, F.P. (1996) Lack of electron transfer from cytochrome b5 in stimulation of catalytic activities of cytochrome P450 3A4. Characterization of a reconstituted cytochrome P450 3A4/NADPH-cytochrome P450 reductase system and studies with apo-cytochrome b5. J Biol Chem, 271, 27438-27444.

Yamazaki, H., Nakajima, M., Nakamura, M., Asahi, S., Shimada, N., Gillam, E.M., Guengerich, F.P., Shimada, T. and Yokoi, T. (1999) Enhancement of cytochrome P-450 3A4 catalytic activities by cytochrome b(5) in bacterial membranes. Drug Metab Dispos, 27, 999-1004.

Yamazaki, H., Nakamura, M., Komatsu, T., Ohyama, K., Hatanaka, N., Asahi, S., Shimada, N., Guengerich, F.P., Shimada, T., Nakajima, M. and Yokoi, T. (2002) Roles of NADPH-P450 reductase and apo- and holo-cytochrome b5 on xenobiotic oxidations catalyzed by 12 recombinant human cytochrome P450s expressed in membranes of Escherichia coli. Protein Expr Purif, 24, 329-337.

Yamazaki, H., Nakano, M., Imai, Y., Ueng, Y.F., Guengerich, F.P. and Shimada, T. (1996) Roles of cytochrome b5 in the oxidation of testosterone and nifedipine by recombinant cytochrome P450 3A4 and by human liver microsomes. Arch Biochem Biophys, 325, 174-182.

Yamazaki, H., Shimada, T., Martin, M.V. and Guengerich, F.P. (2001) Stimulation of cytochrome P450 reactions by apo-cytochrome b5: evidence against transfer of heme from cytochrome P450 3A4 to apo-cytochrome b5 or heme oxygenase. J Biol Chem, 276, 30885-30891.

Yamazaki, H., Ueng, Y.F., Shimada, T. and Guengerich, F.P. (1995) Roles of divalent metal ions in oxidations catalyzed by recombinant cytochrome P450 3A4 and replacement of NADPH--cytochrome P450 reductase with other flavoproteins, ferredoxin, and oxygen surrogates. Biochemistry, 34, 8380-8389.

Yang, C.S. (1975) The association between cytochrome P-450 and NADPH-cytochrome P-450 reductase in microsomal membrane. FEBS Lett, 54, 61-64.

Yano, J.K., Wester, M.R., Schoch, G.A., Griffin, K.J., Stout, C.D. and Johnson, E.F. (2004) The structure of human microsomal cytochrome P450 3A4 determined by X-ray crystallography to 2.05-A resolution. J Biol Chem, 279, 38091-38094.

Yano, J.K., Wester, M.R., Schoch, G.A., Griffin, K.J., Stout, C.D. and Johnson, E.F. (2004) The structure of human microsomal cytochrome P450 3A4 determined by X-ray crystallography to 2.05-angstrom resolution. Journal of Biological Chemistry, 279, 38091-38094.

Yasukochi, Y. and Masters, B.S. (1976) Some properties of a detergent-solubilized NADPH-cytochrome c(cytochrome P-450) reductase purified by biospecific affinity chromatography. J Biol Chem, 251, 5337-5344.

Yun, C.H., Kim, K.H., Calcutt, M.W. and Guengerich, F.P. (2005) Kinetic analysis of oxidation of coumarins by human cytochrome P450 2A6. J Biol Chem, 280, 12279-12291.

Zhang, H., Im, S.C. and Waskell, L. (2007) Cytochrome b5 stimulates the rate of product formation by cytochrome P450 2B4 and competes with cytochrome P450 reductase for a binding site on cytochrome P450 2B4. J Biol Chem.

Zhao, Q., Modi, S., Smith, G., Paine, M., McDonagh, P.D., Wolf, C.R., Tew, D., Lian, L.Y., Roberts, G.C. and Driessen, H.P. (1999) Crystal structure of the FMN-binding

domain of human cytochrome P450 reductase at 1.93 A resolution. Protein Sci, 8, 298-306.

Zhao, Q., Smith, G., Modi, S., Paine, M., Wolf, R.C., Tew, D., Lian, L.Y., Primrose, W.U., Roberts, G.C. and Driessen, H.P. (1996) Crystallization and preliminary X-ray diffraction studies of human cytochrome P450 reductase. J Struct Biol, 116, 320-325.

Ziegler, M., Blanck, J., Greschner, S., Lenz, K., Lau, A. and Ruckpaul, K. (1983) Kinetics of elementary steps in the cytochrome P-450 reaction sequence. V. Laser temperature-jump investigation of the spin relaxation kinetics of cytochrome P-450 LM2. Biomed Biochim Acta, 42, 641-649.